Mayer, Leonard

STUDIES OF THE EFFECTS OF MAGNESIUM ION ON THE STRUCTURE AND MECHANISM OF OROTATE PHOSPHORIBOSYL TRANSFERASE AND NICOTINATE PHOSPHORIBOSYL TRANSFERASE FROM YEAST

City University of New York PH.D. 1983

PLEASE NOTE:

In all cases this material has been filmed in the best possible way from the available copy. Problems encountered with this document have been identified here with a check mark __✓__.

1. Glossy photographs or pages __✓__
2. Colored illustrations, paper or print _____
3. Photographs with dark background __✓__
4. Illustrations are poor copy _____
5. Pages with black marks, not original copy _____
6. Print shows through as there is text on both sides of page _____
7. Indistinct, broken or small print on several pages __✓__
8. Print exceeds margin requirements _____
9. Tightly bound copy with print lost in spine _____
10. Computer printout pages with indistinct print _____
11. Page(s) _____ lacking when material received, and not available from school or author.
12. Page(s) _____ seem to be missing in numbering only as text follows.
13. Two pages numbered _____. Text follows.
14. Curling and wrinkled pages __✓__
15. Other _____

STUDIES OF THE EFFECTS OF Mg^{2+} ON THE STRUCTURE AND MECHANISM OF OROTATE PHOSPHORIBOSYLTRANSFERASE AND NICOTINATE PHOSPHORIBOSYLTRANSFERASE FROM YEAST

by

LEONARD MAYER

A dissertation submitted to the Graduate Faculty in Biochemistry in partial fulfillment of the requirements for the degree of Doctor of Philosophy, The City University of New York.

1983

This manuscript has been read and accepted for the Graduate Faculty in Biochemistry in satisfaction of the dissertation requirement for the degree of Doctor of Philosophy.

1/13/83
Date

Chairman of Examining Committee

January 24, 1983
Date

Executive Officer

Supervisory Committee

ABSTRACT

STUDIES ON THE STRUCTURE AND MECHANISM OF OROTATE PHOSPHORIBOSYLTRANSFERASE AND NICOTINATE PHOSPHORIBOSYLTRANSFERASE

by

Leonard Mayer

Adviser: Professor Donald L. Sloan

The purpose of this investigation was to explore the role that Mg^{2+} *plays in the structure and mechanism of orotate phosphoribosyltransferase (OPRTase) and nicotinate phosphoribosyltransferase (NPRTase) using nuclear magnetic relaxation (NMR) and SDS acrylamide gel electrophoresis. Crosslinking of OPRTase by glutaraldehyde (GTA) in the presence of* Mg^{2+} *did reveal by SDS electrophoresis the existence of a dimeric form of yeast OPRTase. At low concentrations of GTA (0.05%) in the absence of* Mg^{2+}*, detectable dimer was not observed while at high concentrations of GTA (0.2%) in the absence of* Mg^{2+}*, the dimer was detectable as a band on SDS electrophoresis gels. The appearance of the crosslinked dimer depended on the concentration of GTA employed and on whether or not* Mg^{2+} *was present.* Mg^{2+} *enhances the appearance of the dimer.* Mg^{2+}*–phosphoribosylpyrophosphate (PRPP) did not protect the enzyme against crosslinking but may have protected against inactivation by GTA. Whereas GTA inactivates OPRTase, dimethyl suberimidate (DMS) does not. Crosslinking of NPRTase at all concentrations of GTA or DMS tested did not occur. Neither GTA nor DMS succeeded in rendering NPRTase inactive. Neither* Mg^{2+}*,* Mg^{2+}*–PRPP, nor* Mg^{2+}*–adenosine triphosphate (ATP) affected the electrophoretic pattern or the activity of NPRTase treated with either GTA or DMS. From the SDS electrophoresis*

results, it has been proposed that the OPRTase monomer is in equilibrium with a dimeric form and that Mg^{2+} promotes the extent of dimer formation. In contrast, NPRTase exists as a monomer in the native form and does not interconvert to higher molecular weight forms.

Proton-NMR was employed to characterize the formation of OMP-metal ion, PRPP-metal ion, and OPRTase-substrate-metal ion complexes. Moreover, when Mg^{2+} was added to solutions of PRPP, OMP, and OPRTase, the changes in the proton resonance amplitudes of PRPP (decreases) and OMP (increases) suggest that a new equilibrium between this substrate/product pair has been established. Such an alteration in the equilibrium in the absence of orotate and PP_i, the other substrate/product pair, can only occur if the kinetic mechanism is Bi Bi Ping Pong. Thus the NMR experiments provide independent evidence of a mechanism that has been suggested from kinetic analysis.

TABLE OF CONTENTS

LIST OF TABLES

LIST OF FIGURES

LIST OF FIGURES (continued)

INTRODUCTION

5-Phosphoribosyl-1-pyrophosphate (PRPP) is the donor of ribose-5'-phosphate in pyrimidine nucleotide biosynthesis (1), in de novo purine nucleotide biosynthesis (2), in salvage purine nucleotide biosynthesis (3), in nicotinic acid mononucleotide synthesis (4), in tryptophan biosynthesis (5), and in the first step of histidine biosynthesis (6). The enzymes which transfer the phosphoribosyl moiety of PRPP are called phosphoribosyltransferases. Divalent metal ions are required for the enzyme catalyzed transfer of the phosphoribosyl group from PRPP to the nitrogenous, generally aromatic base. The phosphoribosyl transfer is accompanied by the anomeric inversion of configuration of the ribofuranose ring. The configuration in PRPP of C-1, to which pyrophosphate is attached, is α. The configuration of the base attached to C-1 of ribose-5'-phosphate is β. The phosphoribosyltransferase reaction is reversible in the presence of pyrophosphate (PP_i) but inorganic pyrophosphatase may render the reaction irreversible in vivo.

Orotate Phosphoribosyltransferase

The two enzymes of de novo pyrimidine nucleotide biosynthesis of interest to this discussion are orotate phosphoribosyltransferase (orotidine phosphate: pyrophosphate phosphoribosyltransferase; OPRTase; EC 2.4.2.10) and orotidine-5'-phosphate decarboxylase (ODCase; EC \$.1.1.23). OPRTase catalyzes the Mg^{++}-dependent reversible formation of a β-glycosidic bond between orotate and the phosphoribosyl moiety of α-PRPP (equation 1). This stereospecific reaction is accompanied by the release of pyrophosphate. Orotidylate decarboxylase catalyzes the decarboxylation of orotidylate (OMP) to form uridylate (UMP)

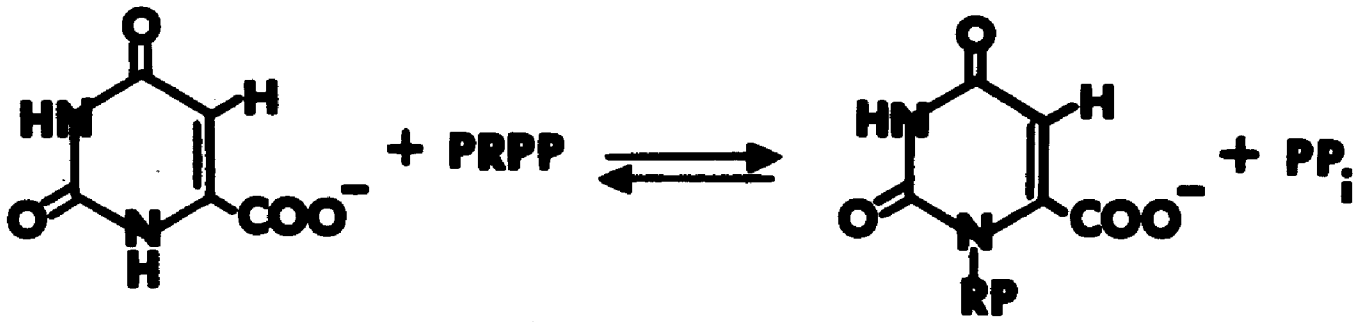

(1)

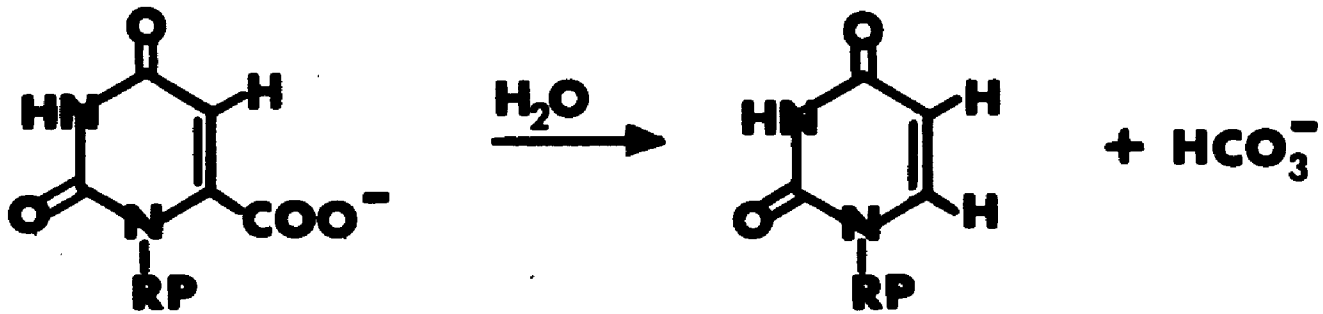

(2)

(equation 2).

In all organisms thus far examined, OPRTase requires magnesium for optimal activity (1, 7, 8, 9, 10, 11, 12). The enzyme is completely inhibited by 5 mM EDTA which removes magnesium ion. The product of the forward reaction, orotidylate (OMP), inhibits the reaction by competing with either orotate or PRPP. Orotidylate decarboxylase does not require magnesium for activity (8).

The purification procedure for the yeast enzyme has been improved in extent of purity and in length of time necessary for purification. Lieberman, et. al. (1) were the first to isolate OPRTase from brewer's yeast. Umezu, et. al. (11) purified OPRTase to homogeneity from baker's yeast and determined some of its properties. Victor, et. al. (13) purified OPRTase from baker's yeast by a modified procedure of Umezu. Reyes, et. al. (14) demonstrated that yeast OPRTase is tightly bound to cibacron blue-linked Sepharose and can be eluted by PRPP and OMP. Maximal purification of OPRTase (1200-1500 fold) was achieved using this single step procedure. Binding of an enzyme to a cibacron blue derivative (a sulfonated aromatic chromophore) suggested but did not prove that OPRTase from baker's yeast possesses a dinucleotide fold. Dodin (15) developed a rapid purification of OPRTase from Escherichia coli K-12 by OMP-Sepharose Column Chromatography.

OPRTase has been purified from a number of sources. Mammalian sources include calf thymus (17), cow brain (18), Ehrlich ascites carcinoma (19), rat liver (20), murine leukemia (21), and human erythrocytes (22). Yeast (1) and Escherichia coli (15) have also served as sources. Recent sources include the human pathogen, Leishmania mexicana mexicana (23), the related flagellate protozoan, Crithidia fasci-

culata (23), and the livers (24) of sparse fur mice (mutant mice with ornithine transcarbamylase deficiency).

OPRTases from all organisms studied thus far except yeast are found in vivo as bifunctional enzyme complexes with ODCase (12). A large body of evidence supports the view that OPRTase and ODCase form a multienzymic protein. OPRTase and ODCase copurify from a number of mammalian tissues or cells (17-24). The two activities cosediment in a centrifugal field, coelute by molecular sieve chromatography, and comigrate in an electric field (25). The protein comprising the two activities has been termed Complex U but is now called pyr5,6 (25-30). In animals, the multienzyme pyr5,6 which is in the cytosol channels orotate directly through to UMP without significantly accumulating the OMP intermediate (27). The activities of both enzymes show a coordinate relationship in rat and human tissues and in erythrocytes from various mammalian sources (31). The two activities remain coordinate as described above in fetal, neonatal, immature, and adult liver and brain of mouse. In yeast, the two catalytic activities are associated with separate proteins; there is no channeling of OMP (16).

The regulation of OPRTase in yeast (Saccharomyces cerevisiae) is different from that in mammals. The gene coding for OPRTase in yeast is designated ura5 and is unlinked to the gene coding for ODCase: ura3 (33, 34, 35). Whereas ODCase is inducible, OPRTase is neither repressible, derepressible, or inducible in yeast (32): OPRTase levels do not change in response to the pyrimidine pool or to the pool levels of prior intermediates. In mammals, the genes for OPRTase and ODCase are linked (25). The linked genes produce a single polypeptide which, as previously stated, is called the multienzyme pyr5,6. OPRTase and ODCase levels

appear to be regulated by induction in mammals (30).

Victor, J., et. al. (13) provided evidence that the kinetic mechanism of formation of OMP from orotate is a Bi Bi Ping Pong mechanism. The double-reciprocal initial velocity patterns for both the forward and reverse reactions were composed of parallel lines. Isotopic exchange studies showed that each half reaction proceeded in the absence of substrates for the other half reaction. Product inhibition studies supported the view that PRPP is the first bound substrate and the interpretation of the kinetic mechanism as ping pong. A Bi Bi Ping Pong kinetic mechanism predicts the existence of two stable enzyme forms: the free enzyme and the enzyme bound with a portion of the substrate. However, Victor, J. et. al. (13) did not isolate such an intermediate. Goitein, R.K. et. al. (36) provided evidence based on kinetic isotope effects which indicate that OPRTase utilizes a carbocation mechanism. The inversion of configuration during formation of OMP and the carbocation mechanism have prompted Victor, J. et. al. (13) to propose the existence of a tightly-bound noncovalent enzyme intermediate, a carbocation intermediate.

Recent studies of divalent metal ion activation of yeast OPRTase catalyzed reaction suggest that the role of Mg^{++} or Mn^{++} is multifunctional and that a metal ion-enzyme complex is the species which catalyzes the reaction via the ping pong mechanism (37). Electron paramagnetic resonance (EPR), UV spectroscopy, and water proton relaxation rate (PRR) measurements have been employed to calculate dissociation constants ($\overline{K_o}$) for the formation of binary complexes between Mn^{++} and orotate ($\overline{K_o}$ = 500 μM), PRPP ($\overline{K_o}$ = 30 μM), PP_i ($\overline{K_o}$ = 12 μM), and OMP ($\overline{K_o}$ = 200 μM). EPR and PRR measure-

ments support the view that a binary Mn^{++}–enzyme complex forms with a maximal stoichiometry of 4:1. The shape of the binding isotherm for Mn^{2+}–enzyme formation is sigmoidal, suggesting cooperation between Mn^{2+} binding sites. The initial velocity patterns for the activation of phosphoribosyl transfer are biphasic. These results can be attributed to catalysis at different rates by an enzyme-metal ion complex and a metal free enzyme. The two sets of intersecting lines exhibited by the initial velocity patterns can be described in terms of two types of Mg^{2+} binding sites on the enzyme, one of which is allosteric in character. The role that Mg^{2+} plays in the OPRTase reaction warrants further study, although kinetic analysis (37) suggests the formations of metal ion–enzyme and metal ion–PRPP complexes lead to optimal activation (equations 3 and 4).

$$M + PRibPP \underset{}{\overset{K_O}{\rightleftharpoons}} M\text{-}PRibPP \qquad (3)$$

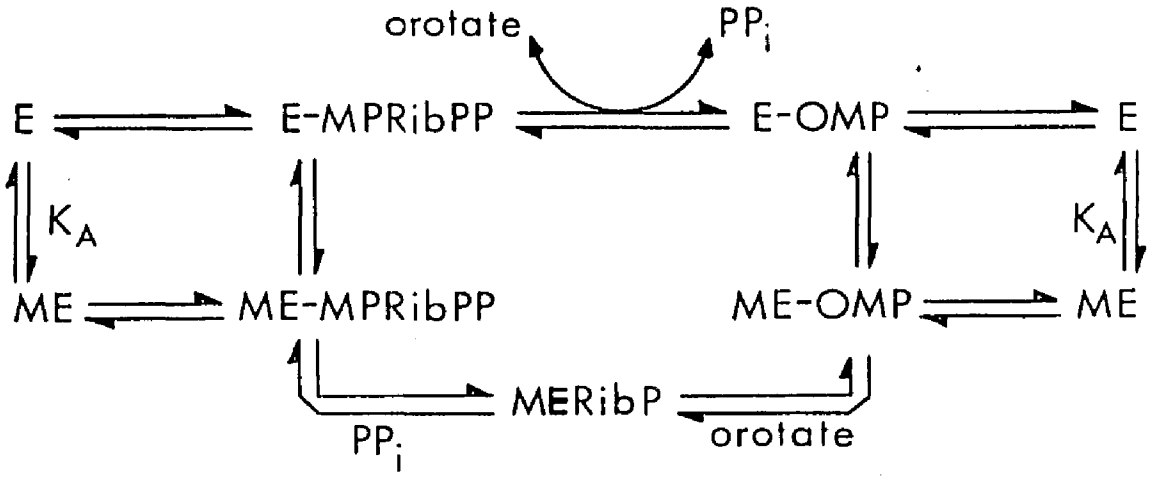

(4)

Nicotinate Phosphoribosyltransferase

Nicotinate phosphoribosyltransferase (nicotinate nucleotide: pyrophosphate phosphoribosyltransferase; NPRTase; EC 2.4.2.11) catalyzes the transfer of the ribose-5-phosphate moiety of PRPP to nicotinic acid to form nicotinate mononucleotide (NaMN). It catalyzes the first step in the Preiss-Handler pathway (38, 39, 40) which is the main route for the biosynthesis of NAD in mammalian tissue, yeast, and E. coli (equations 5-7). Nicotinic acid is obtained either through nutritional sources or from the biodegradation of tryptophan (41).

$$\text{Nicotinate} + \text{PRibPP} \xrightarrow[\text{ATP}]{\text{ADP} + P_i} \text{Na MN} + PP_i \qquad (5)$$

$$\text{Na MN} + \text{ATP} \longrightarrow \text{Na AD} + PP_i \qquad (6)$$

$$\text{Na AD} + \text{Gln} \xrightarrow[\text{ATP}]{\text{AMP} + PP_i} \text{NAD} + \text{Glu} \qquad (7)$$

NPRTase was first purified from beef liver by Imsande and Handler (42) who demonstrated an absolute requirement for a divalent metal ion, the irreversibility of the reaction, and a stimulation of NPRTase activity by orthophosphate and by ATP. The enzyme has subsequently been isolated from Bacillus subtilis (43), yeast (44-47), Ehrlich ascites cells (48), the protozoan Astasia longa (49), human erythrocytes (50), and E. coli (51).

The regulation of NPRTase in Salmonella typhimurium has been studied (53). The genetic marker for NPRTase is designated pncB. NPRTase is not controlled by feedback inhibition, but does exhibit end-product repression. Foster, J.W. et. al. (53) has suggested that NAD is the corepressor molecule since repression of NPRTase by various pyridine nucleotides appears to result from conversion of these nucleotides to NAD.

Kosaka, A. et. al. (46,47) purified yeast NPRTase and reported some of its characteristics. Yeast NPRTase absolutely requires ATP for reaction. Honjo, T. et. al. (45) reported that ATP is stoichiometrically cleaved to ADP and orthophosphate in the reaction catalyzed by the yeast enzyme. The molecular weight of the yeast enzyme was estimated from Sephadex Chromatography to be 43,000. Magnesium ion is required for the reaction. Kosaka, A. et. al. (46) have suggested that ATP-Mg^{2+} is the true substrate of the reaction and that nicotinate mononucleotide production is catalyzed by two different kinetic mechanisms: a partial ordered substrate binding with partial random product release and a partial ping pong substrate binding with partial random product release (47).

Sloan et. al. (52) proposed that NPRTase proceeds via an Ordered Uni Uni Bi Bi Ping Pong kinetic mechanism on the basis of initial velocity studies (using different fixed concentration ratios of two of the three substrates), product (pyrophosphate) inhibition analysis, isotope exchange between substrate/product pairs and flow dialysis studies of the nicotinate-NPRTase interaction. According to this mechanism, ATP binds initially to form P_i–NPRTase and ADP. PRPP and nicotinate then bind P_i–NPRTase (in that order) whereupon PP_i and nicotinate mononucleotide are released randomly (followed by phosphate release).

Niedel, J. et. al. (50) have purified NPRTase from human erythrocytes. ATP stimulates the enzymatic reaction but is not an obligatory substrate. When ATP is present, ATP hydrolysis is stoichiometric with nicotinate mononucleotide formation. ATP stimulates activity by lowering the K_m of both nicotinate and PRPP by one or two orders of magnitude. The molecular weight of the human erythrocyte enzyme was found to be 86,000 by gel filtration.

The analysis of metal ion activation has not yet been done. Kosaka, A. et. al. (46) showed the effects of metal ions on activity and suggested that a metal ion-enzyme complex may form. Metal activation analysis should be complicated since the enzyme, PRPP, and ATP all bind metals. The role of the metal must therefore be multifaceted.

RATIONALE

Traut, T.W. (16) suggested that subunit association/dissociation may be the primary route for the control of the phosphoribosyltransferases. The research described in this thesis was initiated to examine the role that metals play in the OPRTase mechanism of action using NMR and SDS-gel electrophoresis with the idea that perhaps the metal ions may affect a monomer/oligomer equilibrium. Because NPRTase can also be purified from the same baker's yeast extract, the SDS-gel studies were also carried out for this enzyme. As will be described in detail, an effect on OPRTase monomer/dimer equilibrium by Mg^{2+} has been revealed, whereas NPRTase has been proven to be composed of a single polypeptide chain which does not form oligomers.

MATERIALS AND METHODS

Materials

Baker's yeast (Budweiser brand) was obtained from Valenti Yeast Inc., Flushing, N.Y. Supplies purchased from Sigma Chemical Co., St. Louis, Mo., included PRPP (sodium salt), ATP (disodium salt), nicotinic acid, dithiothreitol, coomassie brilliant blue R, SDS molecular weight markers 70 kit, 2-mercaptoethanol, dimethyl suberimidate, Trizma HCl, Trizma Base, acrylamide, hemoglobin, ferritin, and bovine serum albumin. Hydroxyapatite HT, Cellex D, SDS, TEMED, glycine, ammonium persulfate, AG 501-X8, riboflavin-5'-phosphate, and Bio-Rad protein assay kit were purchased from Bio-Rad Laboratories, Richmond, Ca. Glutaraldehyde was obtained from Aldrich Chemical Co., Milwaukee, Wisconsin. Sodium pyrophosphate was purchased from Merck Co., Rahway, N.J. Sodium dichromate, glatial acetic acid, methanol, potassium hydroxide, ammonium phosphate, potassium phosphate (monobasic and dibasic), phenol reagent, sodium carbonate, copper sulfate, sodium potassium tartrate, sodium hydroxide, toluene, octanol, sodium chloride, glycerol, and triethanolamine were purchased from Fisher Scientific Co., Springfield, N.J. Kodak Photo-Flo 200 solution, Kodak technical pan film 2415, bisacrylamide, and bromophenol blue were purchased from Eastman Kodak Co., Rochester, N.Y. Blue Sepharose CL-6B and Sephadex G-100 were purchased from Pharmacia Fine Chemicals, Piscataway, N.J. Orotic acid was bought from Calbiochem, La Salle, Ca. Phosphocellulose was obtained from Brown Co., Berlin, N.H. Magnesium chloride was bought from Thiokol Alfa Products, Danvers, Ma. All other chemicals were reagent grade.

Enzyme Assays

Orotate Phosphoribosyltransferase

The activity of OPRTase was monitored by the decrease in absorption at 295 nm. due to depletion of orotate. The reference cuvette contained 0.29 ml. H_2O, 0.5 ml. 100 mM Tris/HCl (pH = 8), 0.1 ml. of 200 mM $MgCl_2 \cdot 6H_2O$, 0.1 ml. of 1 mM orotate, and 0.01 ml. of enzyme extract. The sample cuvette contained 0.090 ml. of H_2O, 0.5 ml. of 100 mM Tris/HCl (pH = 8), 0.1 ml. of 200 mM $MgCl_2 \cdot 6H_2O$, 0.1 ml. of 1 mM orotate, 0.01 ml. of enzyme extract, and 0.2 ml. of 1 mM PRPP. In certain situations such as the assay of fractions eluted from a column of Blue Sepharose CL-6B, 10 mM PRPP was used in place of 1 mM PRPP. In general the PRPP aliquot was added last, but in some cases such as the monitoring of activity during crosslinking, the enzyme aliquot was added last.

Nicotinate Phosphoribosyltransferase

A previously described HPLC assay procedure (54) was employed during NPRTase purification and thereafter to monitor the activity of NPRTase during crosslinking. The standard NPRTase assay mixture contained 5.0 mM $MgCl_2 \cdot 6H_2O$, 0.1 mM nicotinate, 0.1 mM ATP and 0.1 mM PRPP in 50.0 mM Tris-phosphate buffer (pH = 8). The reaction was initiated with the addition of approximately 0.1 milliunit of enzyme and was terminated (after incubation for 15 min. at 37°C) by heating the solution in a boiling water bath for 2 minutes. The samples were then clarified, first by centrifugation and then by passage through a 0.45 micron HA-type Millipore filter. Volumes of 5.0 µl. of these samples were then injected into a Waters µbondpak C_{18} column.

Protein Determination

The concentrations of OPRTase and NPRTase were determined by both the Lowry method (55) and the Bio-Rad protein assay (56). The Lowry reaction for protein determination involves the formation in alkaline solution of a copper-protein complex which reduces the phosphomolybdic-phosphotungstate reagent (Folin-Ciocalteu phenol reagent) to yield an intense blue color whose absorption can be measured at 650 nm. Any substance that can reduce copper interferes with the Folin reagent: ammonium salts (such as Trizma Base), organic amines, and sulfhydryl reagents. Strongly acidic samples must be neutralized prior to assay by the Lowry method because the reduction of the Folin reagent occurs only at pH of 10.

The Bio-Rad protein assay is based on the differential color change of a dye in response to various concentrations of protein. The absorbance at 595 nm. of the dye-protein complex is stable for more than one hour. 2-Mercaptoethanol and Trizma Base do not interfere with the Bio-Rad Assay. However, basic samples must be neutralized prior to assay by the Bio-Rad method.

Determination of Specific Activity of Enzymes

The specific activity of OPRTase is the number of μmoles of orotate which are converted to OMP per minute per mg. of protein. The determination of activity of OPRTase is based on the disappearance of the absorbance of the orotate at 295 nm. as OPRTase converts orotate to OMP. The extinction coefficient of orotate is 3950 M^{-1} cm^{-1}.

The specific activity of NPRTase is the number of μmoles of nicotinate mononucleotide (NaMN) formed per minute per mg. of protein.

Purification of Enzymes

All steps were performed at 4°C unless otherwise indicated. The purification procedure was adapted from Umezu, K., et. al. (11).

Autolysis

Pressed baker's yeast was suspended in 15 l. of 0.3 M phosphate buffer (pH = 8) and 2.4 l. of toluene. The suspension was stirred for 4 hours at 30°C, while maintaining the pH at 8, and then allowed to stand overnight. Cell debris was removed by centrifugation and the supernatant was clarified by filtration.

Ammonium Sulfate Fractionation

The filtered solution (24 l.) was adjusted to pH of 5 with 8 N acetic acid, brought slowly to 50% saturation with ammonium sulfate (in the presence of octanol), and allowed to stand overnight. The protein precipitate was collected by centrifugation, dissolved in 10 mM phosphate (pH = 8), and dialyzed against this same buffer. Crystalline $MnCl_2$ (50 mM final concentration) was then added to the protein solution which was clarified by centrifugation. Orotic acid was added to the solution (1 mM final concentration) and the pH was adjusted to 6 with concentrated acetate buffer (pH = 5.5).

Ethanol Fractionation

The protein solution was then cooled to 0°C in preparation for the ethanol fractionation procedure. Protein was precipitated from the solution with the addition of pre-cooled (-20°C) ethanol to a final volume fraction of 50% while maintaining the solution temperature below 0°C (final temperature -10°C). The precipitate was collected by centrifugation (at -15°C), dissolved in 10 mM phosphate (pH = 6) and dialyzed

against this buffer in preparation for phosphocellulose chromatography. The final volume of this protein extract was 4.6 l.

Phosphocellulose Column Chromatography

The extract, which contained both OPRTase and NPRTase activities, was eluted through a 5 X 60 cm. phosphocellulose column equilibrated with 5 mM phosphate (pH = 6). Both activities were retained on the column, but continued washing with this buffer eluted OPRTase. The NPRTase activity was then eluted with 40 mM phosphate (pH = 6.7). Active fraction were pooled and NPRTase was precipitated from the solution with the addition of ammonium sulfate (to 70% saturation). The enzyme was dissolved in 5 mM phosphate (pH = 7.5) and dialyzed against the same buffer (final volume 165 ml.).

Hydroxylapatite Chromatography of NPRTase Extract

The NPRTase solution was incubated at 25°C (15 min) with 10 mM $MgCl_2 \cdot 6H_2O$, *5 mM nicotinate, and 2 mM PRPP in order to convert any phosphorylated-enzyme to its native form. Thereafter, NPRTase was adsorbed onto a 6 X 10 cm. hydroxylapatite column equilibrated with 5 mM phosphate (pH = 7.5) and eluted with a linear phosphate gradient (5-100 mM, pH = 7.5). Active fractions were pooled and the NPRTase was concentrated using the above described ammonium sulfate precipitation technique. The enzyme was then dissolved in 2 mM Tris/HCl (pH = 6.0) and dialyzed against this buffer (final volume = 60 ml.).*

Blue Sepharose Chromatography of NPRTase Extract

The dialyzed NPRTase solution was divided into three 20 ml. parts and each aliquot was layered onto a 2.5 X 30 cm. Blue Sepharose CL-6B column equilibrated with 2 mM Tris buffer (pH = 6). After washing the column to remove extraneous protein, NPRTase was eluted with a 2-200 mM

Tris/HCl linear gradient (pH = 6). Active fractions were pooled and lyophilized, and the enzyme was dissolved and dialyzed in 5 mM phosphate (pH = 7.5). The volume of the NPRTase solution was 57 ml.

DEAE Cellulose Chromatography of NPRTase Extract

A 2.5 X 30 cm. DEAE cellulose column was used to purify NPRTase. The enzyme solution was layered onto the column equilibrated with 5 mM phosphate (pH = 7.5). A linear phosphate gradient (5-100 mM) was employed to elute the enzyme which was concentrated once again using lyophilization. The final volume of the purified NPRTase was 10 ml.

Ammonium Sulfate Fractionation of OPRTase Extract

The protein fractions which did not bind to the phosphocellulose column were pooled and subject to 70% saturation with ammonium sulfate (472 gms./liter). The precipitate was collected by filtration through Whatman #1 filter paper. The precipitate was dissolved in 1250 ml. of 10 mM Tris/HCl (pH = 8), 3 mM orotate. The solution was dialyzed against 16 liters of 10 mM Tris/HCl (pH =8), 3 mM orotate for 5 hours.

Sephadex G-100 Gel Chromatography of OPRTase Extract

25 grams of Sephadex G-100 was swelled in a buffer consisting of 10 mM Tris/HCl (pH = 8), 1 mM orotate, and 40 mM NaCl. The Sephadex G-100 was then degassed in the cold room and packed continuously in a column (2.5 cm. X 60 cm.) of volume 290 ml.

1250 ml. of dialysate was divided into 25 portions of 50 ml. Each 50 ml. aliquot was applied to the column of Sephadex G-100 equilibrated with buffer consisting of 10 mM Tris/HCl (pH = 8), 1 mM orotate, and 40 mM NaCl. After loading, the column was developed with the aforementioned equilibrating buffer. 9 racks of 10.6 ml. per fraction were collected. Those fractions whose decrease in absorption was greater

than or equal to 0.01 at 295 nm. were collected. The total extract volume from 25 runs of Sephadex G-100 from 285 pooled test tubes was 3025 ml.

DEAE Cellulose Chromatography of OPRTase Extract

The pooled extract from Sephadex G-100 was dialyzed against 15 liters of 10 mM KP_i (pH = 8), 1 mM orotate. Cellex D was swelled in 10 mM KP_i (pH = 8), 1 mM orotate, degassed, and packed in sections in a 290 ml. volume column (2.5 cm. X 60 cm.). The DEAE cellulose was equilibrated with 1 liter of buffer consisting of 10 mM KP_i (pH = 8) and 1 mM orotate.

Five runs of DEAE cellulose chromatography were performed. In each run, 600 ml. of dialyzed G-100 extract was applied to the column. The column was washed with 3 liters of equilibrating buffer. A protein whose fractions exhibited a yellow discoloration and no OPRTase activity eluted during the wash. The enzyme was eluted with a linear gradient between 750 ml. each of 10 mM KP_i (pH = 8), 1 mM orotate, and of 200 mM KP_i (pH = 8), 1 mM orotate. The 1 mM orotate was not completely soluble in 200 mM KP_i (pH = 8); so the precipitate was filtered before the buffer was placed in the reservoir of the linear gradient apparatus. Fractions of 10 ml. were collected. It was observed that two peaks exhibiting OPRTase eluted. The first peak represents isozyme I while the second peak represents isozyme II. The column was washed with 300 ml. of 200 mM KP_i (pH = 8). The column was reequilibrated with 2000 ml. of 10 mM KP_i (pH = 8), 1 mM orotate. Failure to reequilibrate with at least 2000 ml. of equilibrating buffer or to remove the insoluble orotate from the 200 mM KP_i (pH = 8) reservoir results in earlier elution and less separation of isozymes I and II. The total extract from the

5 runs yielded 1480 ml. of OPRTase extract.

Hydroxylapatite Chromatography of OPRTase Extract

The extract from the pooled DEAE cellulose fractions was dialyzed twice against 10 mM KP_i (pH = 8), 1 mM orotate. 37.5 gms. of hydroxylapatite were swelled in buffer containing 10 mM KP_i (pH = 8) and 1 mM orotate. The hydroxylapatite was packed in a column (2.5 cm. X 30 cm.) of 150 ml. volume. The column was equilibrated with 1 liter of the aforementioned buffer.

Three hydroxylapatite columns were run. In the first column, 500 ml. of extract were loaded. Active fractions eluted during the latter part of loading. So in the second and third runs, 330 ml. of extract were loaded. The enzyme was eluted with a linear gradient of 500 ml. of 10 mM KP_i (pH = 8), 1 mM orotate, and of 500 ml. of 200 mM KP_i (pH = 8), 1 mM orotate. Each fraction had 10 ml. volume. 150 test tubes were collected.

In each of three runs, the active peak appeared as an asymmetrical singlet. The volume of pooled fractions in the first run was 280 ml., in the second run was 130 ml., and in the third run was 100 ml. The fractions collected during the development exhibited no detectable activity. The hydroxylapatite column was regenerated by application of 1 liter of 0.5 M KP_i (pH = 8) and was reequilibrated by 1 liter of equilibrating buffer. The pooled hydroxylapatite fractions appeared clear with no discoloration.

Blue Sepharose CL-6B Chromatography of OPRTase Extract

The pooled hydroxylapatite fractions were dialyzed twice against 16 liters of 10 mM Tris/HCl (pH = 8). A fresh batch of Blue Sepharose CL-6B was allowed to swell in 2 mM Tris/HCl (pH = 8) and poured into

a column of 2.5 cm. X 30 cm. The Blue Sepharose CL-6B column was equilibrated with 1600 ml. of 2 mM Tris/HCl (pH = 8). 200 ml. of dialyzed OPRTase extract was loaded onto the column. Development succeeded the loading with application of 2 mM Tris/HCl (pH = 8). Thirty test tubes with 25 ml. per fraction were collected during loading and development. The enzyme was eluted by application of 25 ml. of 1 mg./ml. of OMP. The buffer applied after OMP was 2 mM Tris/HCl (pH = 8). Twenty test tubes with 6.25 ml. per fraction were collected during elution. The test tubes were assayed for OPRTase activity and for absorption at 268 nm. The column was washed with 200 ml. of 200 mM Tris/HCl (pH = 8) before the next run.

The regeneration of a used Blue Sepharose CL-6B column involved: (1) washing the column with 1 liter of 0.1 M Tris/HCl buffer containing 0.5 M NaCl, adjusted to pH = 8.5, (2) washing the column with 1 liter of 0.1 M sodium acetate buffer containing 0.5 M NaCl, adjusted to pH of 4.5, and (3) reequilibrating the column with 1 liter of 2 mM Tris/HCl (pH = 8).

The enzyme extract from three runs of Blue Sepharose CL-6B appeared clear and amounted to 80 ml., 50 ml., and 70 ml., or a total of 200 ml. The mean of the concentrations determined by both Lowry and Bio-Rad protein assays was 0.075 ± 0.010 mg./ml., 0.170 ± 0.060 mg./ml., and 0.049 ± 0.003 mg./ml., respectively.

The three OPRTase extracts were dialyzed twice against 16 liters of 2 mM Tris/HCl (pH = 8) for 5 hours. The enzyme binds OMP very tightly as suggested by intense absorbance at 268 nm. To remove OMP, the OPRTase extract was subjected to flow dialysis. In a chamber

encased by two plates was inserted a sheet of dialysis tubing material. On one side of the dialysis tubing material was placed 1 ml. of OPRTase to which OMP was bound. On the other side of the dialysis sheet 250 ml. of 10 mM Tris/HCl (pH = 8) was allowed to flow for 5 hours. Then, 250 ml. of 10 mM Tris/HCl (pH = 8), 1 mM sodium pyrophosphate, 1 mM $MgCl_2 \cdot 6H_2O$ was allowed to flow from the reservoir through the chamber over a period of 6 hours. The final dialysis buffer employed was 250 ml. of 10 mM Tris/HCl (pH = 8). Afterward, the enzyme was removed (using a syringe with a flexible rubber tubing) and its activity was monitored. The enzyme without OMP is not stable and subject to denaturation. However, the absorbance at 268 nm. attributed to the presence of OMP was no longer observed.

Nondenaturing Gel Electrophoresis

Electrophoresis Apparatus

The apparatus consists of two reservoirs connected electrically by glass tubes containing the gels. The gel system is prepared in a vertical column. It consists of the stacking gel and the separating gel. The stacking gel is less concentrated (larger pore size) then the separating gel and is prepared in a buffer of lower ionic strength and different pH. The larger pore size in the stacking gel results from low crosslinking and permits the stacking gel to effectively concentrate the components of the protein sample into a sharp starting zone. A low ionic strength results in higher electrical resistance so that the electric field is higher in the stacking gel and hence makes the molecules move faster than in the separating gel.

On polyacrylamide gel, the amount of molecular sieving is controlled by the concentration of gel and the adsorption of proteins is negligeable. The migration of proteins in the stacking gel is based on net charge. The migration of proteins in the separating gel is based on net charge, size, and shape.

Theory

Electrophoresis is the transport of particles through a solvent by an electric field. The force experienced by the particle is given by $F = q\,E$, where q is the charge and E is the electric field. The velocity of the particle is countered by a viscous drag, $f\,v$, where f is the frictional coefficient and v is the velocity: $q\,E = f\,v$. The mobility is defined as the velocity per unit field:

$$\text{Mobility} = u = \frac{v}{E} = \frac{q}{f} \qquad (8)$$

If a protein has zero charge, its mobility will be zero. The mobility depends on the net charge, the size, and the shape of the particle. f is a function of the size and the shape of a macromolecule. The migration of the macromolecule is hindered by the gel matrix, a factor dependent on the size of the macromolecule. The mobility also depends upon the local field which the particle experiences, E. A protein is not an isolated particle. It is surrounded by an environment of small ions. There is an ion atmosphere predominantly of opposite charge which influences the motion of the particle (57).

Movement of Ionic Species in Stacking Gel

In the electrode buffer, glycine exists as both a zwitterion with a net charge of zero and a glycinate anion with a negative charge:

$$^{+}NH_3CH_2COO^{-} = NH_2CH_2COO^{-} + H^{+} \qquad (9)$$

In the presence of an electric field, chloride, protein, bromophenol blue, and glycinate anions all migrate toward the anode.

The low pH of the sample buffer and of the stacking gel shifts the equilibrium between glycinate anion and zwitterion toward formation of immobile zwitterions. The glycine zwitterions do not move into the sample and stacking gels which creates a deficiency of mobile ions. The deficiency of mobile ions diminishes the current flow. In any electrophoretic system, the current must be uniform, and the electrical neutrality must be maintained; hence, the number of charges crossing any given cross-section must be the same in both directions. To maintain the current constant in the region between the chloride ions and the trailing glycinate ions, the voltage decreases. The larger the field

strength, the faster the rate of migration. The deficiency of mobile ions increases the field strength in the region between the chloride ions and the glycinate ions. The relative mobilities of the ions in the stacking gel are from lowest to highest:

GLYCINATE < PROTEIN < BROMOPHENOL BLUE < CHLORIDE

In the stacking gel, the migration of the proteins is rapid not only because of the large field strength, but also because the large pores do not impede their movement. If any of the proteins overtake the leading chloride ions, they slow down because there is no ion deficiency in the region occupied by the chloride ions and hence the field strength diminishes. The rapid movement of proteins behind the chloride front result in a piling up of protein sample in a tight disc between the glycinate and chloride ions. The small pores of the separating gel slow down the migration of the protein disc and permit the glycinate ions to catch up with the proteins. The protein sample enters the running gel as a narrow zone (58).

Movement of Ionic Species in Separating Gel

The average net charge and hence the effective mobility of a solution of glycine varies with pH. Crossing the interface between the stacking gel (pH = 6.9) and the running gel (pH = 8.9), glycinate ions become fully charged. There is no longer an ion deficiency. From this point on, there is a constant field strength.

Tris exists as both an uncharged base: Tris°, and as a positively charged acid: $Tris^{+}$. In the stacking gel the concentration of Tris base is low because the pH is 6.9. In the separating gel, the concentration

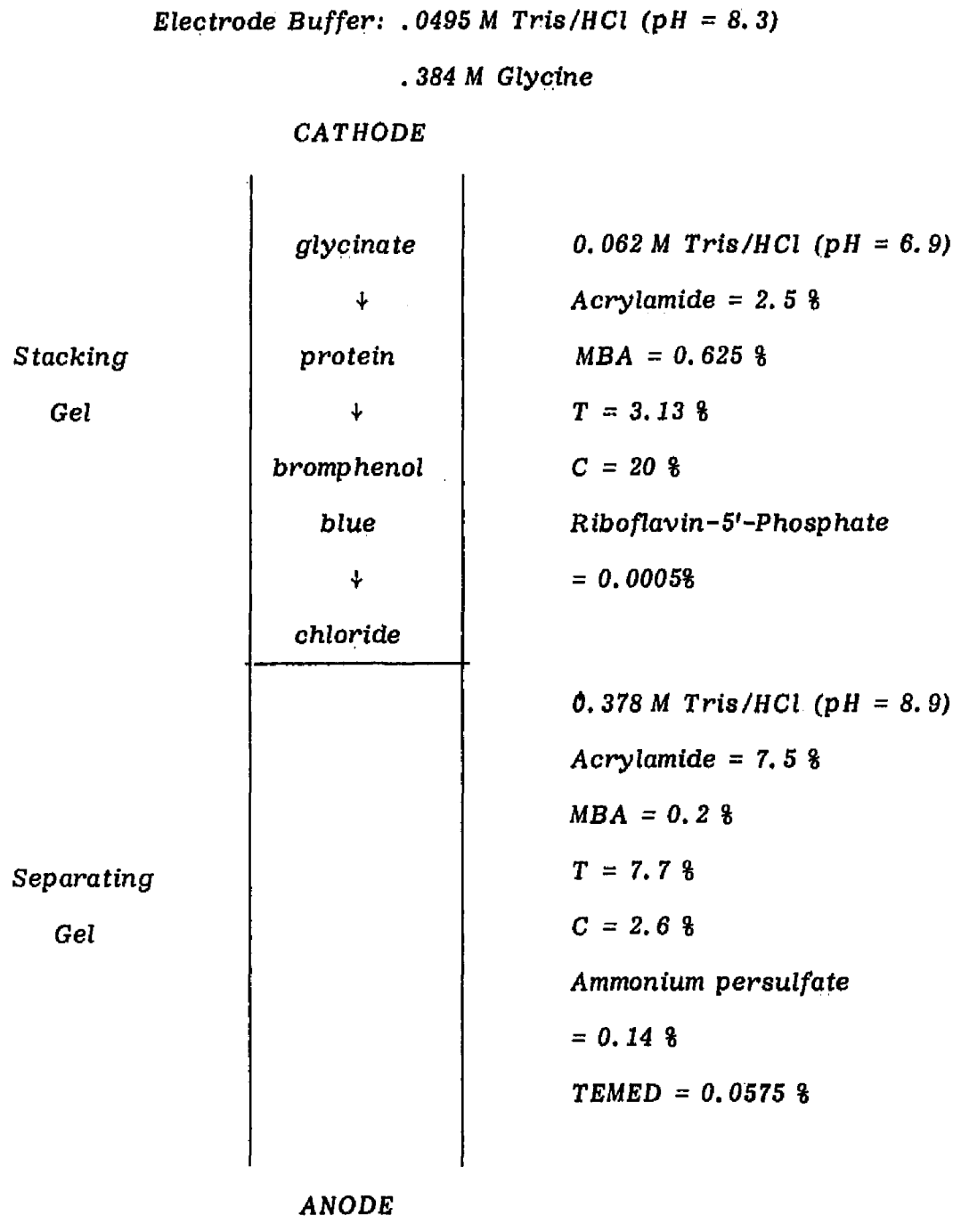

Figure 1. Components of Nondenaturating Gel Electrophoresis. (Tris = 2-Amino-2-(hydroxylmethyl)-1,3-propanediol, MBA = N,N-Methylene bisacrylamide, TEMED = N,N,N',N'-Tetramethylethylenediamine, T = total gel concentration, and C = per cent crosslinker)

of Tris base is high because the pH is 8.9.

As the glycine front crosses the interface, the number of negative ions migrating toward the anode (positive electrode) increases. But the number of negative ions crossing any given cross-section toward the anode must equal the number of positive ions per unit cross-sectional area migrating toward the cathode. Since most of the Tris is uncharged, then the increase in cations must be fulfilled by H^+. There must be an increase in H^+ migrating toward the cathode which leads to a reduction in H^+, i.e., a rise in pH from 8.8 to 9.5. 9.5 is called the running pH. The average charge of the glycinate will increase; hence, the effective mobility of glycine in the lower gel becomes higher than the effective mobility of the proteins but not of the chloride ions. The glycine front passes through the protein zone; hence, the proteins will now be electrophoresing in the glycine solution at the running pH (Figure 1).

Preparation of Stock Solutions

Polyacrylamide gels are generated by the free radical polymerization of acrylamide monomer ($CH_2 = CH - CO - NH_2$) and the crosslinking monomer N,N'-methylene-bisacrylamide ($CH_2=CH-CO-NH-CH_2-NH-CO-CH=CH_2$). Increasing the concentration of polyacrylamide decreases the size of the pores in the pore gradient gel.

The polymerization reaction is initiated by a catalyst redox system which furnishes free radicals. The most commonly used catalyst-initiator system uses the tertiary amine, TEMED (N,N,N',N'-tetramethylethylenediamine), as catalyst and an initiator, ammonium persulfate, which generates oxygen free radicals. Another free radical source is provided

by the photoreduction of riboflavin in the presence of oxygen. The photoreduction of riboflavin, with the subsequent reoxidation of leucoflavin and production of free radicals, is initiated by visible or ultraviolet light. Riboflavin-5'-phosphate is the preferred substitute for riboflavin due to its superior solubility. So, riboflavin-5'-phosphate may serve as catalyst.

TEMED serves the role of accelerator of gelation of the separating gel solution. Potassium ferricyanide is added to the separating gel solution to control the gel time so that the user may prepare a large number of separation gels simultaneously (59).

In water, ammonium persulfate forms free radicals which form free radicals with acrylamide:

$$S_2O_8^{2-} \rightarrow 2\ SO_4^{-\bullet} \qquad (10)$$

Preparation of Concentrated Lower Buffer (A)

96 ml. of 1 N HCl, 73.2 gms. of Trizma Base, and 0.92 ml. of TEMED were dissolved in a final volume of 200 ml. of deionized water. The resulting pH is 8.9. The clear solution is stored at 4°C and brought to room temperature before use.

Preparation of Stacking Buffer (B)

98 ml. of 1 N HCl and 11.96 gms. of Trizma Base are dissolved in a final volume of 200 ml. with deionized water. The resulting pH is 6.7. The clear solution is stored at 4°C and brought to room temperature before use.

Preparation of Crosslinking Reagent for Separating Gel (C)

60 gms. of acrylamide, 1.6 gms. of bisacrylamide, and 30 mgs. of

ferricyanide are dissolved in a final volume of 200 ml. with deionized water. The mixture is filtered with Whatman #1 filter paper to yield a solution and stored in a brown bottle at 4° C. The solution is brought to room temperature before use.

Preparation of Crosslinking Reagent for Stacking Gel (D)

20.0 gms. of acrylamide and 5.0 gms. of bisacrylamide are dissolved in a final volume of 200 ml. with deionized water. The solution is stored in a brown bottle at 4° C and brought to room temperature before use.

Preparation of Riboflavin-5'-Phosphate Solution (E)

8 mg. of riboflavin-5'-phosphate is dissolved in a final volume of 200 ml. with deionized water. The solution is stored in a brown bottle at 4° C and brought to room termperature before use.

Preparation of Ammonium Persulfate Solution (F)

0.28 gms. of ammonium persulfate is dissolved in a final volume of 100 ml. of deionized water. The solution is prepared fresh daily and the day's leftover solution is discarded.

Preparation of Electrode Buffer

12 gms. of Trizma Base and 57.6 gms. of glycine are dissolved in a final volume of 2000 ml. with deionized water. The resulting pH is 8.3 and is not adjusted!

Preparation of Gels from Working Solutions

Gels are made in glass tubes 6 inches in length and 6 mm. in diameter. The glass tubes are inserted into rubber caps and placed vertically into a loading rack. PVC gloves are worn during preparation of the gels in order to avoid getting acrylamide, methylene bis-acrylamide, TEMED, or ammonium persulfate on external or internal

body surfaces. Prior to use the glass tubes were washed by soaking in chromic acid cleaning solution overnight, rinsed with distilled water, soaked about a minute in 10% KOH in 95% ethanol (w/v), and rinsed thoroughly again with distilled water. Dirty rubber caps were washed by suspending them in distilled water with potassium hydroxide pellets (5 g. per 100 ml.). After the solution cooled to room temperature, the rubber caps were rinsed in distilled water, 0.1 N HCl and twice more in distilled water.

Preparation of Separating Gel Layer

The stock solutions were removed from the refrigerator and permitted to warm to room temperature before use. 24 ml. of separating gel solution was prepared by mixing 3 ml. of solution A, 6 ml. of solution C, 3 ml. of distilled water, and 12 ml. of solution F. Solution F was added last because ammonium persulfate initiates polymerization within 20-30 minutes. The mixture was well shaken.

The glass tubes were marked with a water soluble marking pen at 3-3/4 inches and at 4 inches from one end of the tube so as to have reproducible and identical lengths of separating gel layer. The separating gel solution was pipetted into the tubes until the 3-3/4 inch mark. The tubes were tapped to insure that no air bubbles had been trapped.

The separating gel solution in each glass tube was overlaid very carefully with 1/4 inch tube length of distilled water by means of a hypodermic syringe with a 23 gauge needle, 2 inches in length. A flat surface results in flat even bands. A sharp refractile boundary which appeared initially at the interface blurred because of diffusion.

The tubes were left undisturbed for 30-40 minutes at room tempera-

ture. During this time a second refractile boundary line appeared parallel to the first but several millimeters below it (the gel was observed to shrink). After 40 minutes, the water and unreacted monomer were removed by inverting and gently shaking the tubes and then draining the excess water with adsorbent Kimax tissue.

Preparation of Stacking Gel Layer

In a 25 ml. graduated cylinder were mixed 2 ml. of solution A, 4 ml. of solution D, 2 ml. of solution E, and 8 ml. of deionized water. 16 ml. of stacking gel solution were used to prepare 24 gels.

The gel tubes were wiped clean of the previous pen marks and then marked at 3/4 inch and at 1 inch above the second refractile line. The unfilled portions of the tubes were rinsed once gently with the stacking gel solution. With a Pasteur pipette, stacking gel solution was dispensed until the 3/4 inch mark on top of the polymerized separating gel layer. Thereafter, deionized water was layered on the stacking gel layer with a syringe bearing a 23 gauge needle 2 inches in length.

The stacking gel solution polymerized upon exposure to light from Cool White fluorescent lamps. A fluorescent lamp was placed behind the gel tubes at about the same level as that of the stacking gel layer, parallel to the line of the tubes in the loading rack and about 3 inches away. The stacking gel solution became opalescent, indicating gel formation. The upper gels photopolymerized within 30 minutes to 2 hours. The opalescent layer measured 3/8 inch to 1/2 inch. The upper gels were not left exposed to the lamp for excessive periods because heat from it would produce air bubbles in the gels as well as convection in incompletely polymerized regions.

The gels were used within 3 hours or stored in the refrigerator

at 4°C because diffusion between the solvents in the upper and lower gels destroys the pH discontinuity desired for efficient stacking.

Preparation of Standards

The hemoglobin standard was prepared by mixing 3 µl. of tracking dye (0.045% bromophenol blue), 1 mg. of hemoglobin, and 1 ml. of 20% sucrose. 20% sucrose was prepared by dissolving 20 gms. of sucrose in distilled water and diluting to 100 ml.

The ferritin standard was prepared by mixing 3 µl. of tracking dye (0.045% bromophenol blue), 1 mg. of ferritin, and 1 ml. of 20% sucrose.

The ferritin/hemoglobin standard was prepared by mixing 1 mg. of ferritin, 1 mg. of hemoglobin, 3 µl. of 0.045% bromophenol blue, and as much 20% sucrose to make the final volume of 1 ml.

The sample volume of each standard applied to the stacking gel for disc gel electrophoresis was 0.100 ml.

Electrophoresis Experiment

The water layer of each gel tube was decanted. The outsides of the gel tubes were dried. The bottoms of the gel tubes were pushed through the rubber grommets of the Polyanalyst Buchler Instrument Electrophoresis Apparatus, which provided a leakproof fit.

In a small borosilicate test tube were placed 2 drops of glycerol, 3 µl. of tracking dye, and 100 µl. of protein extract. The presence of large amounts of salt in the protein extract delayed stacking; hence, the protein was dialyzed against a low buffer concentration before electrophoresis was undertaken.

550 ml. of electrode buffer was placed in the lower chamber. All the gel tubes suspended by grommets in the central component of the

electrophoresis apparatus were then inserted into the lower buffer chamber. Air bubbles were removed from the bottoms of the gel tubes.

Each protein mixture was slowly vortexed. Precautions were taken to avoid bubble formation because this leads to protein denaturation (which is undesirable since the native protein and the denatured protein may form separate bands). The protein mixture was carefully pipetted on top of the stacking gel layer of one of the gel tubes.

The electrode buffer was carefully pipetted onto this protein layer without disturbing the integrity of the protein layer. The buffer was then poured into the upper reservoir via a funnel. The level of the buffer in the upper reservoir was well above the tops of the gel tubes; otherwise, no electrophoretic movement of ions occurred for the gel tubes which were not submerged.

The lid was placed on top of the upper bath. The power unit was switched on and two minutes were allowed for warming up. The power supply was connected to the apparatus (red outlet to electrode with red dot and black outlet to alternative electrode). The current control knob was adjusted to bring the current to 3 mA per gel. The electrophoresis was continued until the tracking dye had migrated to within 2-5 mm. of the bottom of the gel tube. The dye was not allowed to run off the gel. The approximate time for the electrophoresis was 5 hours. If the level of the lower bath had risen with time during the electrophoresis, then the grommets did not provide a leakproof fit and the power was turned off momentarily to check the fitting around each gel tube for leaks.

Selection of Mode of Power Supply

Buffer systems, which are discontinuous, result in increased cell

resistance because an ionic species with a low mobility (protein) is substituted for one with a high mobility (glycine). Techniques which involve increasing cell resistance are regulated either by constant voltage or constant power.

In the constant voltage mode, an increase in resistance must be accompanied by a decrease in current to maintain the voltage at a constant value. This involves a decrease in the total applied power while maintaining the applied voltage. Constant current operation in cases of increased cell resistance results in increasing voltage and hence potentially damaging heat production.

Constant power operation avoids the problems associated with either constant voltage or constant current. By operating at a constant power output, the power supply adjusts either the voltage or the current to maintain constant heat production in the gel, producing the maximum separation and resolution while avoiding the damaging effects of overheating. This mode of operation allows the run to be completed in the minimum amount of time.

All electrophoreses in this discussion were performed using constant voltage as the mode of power supply!

Termination of Electrophoresis Experiment

The gels were removed from the glass tubes by rimming. A hypodermic needle was inserted between the gel and the glass tube at the bottom of the gel tube. Keeping the needle flat against the glass surface to avoid scratching the gel, it was rotated completely around the circumference of the gel. While rotating, ice cold water was squeezed between the gel and the glass tube to lubricate movement of gel and to make the gel contract somewhat. The gel slipped out

about 1/4 inch. The gel was then squeezed out further by applying air pressure through the top of the gel tube using a rubber bulb.

The electrode buffer was retrieved for future use. It was stored in a brown bottle at 4°C.

The gels were cut with a razor at the center of the tracking dye band. If the standard gels were left in 7% acetic acid instead of being stained (the hemoglobin and/or ferritin are clearly visible and do not require staining to be visualized), the tracking dye band diffused and disappeared.

Staining of Gels from Nondenaturing Gel Electrophoresis

A solution of 0.04% coomassie brilliant blue R-250 in 7% acetic acid was prepared by dissolving 0.4 gms. of coomassie blue powder in a final volume of 1 liter of 7% acetic acid. The acetic acid precipitated the protein within the polyacrylamide gel matrix to prevent it from diffusing. 4 liters of 7% acetic acid were prepared by dissolving 280 ml. of glatial acetic acid in a final volume of 4 liters with distilled water.

Each gel was placed in a test tube filled with 0.04% coomassie blue in 7% acetic acid. The recommended time for staining was 12 hours.

Destaining of Gels from Nondenaturing Gel Electrophoresis

The gels stained with 0.04% coomassie brilliant blue R-250 were destained in 7% acetic acid. The destaining time for diffusion destaining in 7% acetic acid was 3 days without the use of any mechanical shaker. Diffusion destaining was enhanced by raising the temperature to 37°C, by agitation on a mechanical shaker, and by adding a knot of white yarn in the destaining solution, which absorbs the dye.

SDS Acrylamide Gel Electrophoresis

Electrophoresis in polyacrylamide gels in the presence of the anionic detergent sodium dodecyl sulfate (SDS) is useful to determine the state of protein purity of a particular preparation and to measure the molecular weights of individual polypeptide chains. The electrophoretic mobility of protein is determined in the presence of SDS and 2-mercaptoethanol. 2-Mercaptoethanol breaks disulfide linkages and keeps the sulfhydryl groups reduced. SDS binds to hydrophobic regions of proteins and denatures them into randomly coiled polypeptides. Multichain proteins, under these circumstances, will unfold and separate into individual chains. The individual chains will separate on the gel if they are different in size.

Hydrodynamic studies (60) suggest that SDS-protein complexes are rodlike particles. The diameters of these micelles appear to be roughly constant and the lengths are proportional to the length of the polypeptide chains, and hence to the molecular weights (MW). So proteins treated in this way behave as though they have uniform shape and an identical charge to mass ratio. Therefore, separation by SDS acrylamide gel electrophoresis depends only on MW.

The net charge of the protein is determined by SDS rather than by the intrinsic charge of the amino acid residues. At a pH of 9, most proteins are negatively charged. The negative charge would impede SDS binding. SDS binding imparts a large negative charge to the denatured, randomly coiled polypeptides. This charge largely masks any charge normally present in the absence of SDS. In aqueous solution, SDS can exist as monomers or as micellar aggregates, the concentration of each depends upon the total SDS concentration, the

ionic strength, and the temperature.

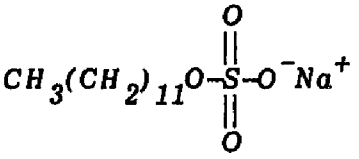

Fig. 2. Structure of Sodium Dodecyl Sulfate.

Only the free SDS monomer binds to proteins, not the micellar structure (61). When the SDS monomer concentration is 5-8 X 10^{-4} M, one protein-SDS complex forms with 0.4 g. of SDS per gram of protein. When the SDS monomer concentration is greater than 8 X 10^{-4} M, another protein-SDS complex forms of 1.4 g. of SDS per gram of protein. Both complexes are rodlike particles.

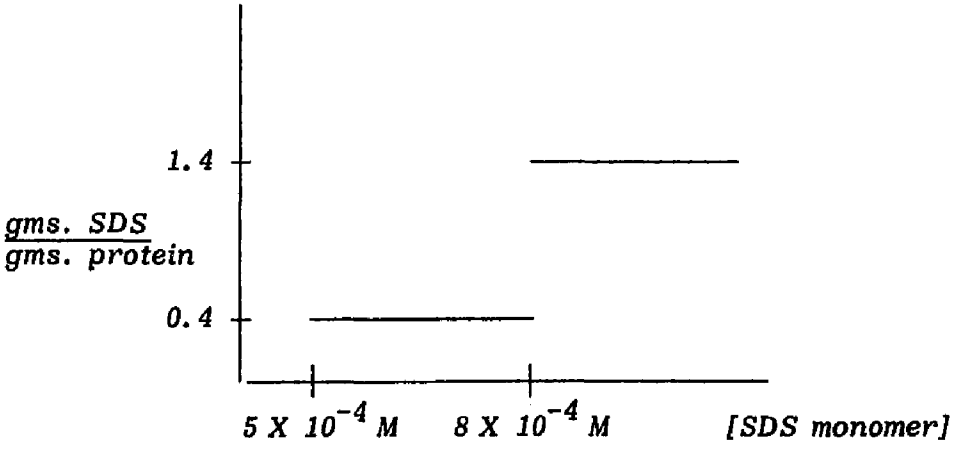

Fig. 3. Binding of SDS to Proteins.

The components of the SDS acrylamide gel electrophoresis system differs from those of the nondenaturing gel electrophoresis system.

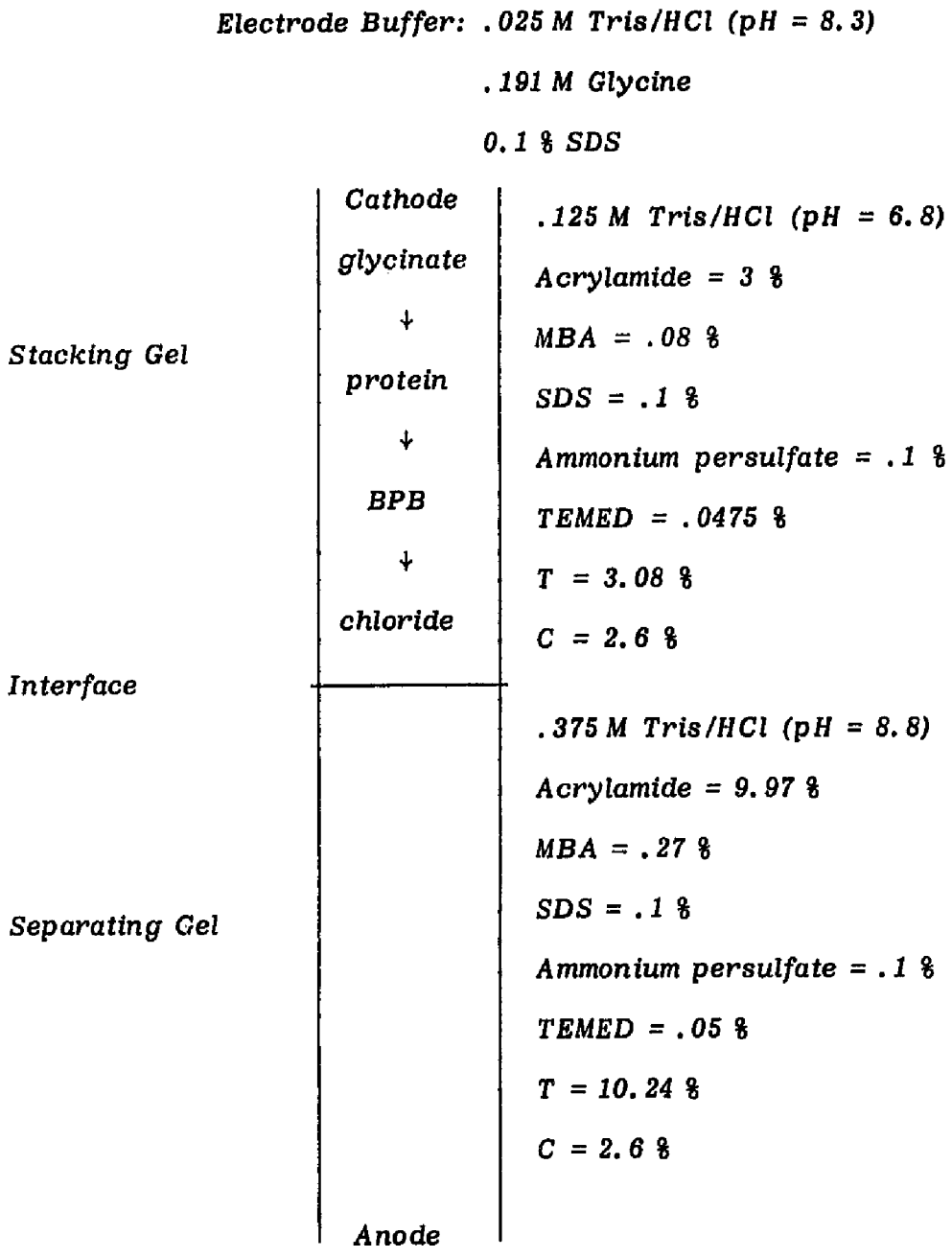

Fig. 4. Components of SDS Acrylamide Gel Electrophoresis System. (BPB = bromophenol blue)

The electrophoresis buffer, the stacking gel, and the separating gel for the SDS gel system contain SDS. The total gel concentration for the separating gel is 10.2% instead of 7.7%. The greater degree of crosslinking leads to a smaller pore size in the separating gel and impedes the migration of the macromolecules more strongly. In the stacking gel where crosslinking is low, the proteins form a narrow starting zone but do not separate on the basis of charge or shape because all proteins have equal charge density and the same shape. In the separating gel where molecular sieving effects predominate, the proteins separate on the basis only of size (Figure 4).

Choice of Buffer for Enzyme Sample Subject to Crosslinking

The buffer serves to maintain a constant pH, to stabilize activity, and to permit crosslinking to occur. The ionic strength and the concentration of the buffer affect loading. The presence of large amounts of salts in the sample to be applied delays stacking for periods proportional to the amount present. If the electrolyte concentration is too high, the amount of current conducted increases while the voltage decreases. This results in a decreased rate of macromolecular migration and in the generation of heat. Convection currents induced by heat may cause loss of sample into the electrode buffer. If the electrolyte concentration is too low, the macromolecules conduct a large portion of the current; hence, they do not form sharp bands but rather spread into diffuse zones.

Crosslinking with di-imidoesters were carried out at pH values above 8 so that a significant proportion of the amino groups would be unprotonated. Protonated amino groups react with imidoesters. Buffers suitable for crosslinking are triethanolamine/HCl or N-ethylmorpholine

acetate for pH of 8-8.5, and sodium borate for pH of 8.5-9. Relatively concentrated buffers (0.2-0.25 M) were used to avoid pH changes on addition of the imidoester hydrochloride and during the course of the reaction. Imidoesters are hydrolyzed very rapidly as the pH is decreased below 7.5. The imidoester solution was prepared fresh each time and used within half a minute of dissolution. The pH of the cross-linking reaction mixture was maintained above neutrality either by dissolving the imidoester hydrochloride in a relatively high concentration of buffer or by adjusting the pH immediately to above 8 with NaOH (62).

The enzyme of interest was contained in 50 mM triethanolamine (pH = 8.5) either by ultrafiltration or by dialysis. In ultrafiltration, 3 ml. of enzyme extract were placed in the Amicon chamber of 10 ml. volume. 50 mM Triethanolamine (pH = 8.5) was added until the 10 ml. mark was reached. The contents were concentrated to a volume of 3 ml. This procedure was repeated twice. In dialysis, the 3 ml. of enzyme extract were placed in a dialysis bag, which was then placed in a reservoir of 50 mM triethanolamine (pH = 8.5) for 5 hours.

Pretreatment of Proteins Before SDS Electrophoresis

Different ligands were incubated with the enzyme for 30 minutes at 4°C in an ice bucket before the crosslinking treatment to assess the effect on crosslinking.

In this paper two types of crosslinking treatment were considered: glutaraldehyde (GTA) treatment or amidination by dimethyl suberimidate (DMS). The protein concentration was at least 0.07 mg./ml. The volume of protein extract used was 0.100 ml. so that the amount of protein was

at least 0.007 mg. The choice of buffer for the protein was 50 mM triethanolamine (pH = 8.5).

The glutaraldehyde was prepared fresh before use. It was used within a minute of dissolution. 2% GTA solution was prepared by dissolving 2 ml. of glutaraldehyde in a final volume of 100 ml. of 0.2 M triethanolamine (TEA) (pH = 8.5). The pH was checked and adjusted to 8.5 with NaOH. 5 µl. of 2% GTA was added per 0.2 ml. of protein extract.

The dimethyl suberimidate was prepared fresh before use and used within one minute of dissolution. 5 mg./ml. of DMS was prepared by dissolving 0.5 g. of DMS in a final volume of 100 ml. of 0.2 M TEA (pH = 8.5). The pH was checked and adjusted to 8.5 if necessary with NaOH. 15 µl. of 5 mg./ml. DMS per 0.1 ml. of protein extract is recommended as starting trial amount of crosslinker. Other concentrations were made up based on results of trial crosslinking.

The final volume of the GTA treated protein would be 102.5 µl. and of the DMS treated protein would be 115 µl. The temperature for the crosslinking reaction was room temperature. The time of incubation for the GTA treated protein was 30 minutes and for the DMS treated protein was 4 hours. For the GTA treated protein the activity was measured at 30 sec. and at 30 minutes after addition of GTA. For the DMS treated protein, the activity was measured 30 sec. and 4 hours after mixing with DMS. The reaction was quenched by freezing in a dry ice acetone bath and the samples were stored at -76°C until denaturation and reduction for SDS electrophoresis. The final concentration of protein for the GTA treated sample was 6.34×10^{-2} mg./ml. and for the DMS treated sample was 5.65×10^{-2} mg./ml.

Denaturation and Reduction Before Electrophoresis

The denaturation buffer was prepared in 100 ml. final volume with distilled water. It was 0.0625 M Tris/HCl (pH = 6.8; 0.927 g. Trizma Base + 0.0464 g. Trizma HCl), 2% SDS [MW = 288.38], 11% glycerol, 0.005% bromophenol blue [MW = 669.98], and 5% 2-mercaptoethanol [MW = 78.1, 1 ml. = 1.1168 g., .005 ml./.105 ml. = 4.76%]. The 0.005 ml. of 2-mercaptoethanol was added to the 0.1 ml. of denaturation buffer immediately before use.

Preparation of Electrophoresis Buffer (pH = 8.3)

The electrophoresis buffer was prepared by combining 6 gms. of Trizma Base [MW = 121.14], 28.8 g. of glycine, 2 g. of SDS, and sufficient deionized water to provide a total volume of 2 liters. It was stored in a brown bottle at 4°C. The pH was not adjusted with HCl or NaOH. The addition of small ions results in artifacts such as diffuse bands and extraneous multiple bands near the top of gel.

Preparation of Crosslinking Reagent (A)

60 g. of acrylamide (30%) and 1.6 g. of bisacrylamide (0.8%) were dissolved in a final volume of 200 ml. with deionized water. The insoluble materials were removed by filtration. The colorless solution was stored in a brown bottle at 4°C. Solutions of acrylamide and bisacrylamide are stable for several months. Unpolymerized acrylamide is a skin irritant and a neurotoxin. Gloves were worn. Pipetting by mouth is hazardous. Before use, the crosslinking reagent was brought to room temperature.

Preparation of Lower Buffer (B)

12.91 g. Trizma Base, 2.37 g. Trizma HCl [.608 M Tris/HCl, pH = 8.8], and 0.32 g. SDS [0.16%] were dissolved in 200 ml. final volume of deionized

water. The solution was stored in a brown bottle at 4°C.

Preparation of Ammonium Persulfate Solution

Ammonium persulfate (10%) was prepared by dissolving 0.5 g. in a final volume of 5 ml. with deionized water. This yielded 0.1% ammonium persulfate in the separating gel. It was stored temporarily in a brown bottle at 4°C. Ammonium persulfate solutions are unstable and were made up just before use.

Preparation of Glass Tubes and Rubber Caps for Separating Gel Layer

Prior to use, the glass tubes were washed clean of polyacrylamide by soaking in chromic acid cleaning solution overnight, rinsing with deionized water, soaking in 10% KOH in 95% ethanol (w/v) for about 1 minute, and rinsing again with deionized water. The glass tubes were then soaked in Kodak Photo-Flo 200 solution to reduce the surface tension of the glass. Chromic acid etches glass and hence raises surface tension. A lower surface tension facilitates removal of the gels from the glass tubes.

Rubber caps were suspended in deionized water with KOH pellets to remove polyacrylamide that sticks. They were then rinsed with deionized water, then with 0.1 N HCl, and then with deionized water. The rubber caps free of shiny polyacrylamide were soaked in Kodak Photo-Flo 200 to prevent the gel once polymerized from adhering too tightly to rubber.

The glass tubes are 6 inches in length and 6 mm. in diameter. They were marked with a water soluble marking pen at 4 inches (10.2 cm.) and at 4-1/4 inches (10.9 cm.). A few drops of separating gel solution (to which no persulfate had yet been added) were added to each rubber cap. The ends of each glass tube were covered. The glass tube was not pushed

all the way into the bottom of the rubber cap. The bottom of the glass tube was inserted to only half the depth of the rubber cap. The gel shrinks when it polymerizes. After sufficient polymerization, the rubber caps were removed; otherwise, the force of the shrinkage of the gels opposes the force of the vacuum created in the rubber cap and leads to the formation of bubbles. Gels broke at areas of bubble formation during rimming. The capped gel tubes were inserted vertically on a loading rack.

Procedure for Preparation of Separating Gel Layer

The stock solutions were removed from the refrigerator and permitted to warm up to room temperature. To 7 ml. of reagent A, 13 ml. of reagent B, 0.84 ml. of deionized water, and 0.01 ml. of TEMED were added. The pH was not adjusted! The solution was deaerated for 15 minutes. The separating gel solution was then kept in an ice bucket for 15-20 minutes. At this point the glass tubes were treated with Kodak Photo-Flo 200.

After equilibration in an ice bucket, a volume of 0.21 ml. of 10% ammonium persulfate was added to the separating gel solution. The solution was well mixed with a small magnetic stirring bar. The total volume was 21.06 ml. from which can be prepared 8 gels. The percentage acrylamide was 10%.

The glass tubes were filled to within 4 inches with separating gel solution to which 10% ammonium persulfate had just been added. The separating gel solution was retained in ice to inhibit polymerization.

The gel solution was added from the bottom of the gel tube, gradually withdrawing the pipette as the gel tube was filled. The tip of the pipette was always kept beneath the surface of the gel solution to prevent

formation of air bubbles in the gel tube. Air pockets were removed by sharply tapping the tube while holding it in a vertical position. The addition of separating gel solution to about 8 glass tubes took only 3 minutes.

The rack with gels was taken into the cold room (4°C) to keep the separating gel layer steady. Water was carefully layered on top of the separating gel layer till the 4-1/4 inch mark using a syringe with a 23 gauge needle that is 2 inches in length. For 8 gels, the layering of water took 5 minutes. Failure to apply water layer soon after application of separating gel layer led to polymerization on the glass at the interface.

The loading rack was removed from the cold room and set on the bench at room temperature. The refractile line between the water layer and the separating gel layer disappeared shortly thereafter. After 6 minutes, while retaining the gel tubes suspended vertically in the loading rack, the rubber caps were removed. If the TEMED and the ammonium persulfate were accurately pipetted, then no separating gel solution fell out of the gel tube. If the separating gel solution from the first gel tube did fall out then the other rubber caps were not removed until the new refractile line appeared succinctly. After rubber cap removal, Kodak Photo-Flo 200 was reinjected from bottom to prevent sticking of gel to bottom of glass tube. The gels were left suspended vertically for 30-40 minutes.

Preparation of Upper Buffer (C)

The upper buffer was 0.147 M Tris/HCl (pH = 6.8) and 0.12% SDS. It was prepared by dissolving 4.36 g. Trizma HCl, 0.209 g. Trizma Base, and 0.24 gms. SDS in a final volume of 200 ml. deionized water. It was

stored at 4°C and brought to room temperature before use.

Preparation of Glass Tubes for Stacking Gel Layer

The previous pen marks were removed from the glass tubes. The water and unreacted monomer were removed by inverting the tubes, shaking, and draining with Kimax adsorbent tissue. The glass tubes were then marked at 3/4 inch (1.8 cm.) and at 1 inch (2.5 cm.) above the new refractile line. They were replaced vertically on the loading rack.

Preparation of Stacking Gel Layer

To 2 ml. of reagent A were added 17 ml. of reagent C, 0.8 ml. of deionized water, and 0.01 ml. of TEMED. The solution was deaerated for 15 minutes and then placed in an ice bucket for 15-20 minutes. The glass tubes were now prepared for the stacking gel layer. 0.2 ml. of 10% ammonium persulfate was added to the stacking gel solution. The total volume was 20.01 ml. The percentage acrylamide was 3.0%. This yielded 0.1% ammonium persulfate in the stacking gel. The stacking gel solution was retained in the ice bucket during the layering of the stacking gel to inhibit polymerization in the container. The stacking gel solution was dispensed into the glass tubes to the 3/4 inch mark. Deionized water was carefully layered with a syringe to the 1 inch mark. The gels were set aside at room temperature for 30-40 minutes. The marks were then removed from the gel tubes. The gels were either stored at room temperature for 24 hours or used immediately. SDS is insoluble below 10°C; hence, storage at 4°C would render the gels unusable.

Preparation of SDS Molecular Weight Markers

Reconstitution of Proteins

The sample buffer for dissolving the SDS molecular weight markers

was 100 mM Tris/HCl (pH = 7, 1.432 gms. Trizma HCl + 0.114 gms. Trizma Base/100 ml.) and 1% SDS.

2 mg. of bovine pancreas trypsinogen [MW = 24,000] was dissolved in 1 ml. of sample buffer and 1 mg. of egg white lysozyme [MW = 14,300], ovalbumin [MW = 45,000], bovine serum albumin [MW = 66,000], and porcine stomach mucosa pepsin [MW = 34,700] were each dissolved in 1 ml. of sample buffer. Each aliquot of protein marker was stored at -20°C.

Denaturation and Reduction Before Electrophoresis of SDS Molecular Weight Protein Markers

0.18 ml. of denaturation buffer and 0.005 ml. of 2-mercaptoethanol were dispensed into each of 4 test tubes. 0.010 ml. of each reconstituted protein marker was dispensed into a test tube sitting in a boiling water bath. The incubation in the boiling water bath was permitted to continue for 2 minutes.

Procedure for Performing SDS Electrophoresis Experiment

Application of Sample to Gels

Water from the glass tubes was removed by inverting, shaking, and draining with adsorbent Kimax tissue. Cold water was perimitted to flow through the outer jacket of the lower reservoir. 550 ml. of electrode buffer was poured into the lower reservoir. The glass tubes were inserted into grommets. The samples and standards were layered on the tops of the gels. Electrode buffer was pipetted on the tops of the sample layers. Electrode buffer was poured into the upper reservoir to a level above the tops of the glass tubes. The power was turned on to warm up the power supply. The current employed was 3 mA per gel. The lid was then placed on top of the upper bath. The

electrodes were connected to the power supply. The voltage was adjusted to attain the calculated current.

Selection of Mode of Power Supply

In all SDS gel electrophoresis experiments performed in this investigation, the mode of power supply was chosen to be at constant voltage to avoid overheating at room temperature.

Termination of SDS Gel Electrophoresis

The electrophoresis was continued until the tracking dye had migrated to within 2-5 mm. of the bottom of the glass tube. The dye was not permitted to run off any of the gels. The gels were removed from the glass tubes by rimming. A hypodermic needle was inserted between the gel and the glass tube at the bottom of the gel tube. Keeping the needle flat against the glass surface to avoid scratching the gel, the needle was rotated completely around the circumference of the gel. During the rotation, Kodak Photo-Flo 200 was squeezed between the gel and the glass tube. Kodak Photo-Flo 200 works best at room temperature. The gels were squeezed out of the glass tubes by applying pressure with either a rubber bulb or an air vent through the top of the tube. The gels dart out. The gels were cut at the center of the tracking dye band.

Staining of SDS Gels for Protein

Preparation of 0.25% Coomassie Blue in 45.5% Methanol and 9.2% Acetic Acid

1.25 gms. of coomassie blue R was dissolved in a solution of 227 ml. deionized water, 227 ml. methanol, and 46 ml. glatial acetic acid. When the dye dissolved, the solution was filtered through Whatman #1 filter paper. Failure to filter the staining solution resulted in the sticking of insoluble coomassie blue particles to the ends of the polyacrylamide

gel: this gave rise to the appearance of artifactual bands at the bottom or at the top of the gels.

Procedure for Staining

The gels were placed in test tubes filled with staining solution and left as such for 1-2 hours. The gels were then rinsed with distilled water and destained. The function of the acetic acid is to denature the proteins and precipitate them within the gel matrix so they will adsorb the stain. SDS prevents this by keeping the proteins soluble inside the gel. SDS was removed by soaking the gels in staining solution which contains methanol. The gels shrink but return to their original size on destaining in 7.5% acetic acid with 5% methanol.

Destaining of Gels

Diffusion Destaining of SDS Gels

The gels were removed from the staining solution and rinsed several times with water. The gels were transferred to plastic test tubes containing many holes. Holes were made by heating a metal file until red hot and then forcing it through the plastic tubes at many different points. The gels in perforated tubes were placed in a 1 liter Ehrlenmeyer flask containing 1 liter of destaining solution and 2 gms of AG 501-X8 (ion exchange resin). With magnetic stirring, the gels were destained in 48 hours.

The gels were removed from the tubes after destaining and rinsed with distilled water. The gels were stored in 7% acetic acid in the dark. Direct sunlight or other strong light sources cause stained bands to fade.

Destaining Solution

The destaining solution was prepared by dissolving 50 ml. of

methanol, 75 ml. of glatial acetic acid, and sufficient deionized water to make a final volume of 1 liter. The destaining solution was discarded after use.

Estimation of Molecular Weight

During the staining process, the gels expand or contract to different degrees; hence, the gels were cut at the center of the tracking dye bands to be able to compare lengths. To determine the relative mobility, R_f, of a protein, the migration distance from the top of the gel to the center of the protein band was divided by the migration distance of the bromophenol blue tracking dye from the top of the gel.

$$R_f = \frac{\text{distance of protein migration}}{\text{distance of tracking dye migration}} \qquad (11)$$

The R_f values were plotted against the known molecular weights on a semi-logarithmic paper. The best straight line was determined by the method of least squares. The molecular weight of the unknown protein was determined either from the graph or from its R_f value using the equation of best fit derived by the method of least squares.

Nuclear Magnetic Resonance Spectroscopy

Nuclear Magnetic Moments

Both protons and neutrons, like electrons, spin and rotate. The spin angular momentum and the orbital angular momentum characterize these motions of the nucleus. The resultant nuclear angular momentum is obtained by combining, in a proper way, the orbital angular momenta and the spins of the nucleons composing the nucleus.

The resulting angular momentum vector is designated $\vec{I}$. *According to a basic principle of quantum mechanics, the maximum experimentally observable component of the angular momentum of a nucleus possessing a spin is a half integral or an integral multiple of* $h/2\pi = \hbar$. *This maximum component is I, the spin quantum number:*

$$I_{max} = I\,\hbar = I\,\frac{h}{2\pi} \qquad (12)$$

The total angular momentum depends on I. The value of I depends on the particular nucleus. The numerical value of the spin number I is related to the mass number and the atomic number. If the mass number A is odd, then the nuclear spin I is half integral. If the mass number A and the charge number Z are both even, then the spin is zero. If the mass number A is even, but the charge number Z is odd, then the spin is integral. Nuclei with I = 0 are spinless. Spinless nuclei have no magnetic resonance spectra.

The magnitude of the total angular momentum is $\hbar\,[I\,(I+1)]^{\frac{1}{2}}$. *The component* m_I *of angular momentum along any selected direction will have values I, (I-1), ..., (-I+1), -I; hence, the nucleus will have 2I + 1 possible spin orientations.* m_I *is the magnetic quantum number.*

The possession of both spin and charge confers on the nucleus a magnetic dipole. A nuclear magnetic moment vector $\vec{\mu}_N$ *characterizes the nuclear magnetic dipole. A spinning charged nucleus produces a magnetic field whose axis is coincident with the axis of spin. The magnetic moment of the spinning nucleus attempts to line up with or against the applied magnetic field because of the action of the magnetic torque. The applied magnetic field* (H_o) *induces the spinning nucleus to rotate in a circle perpendicular to the direction of the applied field. The magnetic moment of the nucleus cannot exactly parallel the applied magnetic field. So the magnetic and spin axis of the nucleus in a given spin state precesses about the direction of the applied field.*

Each nucleus for which I is greater than zero will have a characteristic magnetic moment. The proton has a spin quantum number of 1/2. The magnetic moment vector ($\vec{\mu}_N$) *is parallel to the angular momentum vector* ($\vec{I}$).

$$\vec{\mu}_N = \gamma_N \hbar \vec{I} \qquad (13)$$

γ_N *is called the magnetogyric ratio of the nucleus and is measured in radians* sec^{-1} $gauss^{-1}$.

<u>*Nuclear Energy Levels in a Magnetic Field*</u>

If a magnetic nucleus is placed in a uniform magnetic field, the magnetic dipole or the magnetic moment vector assumes only a discrete set of orientations. Each orientation of the magnetic moment vector corresponds to a different nuclear spin state. In general, there are $2I + 1$ *possible orientations of the nucleus. In the absence of a magnetic field, these states all have the same energy. In the presence of a uniform magnetic field* (H_o) *they correspond to states of different potential energy.*

The splitting of the energy levels of a nucleus by its introduction into a uniform magnetic field is known as nuclear Zeeman splitting. The 2I + 1 equally spaced magnetic energy levels will be separated in energy by $\Delta E = \mu H_0/I$.

For a proton, $I = 1/2$. m_I *may only take the values +1/2 or -1/2. These two values of* m_I *describe states in which the nuclear moment is aligned with or against the field* H_0. *The state in which the nuclear moment is aligned with the field is lower in energy. The orientation in which the nuclear moment is antiparallel to the applied field is higher in energy. The energy difference of the spin states is a function of the strength of the applied magnetic field.*

Magnetic Shielding by Electrons

If any atom or molecule is placed in a magnetic field, the external field induces a circulation of electrons around the nucleus in a plane perpendicular to the external field. These moving electrons in turn produce a secondary magnetic field in the region of the nucleus. If the induced field opposes the external field, the electrons surrounding the nucleus shield the nucleus. If the induced field augments the external field, the electrons deshield the nucleus. Different nuclei flip at different field strengths because they are shielded to different extents depending on their electronic environments. Electronic screening of the nucleus brings the nuclear Zeeman levels closer together; hence, the energy quantum required for a transition is smaller. A shielded nucleus absorbs at a higher magnetic field strength while a deshielded nucleus absorbs at a lower magnetic field strength.

Distribution of Nuclear Spins in a Magnetic Field

Consider a whole assembly of nuclei in thermal equilibrium at tem-

perature T. In the absence of an external magnetic field, an equal number of nuclei are in the upper and lower spin states. Thermal motions tend to equalize the populations in the 2I + 1 energy levels. In the presence of an external magnetic field, the tendency of the nuclei to align with the magnetic field and thus to drop into the lowest energy level opposes these thermal motions. The resultant equilibrium distribution is the compromise predicted by the Boltzman distribution: the lower of the two states will be more populated.

The slight excess population in the lower energy level is responsible for the appearance of a very small macroscopic magnetic moment along $\vec{H}_o$. The sample becomes magnetized. A net absorption of energy is observed during irradiation with an electromagnetic field of suitable frequency (64, 65). If the population of nuclei were populated exactly equally, the number of upward transitions would equal the number of downward transitions and there would be no observable nuclear resonance effect.

Spin Lattice Relaxation Time

Whenever the population of the different spin states deviates from the Boltzman distribution, the system is not in equilibrium. The populations change with time until the Boltzman distribution is attained. The spin lattice relaxation time, T_1, is the time required for the difference between the excess spin population before equilibrium and at equilibrium to be reduced by the factor e. T_1 is a measure of the rate at which the spin system comes into thermal equilibrium with the other degrees of freedom. Except for a static collection of nuclei, spin lattice relaxation through molecular motion always occurs although it may be very slow.

Classical Treatment of Magnetic Resonance Absorption

Consider the classical motion of a magnetic dipole $\vec{\mu}$ *in a magnetic field* $\vec{H}_o$. *The moment* $\vec{\mu}$ *lies at some angle* θ *with respect to the field.*

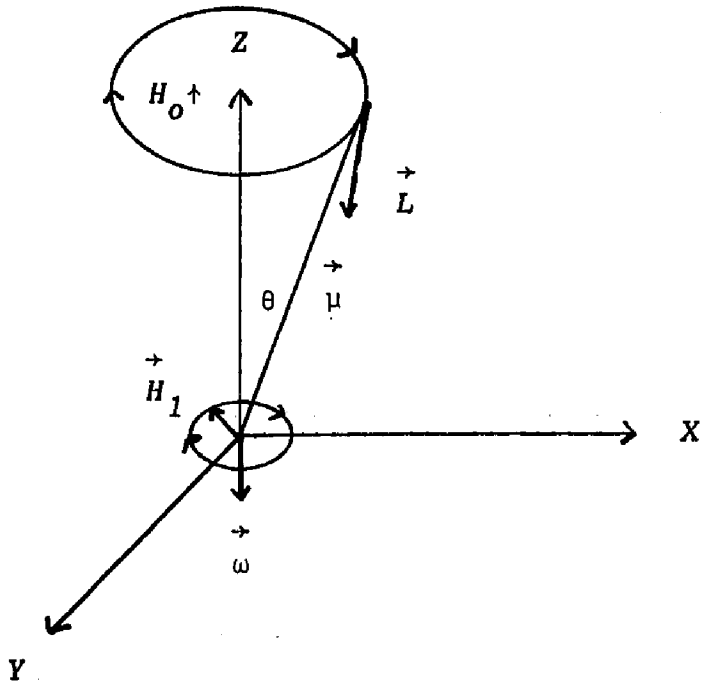

Fig. 5. Precession of Magnetic Moment $\vec{\mu}$ *in a Magnetic Field* $\vec{H}_o$ *Viewed in a Fixed Coordinate System.*

The magnetic interaction between $\vec{H}_o$ *and* $\vec{\mu}$ *generates a torque* $\vec{L}$ *tending to tip the moment* $\vec{\mu}$ *toward* $\vec{H}_o$. *Because the nucleus is spinning, the resultant motion does not change* θ, *but rather causes the magnetic moment to precess around the magnetic field. The torque is a measure of the rotating effectiveness of* $\vec{H}_o$. *The magnetic moment vector* $\vec{\mu}$ *rotates with angular velocity* $\vec{\omega}$. *The angular velocity is the time rate of change of* θ. *The effect of* $\vec{H}_o$ *is exactly equivalent to a rotation with angular velocity* $\vec{\omega}$.

The nuclear moment precesses about $\vec{H}_o$ with the Larmor frequency ν_o. The Larmor frequency is directly proportional to the applied magnetic field and depends on γ which varies from one nucleus to another. The nucleus precesses at a frequency governed by its own properties and that of the magnetic field.

If a small magnetic field $\vec{H}_1$ is placed at right angles to the field $\vec{H}_o$ and is made to rotate about $\vec{H}_o$ at a frequency ν_o, then the nucleus experiences the torque of the resultant of $\vec{H}_o$ and $\vec{H}_1$ and θ changes by $d\theta$. The torque on the nucleus tends to tip the nuclear moment toward the plane perpendicular to $\vec{H}_o$. Energy is thus absorbed from the field $\vec{H}_1$ into the nuclear spin system.

If $\vec{H}_1$ rotates at any frequency ν different from the Larmor frequency ν_o, then it is alternately in and out of phase with $\vec{\mu}$ and no net energy absorption occurs (66).

Quantum Mechanical Treatment of Magnetic Resonance Absorption

Only transitions in which the quantum number m_I is changed by ± 1 can occur so that transitions are permitted only between adjacent energy levels. For nuclei with $I = 1/2$, there is only one transition.

The quantum mechanical treatment predicts absorption only if the frequency ν exactly coincides with the frequency corresponding to the energy gap between the two states between which transition occurs. This corresponds to an infinitely sharp absorption or emission line. In practice, the lines are broadened by spontaneous emission of radiation, spin lattice relaxation, spin spin relaxation, and variations of the static field over the dimensions of the sample.

Visualization of Macroscopic Nuclear Magnetization

Consider the assembly of identical nuclei with magnetogyric ratio γ

and $I = 1/2$. The total moment is defined as the resultant sum per unit volume of all the individual nuclear moments. The total moment is designated $\vec{M}$. In the absence of an applied field H_o, M_z, M_x, and M_y all decay to zero at the same rate with a characteristic time T_1. The orientations of the spins are random in the absence of H_o.

When a population of spins is first thrust into a magnetic field the populations of spins in the upper and lower energy states are equal. Spin lattice relaxation must occur in order to establish an equilibrium spin population and permit a resonance signal to be observed. So T_1 is the time required for the establishment of the thermal equilibrium distribution of the populations of the spin states.

The magnetization and the nuclear magnetic moment may be viewed in either a fixed coordinate system or a rotating coordinate system.

Fixed Coordinate System

Equilibrium Situation

At equilibrium there is a net magnetic moment only in the field direction (Z direction) since the X and Y components of $\vec{\mu}$ average to zero over the spin ensemble. There is a slight excess of nuclear moments oriented with the applied field. M_z is constant. The thermal equilibrium value of M_z is M_o.

Resonance Situation

A short pulse of H_1 at the Larmor frequency flips $\vec{M}$ towards the XY plane. The nuclei flip by absorbing energy from H_1 so that the populations in the two states become more nearly equal. The field H_1 forces the nuclei to precess in phase, thus creating a component M_{xy} in the XY plane. The transverse relaxation time, T_2, is the characteristic time constant of this phasing process (Fig. 6).

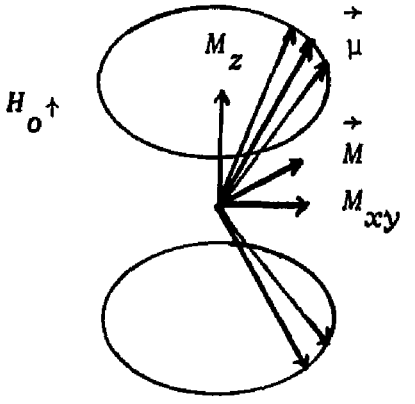

Figure 6. Phase Precession of Nuclei in a Partially Saturated System. Nuclear moments are forced into phase by radiofrequency field with generation of M_{xy}.

Relaxation

After the 90° pulse of H_1, *the nuclei are subject to the applied magnetic field and different magnetic microenvironments. Each nucleus will precess at a different frequency. Variations in the precessional frequencies about the Z axis will lead to the shrinking of* $\vec{M}$ *through the decay of* M_{xy}. T_2, *the transverse relaxation time, is the lifetime for the loss of phase coherence.* M_{xy} *decays exponentially to zero in time* T_2. M_z *decays exponentially to* M_0 *in time* T_1.

Restoration of Equilibrium

T_1 *is not in general equal to* T_2. *The decay time of* M_z *is generally different from the decay time of* M_{xy}. *Changes in* M_{xy} *do not alter the total Zeeman energy of the nuclear spins, whereas changes of* M_z *need an exchange of Zeeman energy with the lattice. Interaction with the lattice causes the magnetic moments of nuclei to flip back to their equilibrium position in the direction of the Z axis.*

Rotating Frame of Reference

Magnetic Moment

Suppose the coordinate system is set up rotating with the Larmor angular frequency $\vec{\omega} = -\gamma \vec{H}_0$. *The applied field exerts a torque on the magnetic moment of the nucleus. However, every time the magnetic moment vector moves by* $\gamma H_0 t$, *so does the coordinate system. To an observer in the rotating frame, the magnetic moment vector appears stationary.*

Suppose another smaller magnetic field of constant magnitude perpendicular to $\vec{H}_0$ *is introduced. If this field* $\vec{H}_1$ *is rotating about the direction of* $\vec{H}_0$ *at the Larmor frequency, then in the rotating system it will behave like a constant field, and the torque, being always in the same direction, will cause large oscillations in the angle between* $\vec{\mu}$ *and* $\vec{H}_0$. *So the direction of* $\vec{\mu}$ *changes.*

Macroscopic Magnetization

If the coordinate system rotates with respect to the laboratory frame with an angular velocity $\vec{\omega}$, *the applied field that an observer in the rotating frame sees exerted on the magnetic moment vanishes. The nuclear magnetization appears fixed and parallel to the +Z direction at equilibrium.*

If an alternating field $\vec{H}_1$ *is applied perpendicular to the static field* $\vec{H}_0$, *as in a typical NMR experiment, it exerts a torque on* $\vec{M}$ *which induces* $\vec{M}$ *to precess about the X axis with angular frequency* γH_1. *The angle* θ *through which* $\vec{M}$ *rotates during time* t_p *is given in radians by* $\theta = \gamma H_1 t_p$. *By proper choice of the duration of the pulse,* t_p, *precessions of M about definite angles* θ *can be obtained.*

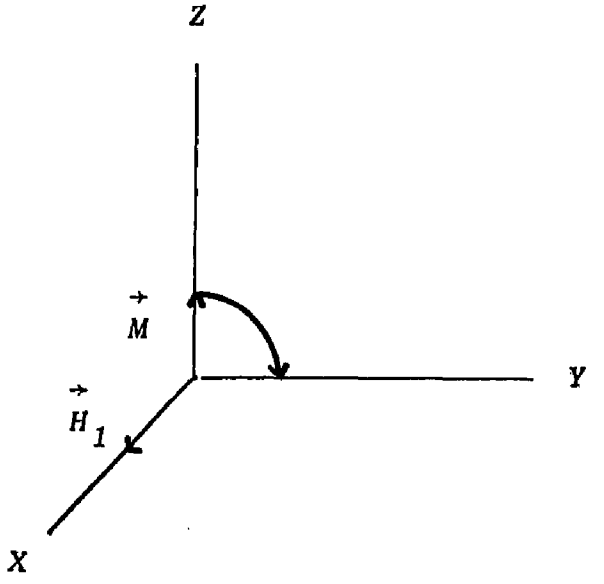

Figure 7. Precession of $\vec{M}$ about $\vec{H}_1$ in the Frame Rotating at the Resonance Frequency $\omega_o = \gamma H_o$. The angle of deflection of $\vec{M}$ is $\theta = \gamma H_1 t_p = 90°$.

The Chemical Shift

The chemical shift is the magnitude of separation of resonance frequencies of nuclei in different structural environments from some arbitrarily chosen standard. The frequency of any given resonance is directly proportional to the applied field strength. Since different models of spectrometers operate at different field strengths, comparison of chemical shift positions measured at different fields is not meaningful. Hence the chemical shift parameter δ is defined by equation 14.

$$\delta = \frac{\nu_{sample} - \nu_{reference}}{\text{Oscillator Frequency in MHz}} \qquad (14)$$

δ is field independent and dimensionless. It is expressed as parts per million (ppm).

Physical Description and Mechanism of T_1 Phenomenon

The establishment of thermal equilibrium between two spin states after application of H_o requires interactions between the nuclei and their surroundings which cause the spin orientations to change, while the excess magnetic energy is transferred to the other degrees of freedom. This process of nonradiative transitions between the two spin states is called the spin lattice relaxation. T_1 is a measure of the time taken for energy to be transferred to other degrees of freedom for the spin system to approach thermal equilibrium. Large T_1 values indicate slow relaxation.

T_1 relaxation occurs by dipolar magnetic interaction of a nucleus with fluctuating magnetic fields caused by various motions of surrounding magnetic dipoles. The surrounding magnetic dipoles are referred to as the lattice. Each nucleus experiences the fluctuating local fields of its neighbors. Those components of the fluctuating local fields in the direction opposite H_1 and at the precession frequency ν_o will shorten T_1 by deflecting the moments away from the H_1 direction and thereby permitting some spins to reenter the low energy state.

Physical Description and Mechanism of T_2 Phenomenon

T_2, the transverse relaxation time, is the characteristic time constant of the phasing of precessing dipoles that results upon superposition of an rf field upon the static field. It is also a measure of the time required for the dipoles to lose the phase of precession if the rf field is suddenly removed.

Two mechanisms of T_2 relaxation are spin spin exchange and spin spin interaction due to inhomogeneous dipolar fields. In spin spin

interaction, the instantaneous dipolar fields cause the precise precessional frequencies of all the moments to differ and hence to lose phase coherence. In spin spin exchange, energy is transferred from a nucleus with $m_I = +1/2$ to another nucleus having $m_I = -1/2$ (67). Both processes remove the phase coherence of the magnetic moments.

Measurement of Nuclear Spin Relaxation

Free Induction Decay

Consider the behavior of a spin system subjected to one or several subsequent 90° and/or 180° pulses. A coordinate system which is rotating at the Larmor frequency ν_0 is adopted so that H_0 is fixed along the Z axis. A given pulse $H_1 t_p$ causes the magnetization in the rotating frame to precess through an angle $\theta = \gamma H_1 t_p$. H_1 is chosen sufficiently large for t_p to be short compared to T_1 and T_2 so that relaxation during the pulse is negligible. Only the NMR signal which arises after the rf pulse has been turned off is considered.

If a 90° pulse is applied along the X axis in the rotating frame, the magnetization $\vec{M}$ will be entirely along the Y axis. Since the receiver coil of the spectrometer is arranged to detect only the component of the magnetization in the XY plane, the magnitude of $\vec{M}$ determines the intensity of the observed NMR signal. The free induction signal is the NMR signal recorded while the nuclear magnetization precesses without the applied field H_1. A 90° pulse produces the maximum signal in the receiver coil, whereas $\vec{M}$ in the relaxed orientation produces no receiver signal.

With time elapsing after the pulse, the transverse relaxation causes M_y and hence the signal to decay exponentially. In a perfectly homogene-

ous field H_o, the free induction signal decays with a time constant T_2. Spin spin exchange, spin spin interactions, and the finite field inhomogeneity contribute to the decay of the free induction signal.

Carr Purcell Pulsed Method for T_1

The basic principle used in measuring the longitudinal relaxation time T_1 is first to deliver a 180° excitation pulse which nutates $\vec{M}$ until it is parallel to the Z axis but oriented against the magnetic field. As the individual spins randomly change energy state, $\vec{M}$ remains parallel with the Z axis but its magnitude M_z increases from $-M_o$ immediately after the 180° pulse through zero to its equilibrium value M_o. A 90° pulse applied after the time τ produces a free induction signal, the initial intensity of which is proportional to the value of M_z at time τ. The magnitude and sign of M_z can be ascertained at any time by introducing a 90° pulse to deflect $\vec{M}$ into the XY plane, where it can be detected by the receiver for a short time before it disappears owing to dephasing. From a combination of 180°–τ –90° experiments with different values of τ, the decay rate of M_z can be measured.

The decay of M_z follows an exponential curve with a time constant T_1: $M_z = M_o\ (1 - 2\,e^{-\tau/T_1})$. At the half time of exponential decay the magnitude of M_z goes through a null: $T_1 = t_{null} / \ln 2$, where t_{null} is the time between the 180° and 90° pulses. The spins must relax to equilibrium before applying the next 180° pulse (68).

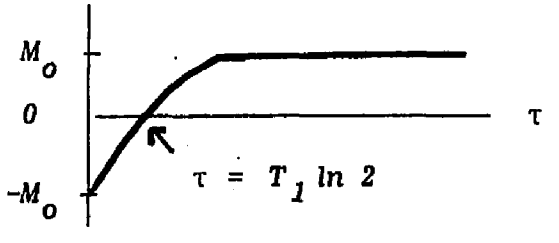

Figure 8. Normalized Values of M_z Observed in 180°–τ–90° Experiments

Sample Preparation

PRPP, OPRTase and OMP together or in separate solutions were dissolved in D_2O/Tris-HCl (pD ≅ 8) using successive lyophilizations of the samples to dryness and additions of D_2O until the HDO content was less than 0.2% D_2O. These samples were then eluted through Chelex-100 to remove metal-ion contaminants and stored in sealed plastic containers at -26°C until the time of the NMR experiment. The samples were transferred to Wilmad 5 mm tubes prior to the experiments.

Peak Assignments

The resonances of OMP and PRPP samples (10-100 mM) were examined at 19°C using a Varian HR-220 NMR Spectrometer (Rockefeller University). Comparisons with known sugar and nucleotide resonances, examination of the peak splitting patterns, and integration procedures were all employed to assign the resonances of these compounds (Table I).

Relaxation Rate Measurements

Carr-Purcell (69, 70) pulse sequences were employed to measure the longitudinal relaxation rates ($1/T_1$) of the resonances of PRPP and OMP under various conditions. The estimation of the relaxation rates was accomplished using the following equation (equation 15) and by plotting τ (the time lapse between the 180° and 90° pulses) versus $\ln [M_\infty - M_\tau]/2M_\infty$ where M_∞ and M_τ represent the signal amplitudes in the Z direction of the rotating frame at $\tau = \infty$ and at any given τ value. The computer procedure of Sass and Ziessow (71) was then employed to obtain refined values of these rates.

$$\frac{-\ln [M_\infty - M_\tau]}{2 M_\infty} = \frac{1}{T_1}(\tau) \qquad (15)$$

RESULTS AND DISCUSSION

Purification of Enzymes

The complete purification of NPRTase was accomplished by L. Hanna and S. Hess of this laboratory, who provided this enzyme for the present studies. The concentration of NPRTase as determined by the Bio-Rad protein assay was found to be 0.22 mg./ml. The purity of the NPRTase extract was ascertained by the observation of a single band on nondenaturing gel electrophoresis, SDS acrylamide gel electrophoresis, and isoelectric focusing.

The OPRTase used for the present studies was purified as described in Materials and Methods. Three eluants from Blue Sepharose CL-6B Chromatography had mean concentrations of 0.075 ± 0.010 mg./ml., 0.170 ± 0.060 mg./ml., and 0.049 ± 0.003 mg./ml. The averages of the mean specific activities of the three extracts were 173 ± 23, 174 ± 62, and 377 ± 245 μmoles OMP formed per minute per mg. of protein, respectively. The purity of the OPRTase preparation used was ascertained by the observation of a single band on nondenaturing gel electrophoresis (Figure 9) and on SDS acrylamide gel electrophoresis (Figure 14).

Pilot Studies of the Use of Crosslinking Reagents

Studies with Hemoglobin

100 μg. of hemoglobin was subject to crosslinking with 5 μl. of 2% GTA, 4% GTA, or 8% GTA for 30 min. Glutaraldehyde, a 1,5-dialdehyde, is a bifunctional reagent which forms Schiff bases with the ε-amino groups of lysyl residues. The side chains of histidine, cysteine, or tyrosine may also be involved in the crosslinking. SDS electrophoresis of samples treated

Figure 9. Disc Gel (Nondenaturing) Electrophoresis of Three OPRTase Samples Eluted Through Blue Sepharose CL-6B. The procedures employed were those described in Materials and Methods.

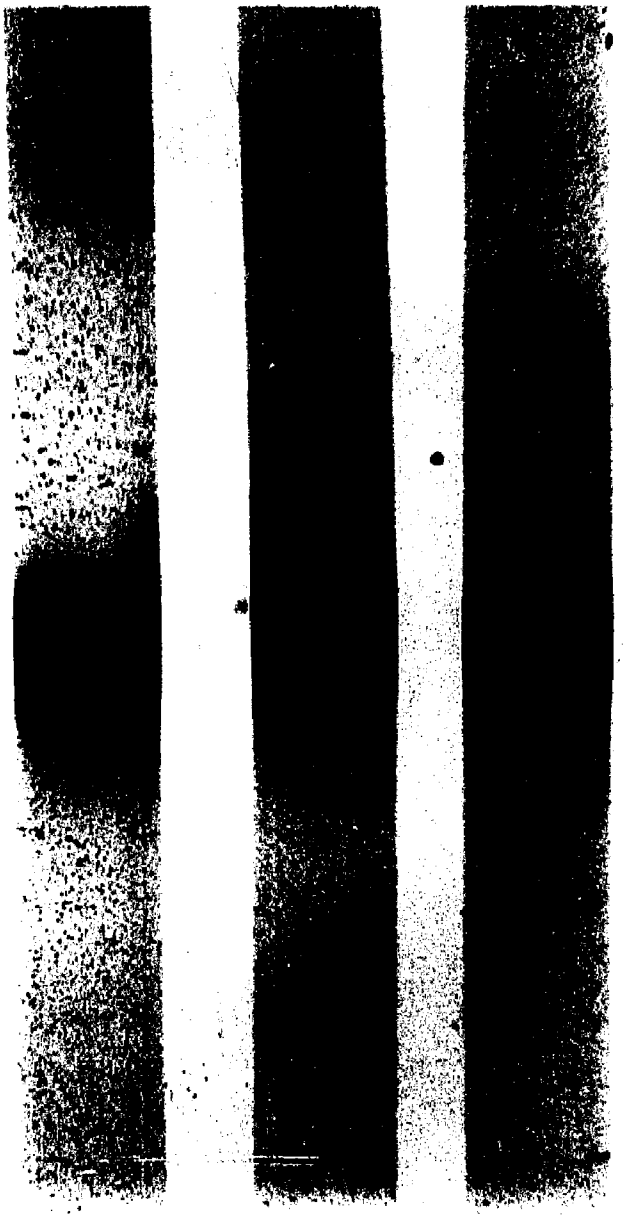

with GTA showed four bands, indicating the number of protomers involved in the oligomer of hemoglobin as four (Figure 10, 2A-4A). The ratio of crosslinker to native protein for the 2% GTA, 4% GTA, and 8% GTA was 880:1, 1800:1, and 3500:1, respectively.

100 μg. of hemoglobin (1.56 X 10^{-3} μmoles) was also subject to crosslinking with 15 μl. of 5 mg./ml., 10 mg./ml., or 15 mg./ml. DMS. Dimethyl suberimidate produces amidine crosslinks among the protomers of oligomeric proteins. SDS electrophoresis of the samples treated with DMS showed four bands corresponding to the monomer, dimer, trimer, and tetramer (Figure 10, 1B-4B). In the absence of the crosslinking reagent only the monomer was observed. The ratio of crosslinker to the native protein for 5 mg./ml., 10 mg./ml., and 15 mg./ml. DMS was 180:1, 350:1, and 530:1, respectively. The more crosslinking reagent used, the greater the possiblity of species being formed with crosslinking between oligomers. However, at lower amounts of crosslinking reagent, crosslinking between oligomers was not significant (Figure 10, 2B).

The molecular weight estimates of the monomer, dimer, trimer, and tetramer are 12,900 ± 1700, 27,500 ± 3500, 45,500 ± 4500, and 57,500 ± 6500, respectively. The bands appeared diffuse due to diffusion occurring while rimming the gels. The range of R_f values was wide. The equation of the line derived by the least squares fit of the midpoints of the range R_f for the standards was: log (MW) = -1.05 R_f + 5.06 (Table 1).

The results show that the procedure for crosslinking by GTA or by DMS did reveal species with molecular weights representing all

Figure 10. The Effect of Crosslinking Reagents GTA (A) and DMS (B) on the SDS Gel Electrophoresis Pattern of Hemoglobin.

1A) 15 µg. lysozyme, 30 µg. trypsinogen, 15 µg. ovalbumin, and 15 µg. bovine serum albumin.

2A) 100 µg. hemoglobin was incubated with 5 µl. .2% GTA for 30 min.

3A) 100 µg. hemoglobin was incubated with 5 µl. 4% GTA for 30 min.

4A) 100 µg. hemoglobin was incubated with 5 µl. 8% GTA for 30 min.

1B) 100 µg. hemoglobin without crosslinking reagent.

2B) 100 µg. hemoglobin was incubated with 15 µl. of 5 mg./ml. DMS for 4 hours.

3B) 100 µg. hemoglobin was incubated with 15 µl. of 10 mg./ml. DMS for 4 hours.

4B) 100 µg. hemoglobin was incubated with 15 µl. of 15 mg./ml. DMS for 4 hours.

5B) 15 µg. lysozyme, 30 µg. trypsinogen, 15 µg. ovalbumin, and 15 µg. bovine serum albumin.

1A 2A 3A 4A

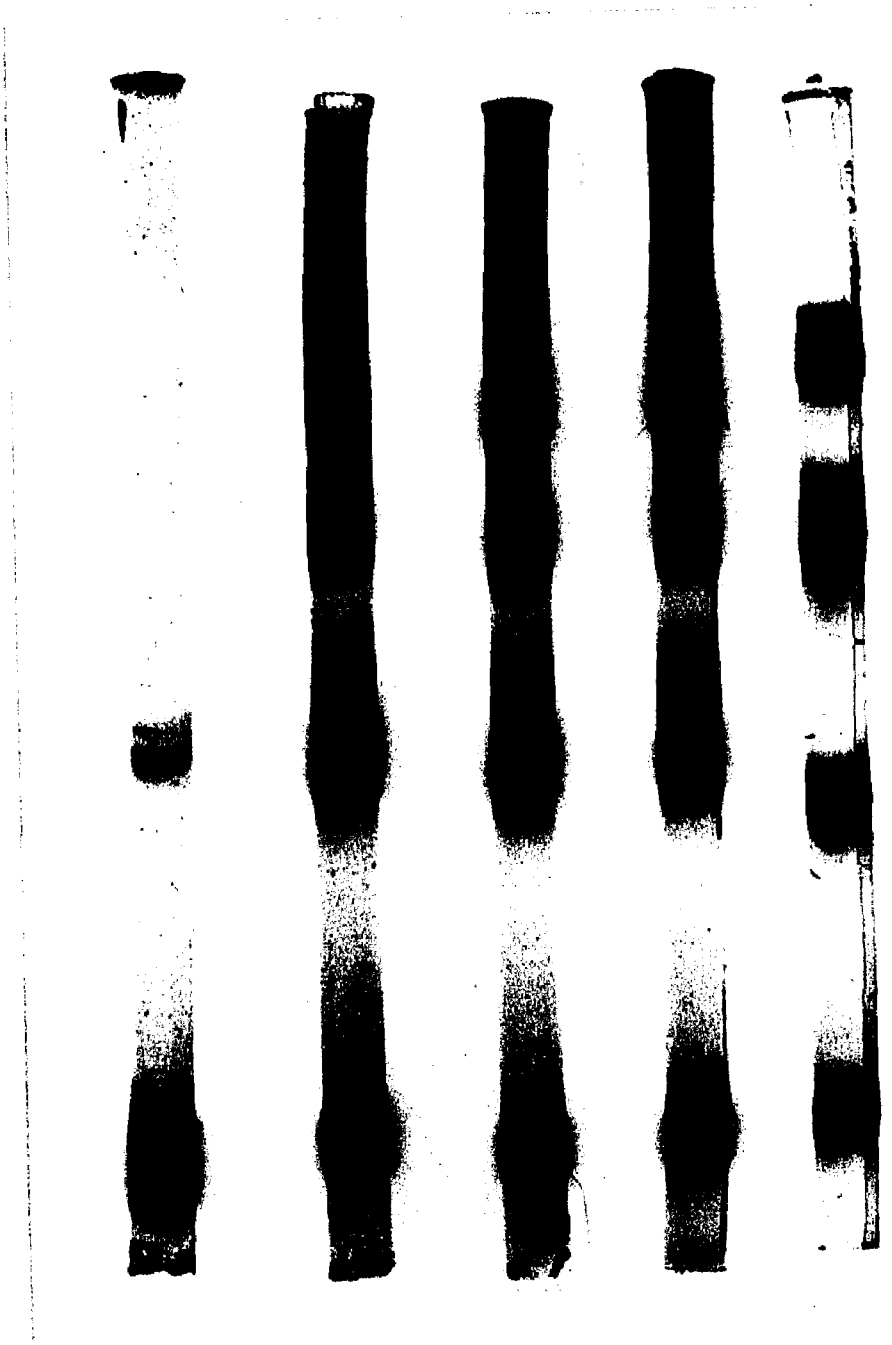
1B
2B
3B
4B
5B

TABLE 1. SDS Electrophoresis of Hemoglobin Subject to Crosslinking

Sample Gel	Distance of Dye Migration	Distance of Protein Migration	Range of R_f	MW
1. *Lysozyme*	*10.3 cm.*	*8.9–9.2 cm.*	*.864–.893*	*14,300*
Trypsinogen		*6.2–6.5 cm.*	*.602–.631*	*24,000*
Ovalbumin		*3.8–4.2 cm.*	*.369–.408*	*45,000*
Bovine Serum Albumin		*2.3–2.6 cm.*	*.223–.252*	*66,000*
2. *Hb w/2% GTA*	*10.7 cm.*	*9.4–9.8 cm.*	*.879–.916*	
		6.2–6.8 cm.	*.579–.636*	
		4.0–4.6 cm.	*.374–.430*	
		2.7–3.5 cm.	*.252–.327*	
3. *Hb w/4% GTA*	*10.8 cm.*	*9.2–9.5 cm.*	*.852–.880*	
		6.0–6.8 cm.	*.556–.630*	
		2.6–3.5 cm.	*.241–.324*	
4. *Hb w/8% GTA*	*10.8 cm.*	*9.3–9.7 cm.*	*.861–.898*	
		6.2–7.0 cm.	*.574–.648*	
		2.8–3.6 cm.	*.259–.333*	
5. *Hb w/o DMS*	*10.7 cm.*	*9.3–10.1 cm.*	*.869–.944*	
6. *Hb w/5 mg./ml. DMS*	*10.6 cm.*	*9.1–9.7 cm.*	*.858–.915*	
		5.7–6.4 cm.	*.538–.604*	
		3.7–4.2 cm.	*.349–.396*	
		2.7–3.0 cm.	*.255–.283*	
7. *Hb w/10 mg./ml. DMS*	*10.5 cm.*	*9.1–9.6 cm.*	*.868–.914*	
		5.7–6.3 cm.	*.543–.600*	
		3.6–4.3 cm.	*.343–.410*	
		2.6–3.1 cm.	*.248–.295*	
8. *Hb w/15 mg./ml. DMS*	*10.6 cm.*	*9.2–9.6 cm.*	*.868–.906*	
		5.8–6.4 cm.	*.547–.604*	
		3.7–4.4 cm.	*.349–.415*	
		2.7–3.3 cm.	*.255–.311*	

possible subunit combinations of hemoglobin. The same procedure was used to investigate the electrophoretic profile produced after crosslinking of OPRTase and NPRTase.

Studies with Partially Pure and Purified OPRTase

7 µg. of partially pure OPRTase (1.75×10^{-4} µmoles) was subjected to crosslinking with 50 µl. of 2% GTA (13.7 µmoles) with and without incubation with Mg^{2+} alone, Mg^{2+} and PRPP, and Mg^{2+} and OMP. The SDS electrophoresis pattern of the partially purified OPRTase without GTA exhibited one band corresponding to the monomer and two close bands corresponding to the impurity (Figure 11). In the presence of GTA the band corresponding to the monomer disappeared and a diffuse band corresponding to the crosslinked monomer appeared. Incubation with Mg^{2+}, Mg^{2+} and PRPP, or Mg^{2+} and OMP did not protect the monomer from crosslinking with GTA to form the diffuse band corresponding to a species with higher molecular weight and lower mobility. The ratio of crosslinker to native OPRTase was 78,000:1.

7 µg. of partially purified OPRTase was also treated with 50 µl. of 5 mg./ml. DMS (0.915 µmoles) with and without Mg^{2+}, Mg^{2+} and PRPP, or Mg^{2+} and OMP. The SDS electrophoresis of the partially purified OPRTase without DMS confirmed the reproducibility of the result of the SDS profile obtained using partially purified OPRTase without GTA (Figure 11). Incubation with Mg^{2+}, Mg^{2+} and PRPP, or Mg^{2+} and OMP before crosslinking with DMS did reveal the novel appearance of bands corresponding to species with molecular weights higher than that of the monomer but did not eliminate the band corresponding to the monomer. The ratio of the crosslinker to native OPRTase was 5200:1.

Figure 11. Pilot Studies of the Effect of Crosslinking Reagents GTA (A) and DMS (B) on the SDS Gel Electrophoresis Pattern of Partially Purified OPRTase.

IA) 7 μg. partially purified OPRTase without GTA.

IIA) 7 μg. partially purified OPRTase was incubated with 50 μl. of 2% GTA for 30 min.

IIIA) 7 μg. partially purified OPRTase pretreated with 5 μmoles Mg^{2+} for 30 min. was incubated with 50 μl. 2% GTA for 30 min.

IVA) 7 μg. partially purified OPRTase pretreated with 5 μmoles Mg^{2+} and 2.54 μmoles PRPP for 30 min. was incubated with 50 μl. 2% GTA for 30 min.

VA) 7 μg. partially purified OPRTase pretreated with 5 μmoles Mg^{2+} and 4.16 μmoles OMP for 30 min. was incubated with 50 μl. 2% GTA for 30 min.

IB) 7 μg. partially purified OPRTase without DMS.

IIB) 7 μg. partially purified OPRTase was incubated with 50 μl. of 5 mg./ml. DMS for 3 hours.

IIIB) 7 μg. partially purified OPRTase pretreated with 5 μmoles Mg^{2+} for 30 min. was incubated with 50 μl. of 5 mg./ml. DMS for 3 hrs.

IVB) 7 μg. partially purified OPRTase pretreated with 5 μmoles Mg^{2+} and 2.54 μmoles PRPP for 30 min. was incubated with 50 μl. of 5 mg./ml. DMS for 3 hours.

VB) 7 μg. partially purified OPRTase pretreated with 5 μmoles Mg^{2+} and 4.16 μmoles OMP for 30 min. was incubated with 50 μl. of 5 mg./ml. DMS for 3 hours.

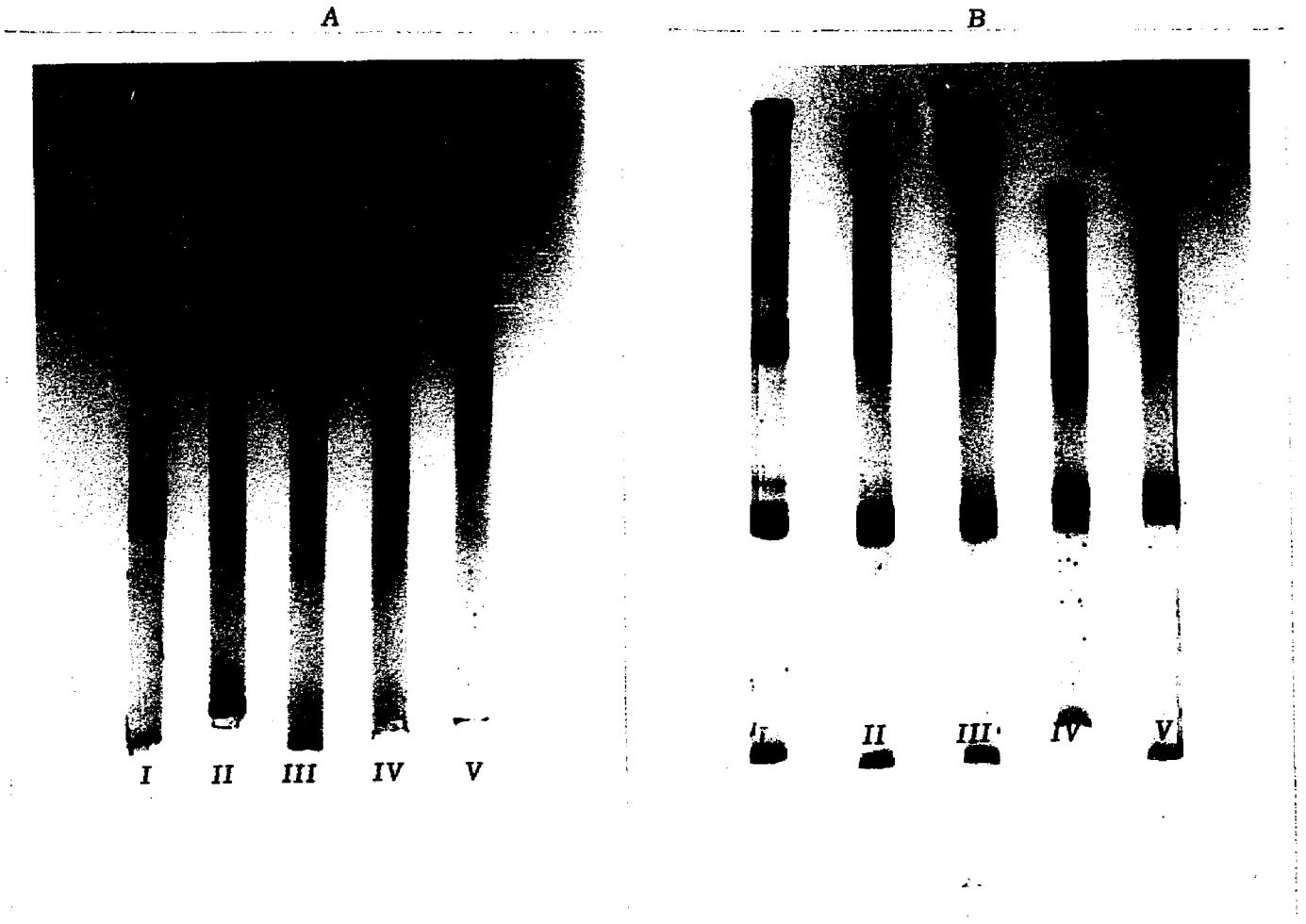
A
B
I
II
III
IV
V
I
II
III
IV
V

The activity of the partially purified OPRTase treated with GTA or DMS was monitored with time. OPRTase decreased dramatically in activity within 30 sec. after addition of GTA (Table 2). Neither incubation with Mg^{2+} nor Mg^{2+}-OMP protected the enzyme against inactivation. Pretreatment with Mg^{2+}-PRPP appeared to protect OPRTase against inactivation by GTA relative to pretreatment with Mg^{2+} alone (vide infra). Wide fluctuations in the activity of OPRTase were observed when this activity was measured in the presence or absence of DMS (Table 3). However, slight activity decreases were observed after a 3 hr. incubation with the crosslinker.

14 μg. of purified OPRTase with and without prior incubation with Mg^{2+} was treated with 5 μl. of 4% GTA (2.75 μmoles). The SDS electrophoretic pattern with the Mg^{2+} exhibited one band corresponding to the monomer and a species with a higher molecular weight than the monomer (Figure 12). Detectable dimer was not observed in the absence of added Mg^{2+}. The band corresponding to the monomer appeared less intense for the OPRTase with Mg^{2+}. Mg^{2+} promoted the crosslinking of OPRTase by GTA presumably by favoring the formation of the dimer of OPRTase. The ratio of crosslinker to native enzyme was 8000:1.

The pilot studies of the use of GTA on OPRTase did reveal by SDS electrophoresis the existence of a crosslinked, slower moving species of OPRTase, the dimer. The effect of Mg^{2+} on crosslinking can be explained as an alteration of the extent of dimer formation.

Concentration Dependence of GTA on OMP-OPRTase Crosslinking

14 μg. of OPRTase in the presence of 5 μmoles Mg^{2+} was treated with 5 μl. of 2% GTA, 4% GTA, or 8% GTA: the ratio of crosslinker to native enzyme was 3900:1, 7900:1, or 16,000:1, respectively.

TABLE 2. Pilot Studies of the Effect of Glutaraldehyde on OPRTase Activity

Sample	*Activity (ΔA_{295}/min) After Incubation For*	
	30 sec.	*30 min.*
1. OPRTase without GTA	*0.103*	*0.103*
2. OPRTase with 50 µl. 2% GTA	*0.006*	*0.0*
3. OPRTase with Mg(II) & 50 µl. 2% GTA	*0.0*	*0.0*
4. OPRTase with MgPRPP & 50 µl. 2% GTA	*0.005*	*0.0*
5. OPRTase with MgOMP & 50 µl. 2% GTA	*0.0*	*0.0*

TABLE 3. Pilot Studies of the Effect of Dimethyl Suberimidate on OPRTase Activity

Sample	*Activity (ΔA_{295}/min) After Incubation For*	
	30 sec.	*3 hrs.*
1. OPRTase without DMS	*.091*	*.130*
2. OPRTase with DMS	*.095*	*.068*
3. OPRTase w/DMS w/Mg^{2+}	*.162*	*.053*
4. OPRTase w/DMS w/MgPRPP	*.092*	*.058*
5. OPRTase w/DMS w/MgOMP	*.035*	*.021*

Figure 12. Pilot Study of the Effects of Addition of GTA and Mg^{2+} on the SDS Gel Electrophoresis Pattern of OMP-OPRTase.

1) 14 µg. OMP-OPRTase was incubated with 5 µl. 4% GTA for 30 min.

2) 14 µg. OMP-OPRTase pretreated with 5 µmoles Mg^{2+} for 30 min. was incubated with 5 µl. 4% GTA for 30 min.

1 2

These samples were run on SDS electrophoresis gels (Figure13). The electrophoretic pattern showed only the non-crosslinked monomer with 5 µl. of 2% GTA but also showed the crosslinked dimer with 5 µl. of 4% GTA and 5 µl. of 8% GTA. As the amount of crosslinker was increased, the intensity of the non-crosslinked monomer diminished while that of the crosslinked dimer increased.

The activity of OPRTase subject to crosslinking with GTA after prior incubation with Mg^{2+} was measured 30 sec. and 30 min. after addition of the crosslinker. The activity decreased markedly after 30 min.: the more crosslinker added, the faster the inactivation of the enzyme (Table 4).

The molecular weight estimates of the monomer and dimer were found to be 26,500 ± 1500 and 50,000 ± 2000, respectively. The equation of best fit derived by the method of least squares using the midpoints of the R_f ranges of the standard proteins was: log(MW) = - 1.02 R_f + 5.10.

Consequently, increasing concentrations of glutaraldehyde did demonstrate the existence of the crosslinked dimer by SDS electrophoresis. The crosslinked dimer had a lower mobility than the non-crosslinked monomer. The appearance of the crosslinked dimer depended on the concentration of glutaraldehyde that was employed.

Effects of Addition of Mg^{2+} on OMP-OPRTase Crosslinking with GTA

14 µg. of OPRTase was incubated with 5 µl. of 2% GTA, 4% GTA, or 8% GTA with and without 25 mM Mg^{2+}: the ratio of crosslinker to native enzyme was 3900:1, 7900:1, or 16,000:1, resepectively. These samples were run on SDS electrophoresis gels. Without crosslinker,

Figure 13. The Effects of Higher Concentrations of GTA on the SDS Gel Electrophoresis Pattern of Mg^{2+}-OMP-OPRTase Solutions.

1) *The zebra gel of standard proteins: 15 μg. lysozyme, 30 μg. trypsinogen, 15 μg. ovalbumin, and 15 μg. bovine serum albumin.*
2) *3.5×10^{-4} μmoles OMP-OPRTase pretreated with 5 μmoles Mg^{2+} for 30 min. was incubated with 1.37 μmoles GTA for 30 min.*
3) *3.5×10^{-4} μmoles OMP-OPRTase pretreated with 5 μmoles Mg^{2+} for 30 min. was incubated with 2.75 μmoles GTA for 30 min.*
4) *3.5×10^{-4} μmoles OMP-OPRTase pretreated with 5 μmoles Mg^{2+} for 30 min. was incubated with 5.49 μmoles GTA for 30 min.*

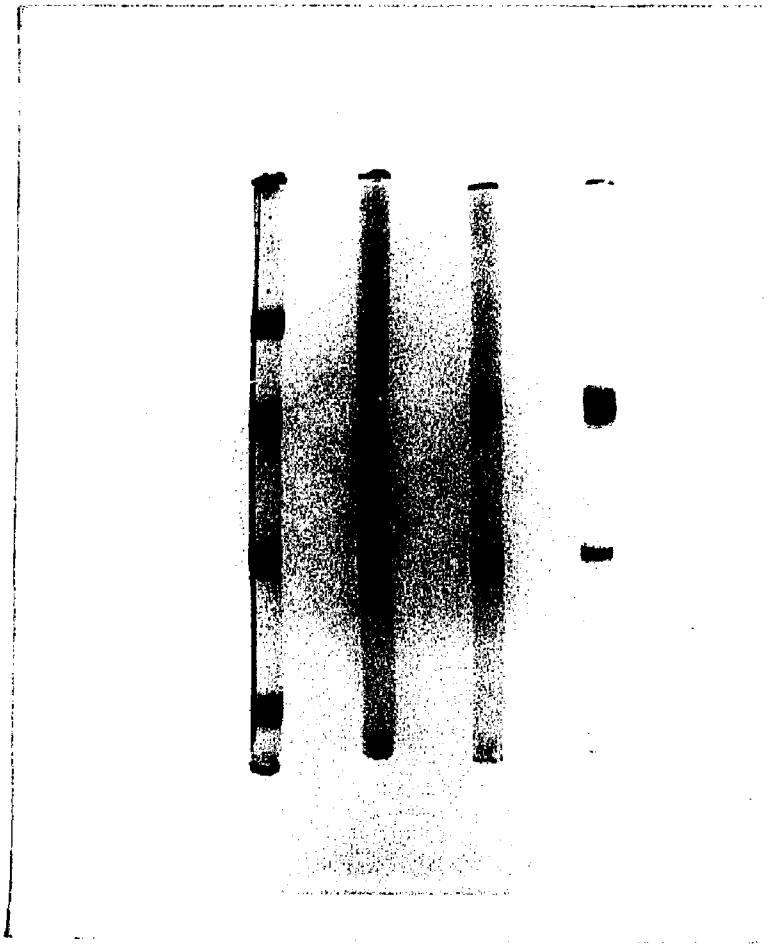

1 2 3 4

TABLE 4. Activities of OMP-OPRTase After Incubation With Increasing Amounts of Glutaraldehyde In the Presence of Magnesium

Sample	Activity (ΔA_{295}/min) After Incubation For	
	30 sec.	30 min.
1. OPRTase without GTA	.059	.049
2. OPRTase with Mg(II) & 2% GTA	.051	.014
3. OPRTase with Mg(II) & 4% GTA	.054	.010
4. OPRTase with Mg(II) & 8% GTA	.021	.001

TABLE 5. SDS Electrophoresis of OMP-OPRTase Subject to Crosslinking by Glutaraldehyde After Prior Incubation with Mg(II)

Sample Gel	Distance of Dye Migration	Distance of Protein Migration	Range of R_f	MW
1. Lysozyme	10.7 cm.	9.5–9.8 cm.	.888–.916	14,300
Trypsinogen		6.7–7.0 cm.	.626–.654	24,000
Ovalbumin		4.3–4.6 cm.	.402–.430	45,000
Bovine Serum Albumin		3.6–3.8 cm.	.336–.355	66,000
2. OPRTase w/Mg/2% GTA	10.5 cm.	6.7–7.1 cm.	.638–.676	
3. OPRTase w/Mg/4% GTA	10.4 cm.	6.8–7.1 cm.	.654–.683	
		4.0–4.2 cm.	.385–.404	
4. OPRTase w/Mg/8% GTA	10.4 cm.	6.7–6.9 cm.	.644–.663	
		3.9–4.3 cm.	.375–.413	

the gel exhibited one band corresponding to the monomer which substantiated the assertion that the preparation was homogeneous. With crosslinker but without Mg^{2+}, the noncrosslinked monomer appeared but the crosslinked dimer was not detectable except when 5 µl. of 8% GTA was included in the incubation mixture. With crosslinker and Mg^{2+}, the crosslinked dimer was not visibly apparent with 5 µl. of 2% GTA but was detectable when 5 µl. of 4% or 8% GTA was included in the incubation mixture (Figure 14).

The activity measurements 30 sec. and 30 min. after addition of GTA were performed. Within 30 sec., the activity diminished the most when 8% GTA was employed whether or not Mg^{2+} was preincubated. After 30 min. of incubation with crosslinker, the activity diminished to a greater extent if Mg^{2+} was preincubated before crosslinking (Table 6).

The molecular weight estimates for the monomer and dimer are 26,500 ± 1500 and 50,000 ± 2500, respectively. The equation derived by the method of least squares using the midpoints of the range of R_f values for the standards of known molecular weights was: log (MW) = - 1.02 R_f + 5.10 (Table 7).

These observations are consistent with the proposal that the monomer and dimer are in equilibrium and that Mg^{2+} promotes the extent of dimer formation. It is intuitive that the more dimer present upon addition of crosslinker, the more intense will be the dimer band and the less intense the monomer band.

Effects of Addition of Mg^{2+} and Mg^{2+}-PRPP on OPRTase Crosslinking with GTA

20 µg. of OPRTase (5 X 10^{-4} µmoles) after complete removal of OMP

Figure 14. SDS Gel Electrophoresis Studies of the Effects of Mg^{2+} Addition to OMP-OPRTase and GTA Incubation Mixtures.

1) 15 µg. lysozyme.

2) 30 µg. trypsinogen.

3) 15 µg. ovalbumin.

4) 15 µg. bovine serum albumin.

5) 3.5×10^{-4} µmoles OMP-OPRTase without GTA.

6) 3.5×10^{-4} µmoles OMP-OPRTase was incubated with 1.37 µmoles GTA for 30 min.

7) 3.5×10^{-4} µmoles OMP-OPRTase was incubated with 2.75 µmoles GTA for 30 min.

8) 3.5×10^{-4} µmoles OMP-OPRTase was incubated with 5.49 µmoles GTA for 30 min.

9) 3.5×10^{-4} µmoles OMP-OPRTase pretreated with 5 µmoles Mg^{2+} for 30 min. was incubated with 1.37 µmoles GTA for 30 min.

10) 3.5×10^{-4} µmoles OMP-OPRTase pretreated with 5 µmoles Mg^{2+} for 30 min. was incubated with 2.75 µmoles GTA for 30 min.

11) 3.5×10^{-4} µmoles OMP-OPRTase pretreated with 5 µmoles Mg^{2+} for 30 min. was incubated with 5.49 µmoles GTA for 30 min.

12) The zebra gel of standard proteins: 15 µg. lysozyme, 30 µg. trypsinogen, 15 µg. ovalbumin, and 15 µg. bovine serum albumin.

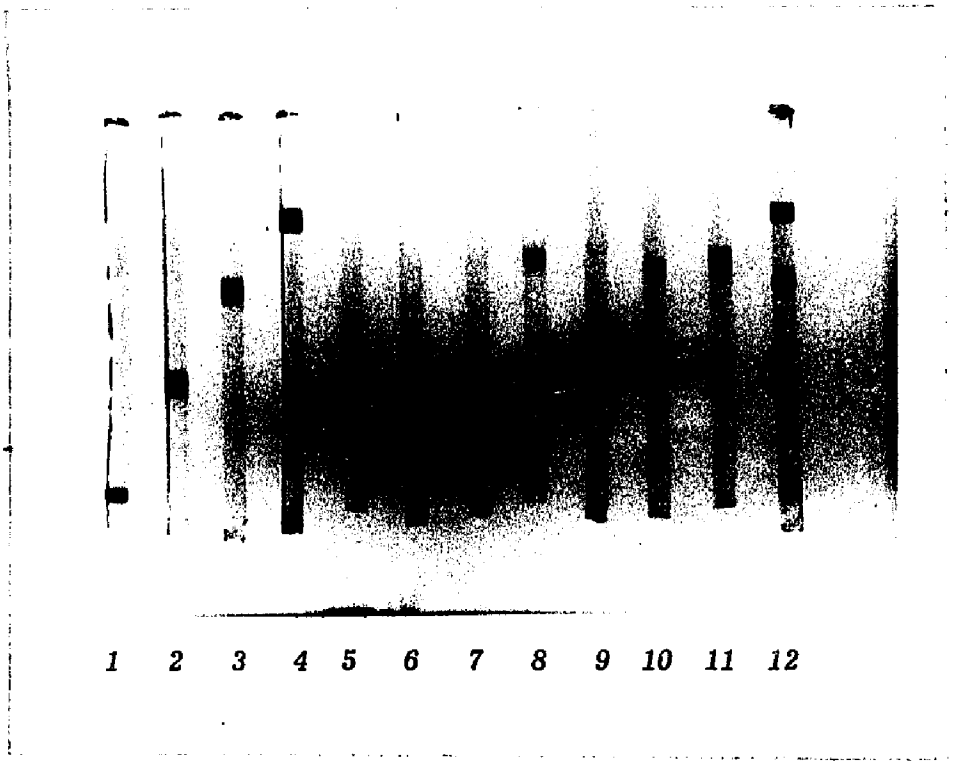
1 2 3 4 5 6 7 8 9 10 11 12

TABLE 6. Measurements of Activity of OMP-OPRTase Treated with GTA with or without Prior Incubation with Mg(II)

Sample	*Activity (ΔA_{295}/min) After Incubation For*	
	30 sec.	*30 min.*
1. OPRTase w/o GTA	*.059*	*.049*
2. OPRTase w/2% GTA	*.058*	*.032*
3. OPRTase w/4% GTA	*.054*	*.031*
4. OPRTase w/8% GTA	*.035*	*.003*
5. OPRTase w/Mg^{2+} & 2% GTA	*.051*	*.014*
6. OPRTase w/Mg^{2+} & 4% GTA	*.054*	*.010*
7. OPRTase w/Mg^{2+} & 8% GTA	*.021*	*.001*

TABLE 7. Effects of Addition of Mg(II) on OMP-OPRTase Crosslinking with GTA by SDS Electrophoresis

Sample Gel	Distance of Dye Migration	Distance of Protein Migration	Range of R_f	MW
1. Lysozyme	10.9 cm.	10.7-10.9 cm.	.982-1.0	14,300
2. Trypsinogen	10.8 cm.	6.8-7.1 cm.	.630-.657	24,000
3. Ovalbumin	10.9 cm.	4.4-4.7 cm.	.404-.431	45,000
4. Bovine Serum Albumin	10.8 cm.	2.7-3.0 cm.	.250-.278	66,000
5. OPRTase w/o GTA	10.3 cm.	6.8-7.1 cm.	.660-.689	
6. OPRTase w/2% GTA	10.6 cm.	6.9-7.2 cm.	.651-.679	
7. OPRTase w/4% GTA	10.4 cm.	6.7-7.0 cm.	.644-.673	
8. OPRTase w/8% GTA	10.1 cm.	6.6-6.7 cm.	.653-.663	
		3.7-4.0 cm.	.366-.396	
9. OPRTase w/Mg/2% GTA	10.5 cm.	6.7-7.1 cm.	.638-.676	
10. OPRTase w/Mg/4% GTA	10.4 cm.	6.8-7.1 cm.	.654-.683	
		4.0-4.2 cm.	.385-.404	
11. OPRTase w/Mg/8% GTA	10.4 cm.	6.7-6.9 cm.	.644-.663	
		3.9-4.3 cm.	.375-.413	
12. Lysozyme	10.7 cm.	9.5-9.8 cm.	.888-.916	14,300
Trypsinogen		6.7-7.0 cm.	.626-.654	24,000
Ovalbumin		4.3-4.6 cm.	.402-.430	45,000
Bovine Serum Albumin		3.6-3.8 cm.	.336-.355	66,000

was treated with 5.49 μmoles GTA, 5.49 μmoles GTA after 30 min. incubation with 5 μmoles Mg^{2+}, or with 5.49 μmoles GTA after a 30 min. preincubation with 5 μmoles Mg^{2+} and 0.2 μmoles PRPP. These samples were subject to SDS electrophoresis. In the absence of GTA, only the noncrosslinked monomer band appeared. In the presence of GTA, both the noncrosslinked monomer band and the crosslinked dimer band appeared. The presence of Mg^{2+} or Mg^{2+}–PRPP during crosslinking did not appear to protect OPRTase from crosslinking. The ratio of crosslinker to OPRTase was 11,000:1 (Figure 15).

The activities of OPRTase without GTA, with 8% GTA, with 8% GTA and Mg^{2+}, or with 8% GTA and Mg^{2+}–PRPP were measured 30 sec. and 30 min. after crosslinker addition. In the absence of crosslinker, the activity remained stable. OPRTase activity diminished the most within 30 sec. after crosslinker addition after pretreatment with Mg^{2+} (Table 8).

The molecular weight estimates for the monomer and dimer were 26,000 ± 2000 and 56,000 ± 9000, respectively. The equation of the line fitted by the method of least squares was: $\log(MW) = -1.05 R_f + 5.06$ (Table 9).

In conclusion, similar crosslinking results were obtained for the enzyme with OMP removed as for the enzyme with OMP tightly bound (Figures 14 and 15). The residues which participate in the crosslinking by GTA do not therefore reside in the OMP binding site. Mg^{2+} did enhance the appearance of the dimer (Figure 15) and may have increased the rate of inactivation (Tables 6 and 8). The ε-amino groups, in an orientation appropriate for interprotomeric crosslinking, seem to be more accessible within the distance spanned by GTA as a consequence of the conforma-

Figure 15. SDS Gel Electrophoresis Studies of the Effects of the Addition of Mg^{2+} and of Mg^{2+}-PRPP to the OPRTase and GTA Incubation Mixture After Complete Removal of OMP.

1) The zebra gel of the standard proteins: 20 µg. lysozyme, 40 µg. trypsinogen, 20 µg. pepsin, 20 µg. ovalbumin, and 20 µg. bovine serum albumin.

2) 5×10^{-4} µmoles OPRTase without GTA.

3) 5×10^{-4} µmoles OPRTase was incubated with 5.49 µmoles GTA for 30 min.

4) 5×10^{-4} µmoles OPRTase pretreated with 5 µmoles Mg^{2+} for 30 min. was incubated with 5.49 µmoles GTA for 30 min.

5) 5×10^{-4} µmoles OPRTase pretreated with 5 µmoles Mg^{2+} and 0.2 µmoles PRPP for 30 min. was incubated with 5.49 µmoles GTA for 30 min.

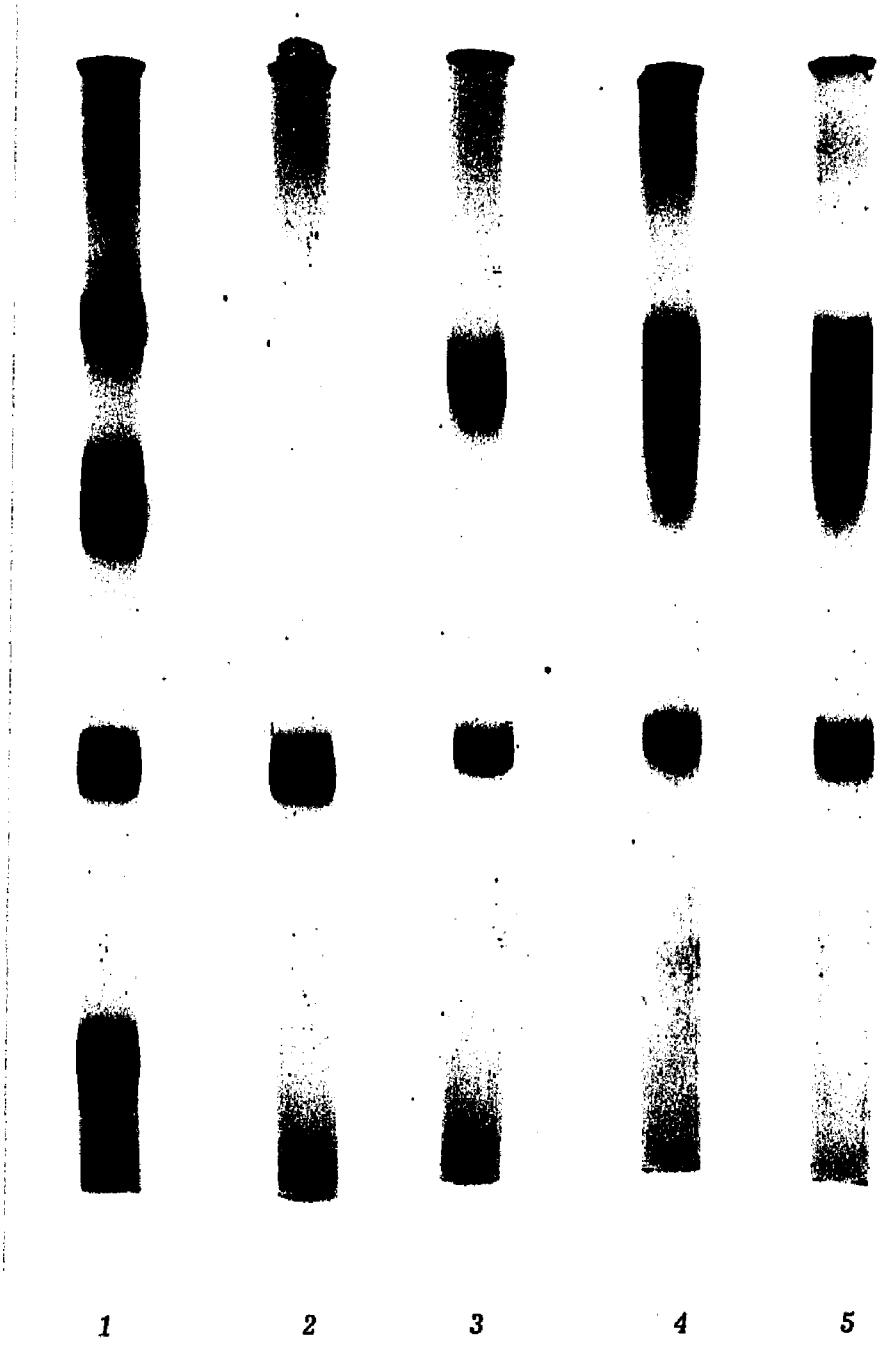
1
2
3
4
5

TABLE 8. Activity Measurements of OPRTase Crosslinking with GTA After Preincubation with Mg(II) or Mg(II)-PRPP

Sample	*Activity (ΔA_{295}/min) After Incubation For*	
	30 sec.	*30 min.*
1. OPRTase without GTA	*.079*	*.081*
2. OPRTase with 5 µl. 8% GTA	*.043*	*.009*
3. OPRTase with Mg^{2+} & 5 µl. 8% GTA	*.017*	*0.0*
4. OPRTase with Mg^{2+}-PRPP & 5 µl. 8% GTA	*.030*	*.003*

TABLE 9. SDS Electrophoresis of OPRTase After Complete Removal of OMP

Sample Gel	Distance of Dye Migration	Distance of Protein Migration	Range of R_f	MW
1. *Lysozyme*	*10.7 cm.*	*9.2–9.6 cm.*	*.860–.897*	*14,300*
Trypsinogen		*6.5–6.8 cm.*	*.607–.636*	*24,000*
Pepsin		*4.0–4.25 cm.*	*.374–.397*	*34,700*
Ovalbumin		*4.25–4.5 cm.*	*.397–.421*	*45,000*
Bovine Serum Albumin		*2.2–2.6 cm.*	*.206–.243*	*66,000*
2. *OPRTase without GTA*	*10.7 cm.*	*6.6–6.9 cm.*	*.617–.645*	
3. *OPRTase with 8% GTA*	*10.6 cm.*	*6.6–6.7 cm.*	*.623–.632*	
		3.0–3.3 cm.	*.283–.311*	
4. *OPRTase with 8% GTA & Mg^{2+}*	*10.6 cm.*	*6.4–6.7 cm.*	*.604–.632*	
		2.6–3.8 cm.	*.245–.358*	
5. *OPRTase with 8% GTA & Mg^{2+}-PRPP*	*10.3 cm.*	*6.1–6.4 cm.*	*.592–.621*	
		2.4–3.8 cm.	*.233–.369*	

tional change(s) induced by Mg^{2+}. In contrast, Mg^{2+}–PRPP had no effect on the crosslinking of the enzyme with GTA since the intensity of the dimer band did not diminish (Figure 15), but in the one experiment that was run, Mg^{2+}–PRPP may have protected the enzyme against inactivation (Table 8). These results do not conclusively establish the relationship between inactivation and crosslinking which can be independent events.

Effects of Addition of Mg^{2+} on OMP-OPRTase Crosslinking with DMS

7 μg. of native OPRTase was incubated with 0.275 μmoles DMS with or without prior incubation with 2.5 μmoles Mg^{2+}. 30 sec. and 4 hrs. after addition of crosslinker, samples were frozen and stored for analysis by SDS electrophoresis (Figure 16). OPRTase without DMS exhibited one band corresponding to the noncrosslinked monomer. OPRTase with DMS for 30 sec. or for 4 hrs. exhibited one band corresponding to the noncrosslinked monomer but failed to show any visibly detectable band corresponding to a crosslinked species with this limited amount of enzyme.

After preincubation with 2.5 μmoles Mg^{2+}, OPRTase with DMS showed the more faint monomer band but failed to visibly display a band corresponding to a crosslinked species. The ratio of DMS to native OPRTase was 1600:1.

The activities of OPRTase with DMS and Mg^{2+}–treated OPRTase with DMS were monitored 30 sec. and 4 hrs. after addition of crosslinker. In all cases the activity of OPRTase did not diminish appreciably (Table 10).

The estimates for the molecular weight for the monomer was found to be 26,000 ± 1000. The equation of best fit derived by the method of least squares from the midpoints of the range of R_f values for the standards of known molecular weight was found to be: $\log (MW) = -0.981\ R_f + 5.00$ (Table 11).

Figure 16. SDS Gel Electrophoresis Studies of the Effects of Addition of Mg^{2+} to OMP-OPRTase and DMS Incubation Mixtures.

1) 20 μg. lysozyme.

2) 40 μg. trypsinogen.

3) 20 μg. ovalbumin.

4) 20 μg. bovine serum albumin.

5) 1.75×10^{-4} μmoles OMP-OPRTase without DMS.

6) 1.75×10^{-4} μmoles OMP-OPRTase incubated with 0.275 μmoles DMS for 30 sec.

7) 1.75×10^{-4} μmoles OMP-OPRTase incubated with 0.275 μmoles DMS for 4 hours.

8) 1.75×10^{-4} μmoles OMP-OPRTase pretreated with 2.5 μmoles Mg^{2+} for 30 min. was incubated with 0.275 μmoles DMS for 30 sec.

9) 1.75×10^{-4} μmoles OMP-OPRTase pretreated with 2.5 μmoles Mg^{2+} for 30 min. was incubated with 0.275 μmoles DMS for 4 hours.

10) The zebra gel of the standard proteins: 20 μg. lysozyme, 40 μg. trypsinogen, 20 μg. ovalbumin, and 20 μg. BSA.

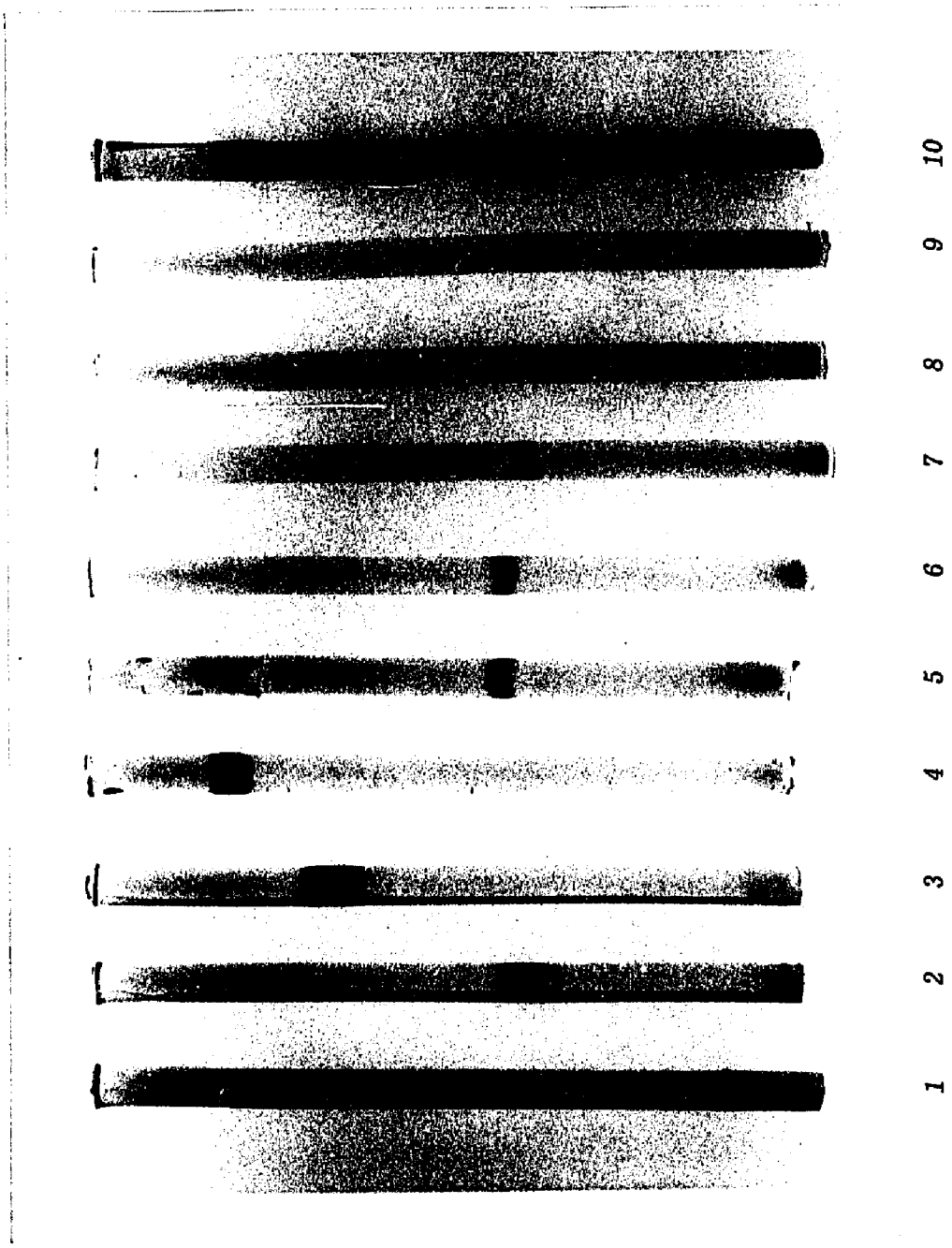
10
9
8
7
6
5
4
3
2
1

TABLE 10. Effects of Treatment with DMS Following Preincubation with Mg(II) on OMP-OPRTase Activity

Sample	*Activity (ΔA_{295}/min) After Incubation For*	
	30 sec.	*4 hrs.*
1. OPRTase without DMS	*.045*	*.044*
2. OPRTase with DMS	*.048*	*.035*
3. OPRTase with Mg(II) & DMS	*.032*	*.032*

TABLE 11. SDS Electrophoresis of OPRTase Subject to Crosslinking by DMS

Sample Gel	Distance of Dye Migration	Distance of Protein Migration	Range of R_f	MW
1. Lysozyme	10.6 cm.	9.1-9.4 cm.	.858-.887	14,300
2. Trypsinogen	10.3 cm.	6.0-6.5 cm.	.583-.631	24,000
3. Ovalbumin	10.3 cm.	3.2-3.7 cm.	.311-.359	45,000
4. Bovine Serum Albumin	10.3 cm.	1.9-2.3 cm.	.184-.223	66,000
5. OPRTase without DMS	10.2 cm.	6.0-6.2 cm.	.588-.608	
6. OPRTase with DMS [30 sec.]	10.6 cm.	6.1-6.3 cm.	.575-.594	
7. OPRTase with DMS [4 hours]	10.9 cm.	6.4-6.6 cm.	.587-.606	
8. OPRTase with Mg^{2+} & DMS [30 sec.]	10.7 cm.	6.4-6.6 cm.	.598-.617	
9. OPRTase with Mg^{2+} & DMS [4 hrs.]	10.8 cm.	6.4-6.6 cm.	.593-.611	
10. Lysozyme	10.6 cm.	9.2-9.5 cm.	.868-.896	14,300
Trypsinogen		6.3-6.6 cm.	.594-.623	24,000
Ovalbumin		3.6-3.9 cm.	.340-.368	45,000
Bovine Serum Albumin		2.0-2.3 cm.	.189-.217	66,000

Consequently, the treatment of OMP-OPRTase (after pretreatment with Mg^{2+}) with DMS at a ratio of DMS to native enzyme of 1600:1 did lead to the decreased intensity of the monomer band. Any statement concerning the monomer/dimer equilibrium cannot be made conclusively since a dimer band was not observed. In addition DMS does not appear to inactivate OMP-OPRTase (Table 10). Thus it appears that DMS is not as good a crosslinker of the OPRTase dimer as GTA. This cannot be because of its size but may be attributed to the greater reactivity of Schiff base formation.

Concentration Dependence of GTA on NPRTase

22 μg. NPRTase (5×10^{-4} μmoles) was incubated for 30 min. with 5 μl. 2% GTA, 5 μl. 4% GTA, or 5 μl. 8% GTA. The samples were run on SDS gel electrophoresis (Figure 17). NPRTase without GTA exhibited one band corresponding to the noncrosslinked monomer; hence, the NPRTase preparation appeared homogeneous. NPRTase with 2% GTA, 4% GTA, or 8% GTA exhibited only one band corresponding to the non-crosslinked monomer: no band corresponding to a crosslinked species was visibly detectable. The ratio of crosslinker to native enzyme was 2700:1, 5400:1, or 11,000:1.

The activity of NPRTase was monitored at 30 sec. or 30 min. after incubation with 5 μl. of 2% GTA. The activity did not diminish upon treatment with the 5 μl. of 2% GTA (Table 12).

The estimate for the molecular weight of NPRTase was 46,000 ± 5500. The equation of the line derived by the method of least squares from the midpoints of the ranges of R_f of the standards of known molecular weight was: $\log (MW) = -1.05 R_f + 5.06$ (Table 13).

Figure 17. SDS Gel Electrophoresis Studies of the Effects of Addition of GTA to NPRTase.

1) 15 µg. lysozyme, 30 µg. trypsinogen, 15 µg. ovalbumin, and 15 µg. bovine serum albumin.

2) 22 µg. NPRTase without GTA.

3) 22 µg. NPRTase with 5 µl. 2% GTA [1.37 µmoles] for 30 min.

4) 22 µg. NPRTase with 5 µl. 4% GTA [2.75 µmoles] for 30 min.

5) 22 µg. NPRTase with 5 µl. 8% GTA [5.49 µmoles] for 30 min.

1 2 3 4 5

TABLE 12. Effect of GTA on NPRTase Activity[a]

Sample	*Incubation Time for Activity Measurement*		
	1 min.	*3 min.*	*10 min.*
1. NPRTase without GTA	——	——	*0.8 cm.*
2. NPRTase with 5 µl. 2% GTA [30 seconds]	*0.5 cm.*	*0.6 cm.*	*0.9 cm.*
3. NPRTase with 5 µl. 2% GTA [30 minutes]	*0.5 cm.*	*0.5 cm.*	*0.6 cm.*
4. NPRTase with Mg^{2+} & 5 µl. 2% GTA [30 seconds]	*0.4 cm.*	*0.5 cm.*	*0.8 cm.*
5. NPRTase with Mg^{2+} & 5 µl. 2% GTA [30 minutes]	*0.5 cm.*	*0.6 cm.*	*0.7 cm.*

a) Activities are represented in terms of peak amplitudes of NaMN as this product elutes from the μC_{18} HPLC column. This peak amplitude is directly proportional to the NaMN concentration.

TABLE 13. SDS Electrophoresis Studies of the Concentration Dependence of GTA on NPRTase Crosslinking

Sample Gel	Distance of Dye Migration	Distance of Protein Migration	Range of R_f	MW
1. Lysozyme	10.3 cm.	8.9–9.2 cm.	.864–.893	14,300
Trypsinogen		6.2–6.5 cm.	.602–.631	24,000
Ovalbumin		3.8–4.2 cm.	.369–.408	45,000
Bovine Serum Albumin		2.3–2.6 cm.	.223–.252	66,000
2. NPRTase w/o GTA	10.4 cm.	3.5–4.1 cm.	.337–.394	
3. NPRTase w/2% GTA	10.8 cm.	4.0–4.5 cm.	.370–.417	
4. NPRTase w/4% GTA	10.5 cm.	3.5–4.3 cm.	.333–.410	
5. NPRTase w/8% GTA	10.7 cm.	3.5–4.5 cm.	.327–.421	

In contrast to OPRTase, NPRTase does not appear to crosslink with either 2%, 4%, or 8% GTA. Also, the activity of NPRTase appears to be unaffected by the presence of GTA. The results support the proposal that NPRTase does not appear to form a crosslinked species to an appreciable extent. The gels appeared colorless above the noncrosslinked monomer (Figure 17).

Effects of Addition of Mg^{2+} and Substrates on NPRTase Treatment with Glutaraldehyde

22 µg. NPRTase (5×10^{-4} µmoles) was incubated with 5 µl. 2% GTA (1.37 µmoles) for 30 sec. or for 30 min. After preincubation with 3 µmoles Mg^{2+}, another 22 µg. NPRTase was incubated with 1.37 µmoles GTA for 30 sec. or for 30 min. These samples were run on SDS electrophoresis gels (Figure 18) to assess the effect of addition of Mg^{2+} on NPRTase treated with GTA. In the absence of GTA, NPRTase exhibited a single band corresponding to the noncrosslinked monomer. In the presence of GTA, whether for 30 sec. or for 30 min., only the noncrosslinked monomer band manifested itself. Above the monomer band, the gels were colorless and virtually identical to the gel on which NPRTase without GTA was run. The monomer band also did not appear to diminish in intensity. After preincubation with Mg^{2+}, NPRTase with GTA, whether for 30 sec. or for 30 min., displayed only one band corresponding to the monomer. The gels appeared identical to the gel on which NPRTase without GTA was run. The section of the gel above the monomer band appeared colorless. There was no apparent dimunition of intensity of the monomer band compared to the gel on which NPRTase without GTA was run. The ratio of crosslinker to native enzyme was 2700:1.

Figure 18. SDS Gel Electrophoresis Studies of the Effects of Addition of Mg^{2+} and GTA to NPRTase.

1) 20 µg. lysozyme.

2) 40 µg. trypsinogen.

3) 20 µg. ovalbumin.

4) 20 µg. bovine serum albumin.

5) 22 µg. NPRTase without GTA.

6) 22 µg. NPRTase and 1.37 µmoles GTA incubated for 30 sec.

7) 22 µg. NPRTase and 1.37 µmoles GTA incubated for 30 min.

8) 22 µg. NPRTase pretreated with 3 µmoles Mg^{2+} for 30 min. was incubated with 1.37 µmoles GTA for 30 sec.

9 & 10) 22 µg. NPRTase pretreated with 3 µmoles Mg^{2+} for 30 min. was incubated with 1.37 µmoles GTA for 30 min.

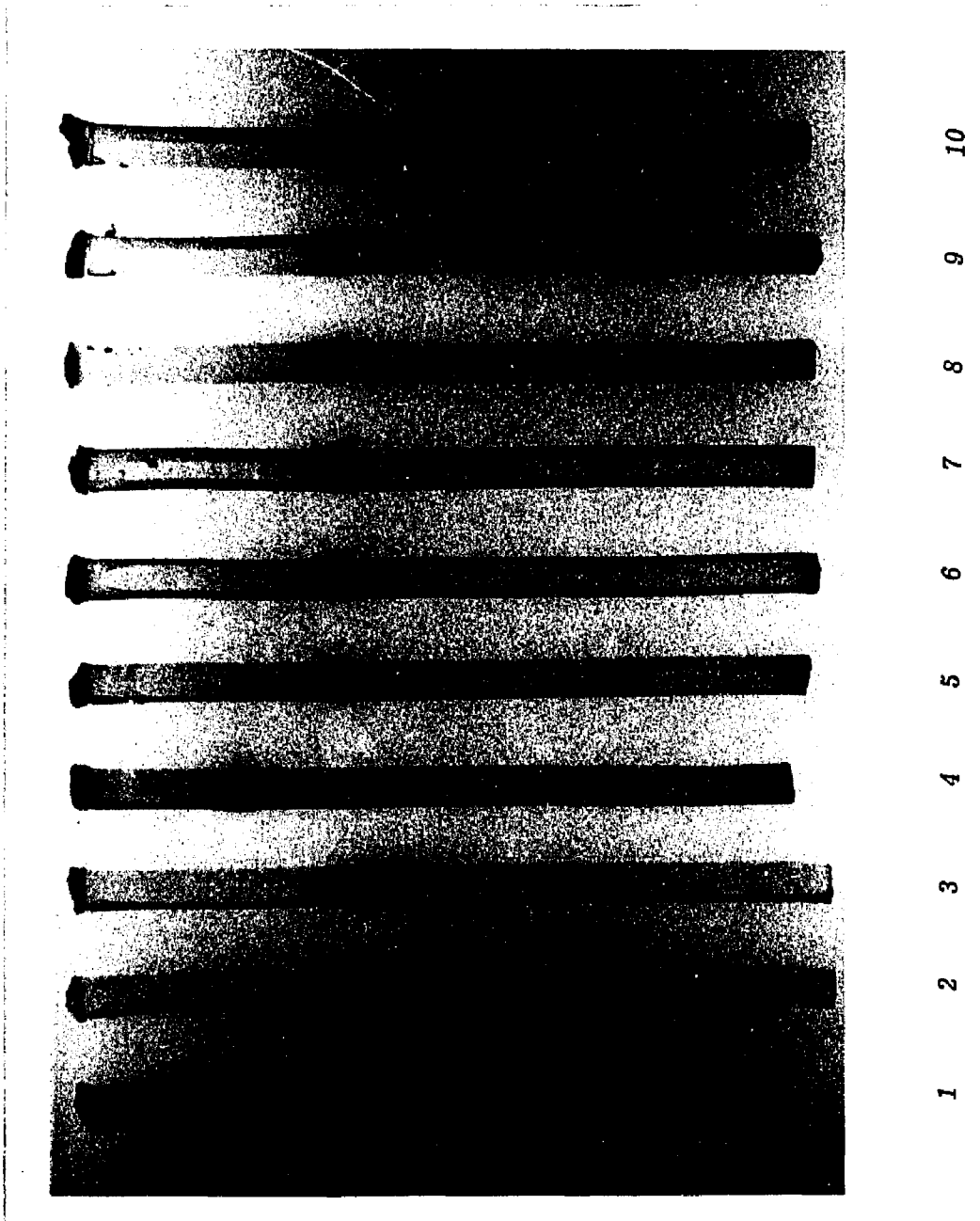
1
2
3
4
5
6
7
8
9
10

The activity of NPRTase was monitored during the attempt at crosslinking NPRTase with GTA, with or without Mg^{2+}. GTA had no effect on the activity of NPRTase whether or not Mg^{2+} was present (Table 12).

The molecular weight estimate for NPRTase during studies of the effect of Mg^{2+} on treatment with GTA was 49,000 ± 2000. The equation of best fit derived by the method of least squares from the midpoints of the range of R_f values of the standards of known molecular weight was: $\log(MW) = -0.986\ R_f + 5.03$ (Table 15).

22 µg. NPRTase was incubated for 30 min. with 5 µl. 2% GTA. Another 22 µg. NPRTase was incubated for 30 min. with 5 µl. 2% GTA after preincubation with 2 µmoles Mg^{2+} and 2×10^{-2} µmoles PRPP. Another 22 µg. NPRTase was incubated with 1.37 µmoles GTA after preincubation with 2 µmoles Mg^{2+} and 4.8×10^{-2} µmoles ATP. As a control, 22 µg. NPRTase was incubated with 2 µmoles Mg^{2+}, 4.8×10^{-2} µmoles ATP, and 2×10^{-2} µmoles PRPP. The ratio of crosslinker to native enzyme was 2700:1.

The aforementioned samples were run on SDS electrophoresis gels (Figure 19). NPRTase with GTA but without substrates exhibited only the noncrosslinked monomer band. After preincubation with PRPP and Mg^{2+}, NPRTase still exhibited only one band corresponding to the monomer. After preincubation with ATP and Mg^{2+}, NPRTase displayed only one band. The profile of NPRTase with Mg^{2+}, ATP, and PRPP but without GTA showed only one band corresponding to the monomer.

The activity of NPRTase was monitored to assess the effect of substrates on treatment with GTA (Table 14). There was no dimunition of

Figure 19. SDS Gel Electrophoresis Study of the Effects of Added Substrates and Mg^{2+} to the NPRTase & GTA Incubation Mixture.

1) 20 µg. lysozyme.

2) 40 µg. trypsinogen.

3) 20 µg. ovalbumin.

4) 20 µg. bovine serum albumin.

5) 22 µg. NPRTase and 1.37 µmoles GTA incubated for 30 min.

6) 22 µg. NPRTase pretreated with 2 µmoles Mg^{2+} and 2 X 10^{-2} µmoles PRPP for 30 min. was incubated with 1.37 µmoles GTA for 30 min.

7) 22 µg. NPRTase pretreated with 2 µmoles Mg^{2+} and 4.8 X 10^{-2} µmoles ATP for 30 min. was incubated with 1.37 µmoles GTA for 30 min..

8) 22 µg. NPRTase pretreated with 2 µmoles Mg^{2+}, 4.8 X 10^{-2} µmoles ATP, and 2 X 10^{-2} µmoles PRPP for 30 min. was not subject to GTA.

1
2
3
4
5
6
7
8

TABLE 14. Effect of Substrates on NPRTase Activity[a]

During Crosslinking by Glutaraldehyde

Sample	*Incubation Time for Activity Measurement*		
	1 min.	*3 min.*	*10 min.*
1. NPRTase with 5 µl. 2% GTA [30 min.]	*0.6 cm.*	*0.7 cm.*	*1.0 cm.*
2. NPRTase with Mg^{2+}-PRPP & 5 µl. 2% GTA [30 min.]	*0.5 cm.*	*0.6 cm.*	*0.7 cm.*
3. NPRTase with Mg^{2+}-ATP & 5 µl. 2% GTA [30 min.]	*0.5 cm.*	*0.6 cm.*	*0.7 cm.*
4. NPRTase with Mg^{2+}, ATP, and PRPP [30 min.]	*0.5 cm.*	*0.6 cm.*	*1.2 cm.*

a) Activity measurements were as described in Table 12.

TABLE 15. SDS Electrophoresis of NPRTase Subject to Glutarlaldehyde To Assess the Effect of Mg(II) on Crosslinking

Sample Gel	Distance of Dye Migration	Distance of Protein Migration	Range of R_f	MW
1. Lysozyme	10.4 cm.	9.4–9.6 cm.	.904–.923	14,300
2. Trypsinogen	10.7 cm.	6.5–6.7 cm.	.607–.626	24,000
3. Ovalbumin	10.4 cm.	3.9–4.1 cm.	.375–.394	45,000
4. Bovine Serum Albumin	10.6 cm.	2.4–2.6 cm.	.226–.245	66,000
5. NPRTase w/o GTA	10.7 cm.	3.6–3.8 cm.	.336–.355	
6. NPRTase w/GTA [30 sec.]	10.8 cm.	3.5–3.9 cm.	.324–.361	
7. NPRTase w/GTA [min.]	10.8 cm.	3.5–3.9 cm.	.324–.361	
8. NPRTase w/Mg/GTA [30 sec.]	10.8 cm.	3.5–3.9 cm.	.324–.361	
9. NPRTase w/Mg/GTA [30 min.]	10.8 cm.	3.5–3.9 cm.	.324–.361	
10. NPRTase w/Mg/GTA [30 min.]	10.8 cm.	3.7–3.9 cm.	.343–.361	

TABLE 16. SDS Electrophoresis of NPRTase
Subject to Crosslinking by Glutaraldehyde in Presence of ATP or PRPP

Sample Gel	Distance of Dye Migration	Distance of Protein Migration	Range of R_f	MW
1. Lysozyme	10.4 cm.	9.9–10.1 cm.	.952–.971	14,300
2. Trypsinogen	10.7 cm.	6.9–7.1 cm.	.645–.664	24,000
3. Ovalbumin	10.6 cm.	4.2–4.4 cm.	.396–.415	45,000
4. Bovine Serum Albumin	10.6 cm.	2.4–2.6 cm.	.226–.245	66,000
5. NPRTase w/GTA [30 min.]	10.7 cm.	3.9–4.0 cm.	.364–.374	
6. NPRTase w/Mg/PRPP/GTA [30 min.]	10.8 cm.	3.8–4.3 cm.	.352–.398	
7. NPRTase w/Mg/ATP/GTA [30 min.]	10.6 cm.	3.7–4.2 cm.	.349–.396	
8. NPRTase w/Mg/ATP/PRPP [30 min.]	10.7 cm.	3.7–4.1 cm.	.346–.383	

activity in the presence of GTA. The preincubation with ATP or PRPP before GTA treatment did not reduce the activity from that found by treatment with GTA alone.

The estimate for the molecular weight for the monomer from SDS electrophoretic analysis of the effect of substrates on treatment with GTA was 47,500 ± 2500. The equation derived by the method of least squares was: log (MW) = - 0.974 R_f + 5.04 (Table 16).

In conclusion, neither Mg^{2+} nor Mg^{2+} and substrates affected the electrophoretic pattern or the activity of NPRTase.

Concentration Dependence of DMS on NPRTase Crosslinking

22 µg. NPRTase was incubated for 4 hrs. with 15 µl. of 5 mg./ml., 10 mg./ml., or 15 mg./ml. DMS. A sample of 22 µg. NPRTase without DMS served as control. The ratio of crosslinker to native NPRTase was 550:1, 1100:1, or 1600:1. The samples were run on SDS electrophoresis gels (Figure 20). NPRTase without DMS exhibited only one band corresponding to the noncrosslinked monomer. NPRTase with 5 mg./ml., 10 mg./ml., or 15 mg./ml. DMS showed only one band corresponding to the noncrosslinked monomer. The band appeared more diffuse than the band of the gel on which NPRTase without DMS was run. The section of gel above the monomer band appeared colorless. The bands of the gels on which NPRTase with DMS was run did not show any appreciable reduction in intensity of the coomassie blue dye.

The estimate for the molecular weight of the monomer was 46,000 ± 2500. The equation of the line fitted by the method of least squares was: log (MW) = - 1.05 R_f + 5.06 (Table 17).

Consequently, increasing concentrations of DMS had no observable effect on the electrophoretic pattern of NPRTase.

Figure 20. SDS Gel Electrophoresis Studies of the Effects of Addition of DMS to NPRTase.

1) *20 μg. lysozyme, 40 μg. trypsinogen, 20 μg. pepsin, 20 μg. ovalbumin, and 20 μg. bovine serum albumin.*
2) *22 μg. NPRTase without DMS.*
3) *22 μg. NPRTase was incubated with 15 μl. of 5 mg./ml. DMS [0.275 μmoles] for 4 hours.*
4) *22 μg. NPRTase was incubated with 15 μl. of 10 mg./ml. DMS [0.549 μmoles] for 4 hours.*
5) *22 μg. NPRTase was incubated with 15 μl. of 15 mg./ml. DMS [0.824 μmoles] for 4 hours.*

1 2 3 4 5

TABLE 17. SDS Electrophoresis of NPRTase

Treated with Increasing Concentrations of DMS

Sample Gel	Distance of Dye Migration	Distance of Protein Migration	Range of R_f	MW
1. Lysozyme	10.7 cm.	9.2–9.6 cm.	.860–.897	14,300
Trypsinogen		6.5–6.8 cm.	.607–.636	24,000
Pepsin		4.0–4.25 cm.	.374–.397	34,700
Ovalbumin		4.25–4.5 cm.	.397–.421	45,000
Bovine Serum Albumin		2.2–2.6 cm.	.206–.243	66,000
2. NPRTase w/o DMS	10.9 cm.	3.9–4.2 cm.	.358–.385	
3. NPRTase w/ 5 mg./ml. DMS	11.1 cm.	4.1–4.4 cm.	.369–.396	
4. NPRTase w/ 10 mg./ml. DMS	10.9 cm.	3.9–4.3 cm.	.358–.394	
5. NPRTase w/ 15 ng./ml. DMS	10.8 cm.	3.8–4.3 cm.	.352–.398	

Figure 21. SDS Gel Electrophoresis Studies of the Effects of Addition of Mg^{2+} and DMS to NPRTase.

1) 20 μg. lysozyme.

2) 40 μg. trypsinogen.

3) 20 μg. ovalbumin.

4) 20 μg. bovine serum albumin.

5) 22 μg. NPRTase without DMS.

6) 22 μg. NPRTase and 0.550 μmoles DMS incubated for 30 sec.

7) 22 μg. NPRTase and 0.550 μmoles DMS incubated for 4 hours.

8) 22 μg. NPRTase pretreated with 2.5 μmoles Mg^{2+} for 30 min. was incubated with 0.550 μmoles DMS for 30 sec.

9) 22 μg. NPRTase pretreated with 2.5 μmoles Mg^{2+} for 30 min. was incubated with 0.550 μmoles DMS for 4 hours.

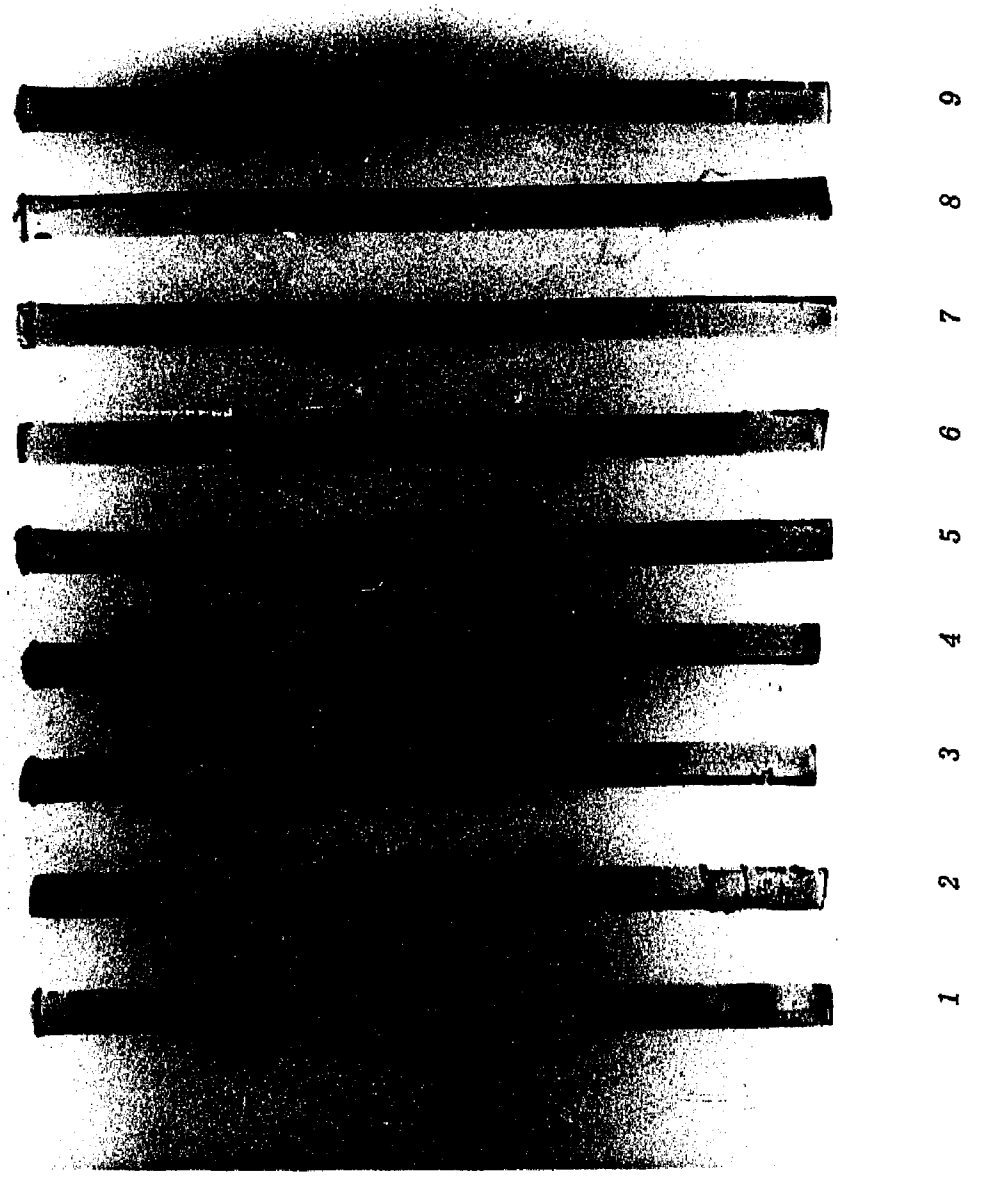
9
8
7
6
5
4
3
2
1

Effects of Addition of Mg^{2+} on NPRTase Crosslinking with DMS

22 μg. NPRTase was incubated with 30 μl. of 5 mg./ml. DMS for 30 sec. or for 4 hrs. Another 22 μg. NPRTase was incubated with 30 μl. of 5 mg./ml. of DMS for 30 sec. or for 4 hrs. after prior incubation with 2.5 μmoles Mg^{2+} for 30 min. 22 μg. NPRTase without DMS served as control. These samples were run on SDS electrophoresis gels (Figure 21). The ratio of DMS to native NPRTase was 1150:1. NPRTase without DMS exhibited only one band corresponding to the noncrosslinked monomer. NPRTase with DMS whether for 30 sec. or for 4 hrs. showed only the noncrosslinked band: there was no apparent reduction of intensity of the noncrosslinked monomer band compared to the gel on which NPRTase without DMS was run. The section of gel above the noncrosslinked monomer band was colorless. After prior incubation with Mg^{2+}, NPRTase with DMS for 30 sec. or for 4 hrs. exhibited only one band corresponding to the noncrosslinked monomer. The section of gel above the noncrosslinked monomer band appeared colorless. The intensity of the monomer band did not appear appreciably less than that of the gel onl which NPRTase without DMS was run.

The activity of NPRTase treated with DMS for 30 sec. or for 4 hrs. was measured in the presence or absence of Mg^{2+}. DMS did not appear to diminish the activity of NPRTase (Table 18). Mg^{2+} did not appear to affect the activity of NPRTase treated with DMS for 30 sec. or for 4 hrs.

The estimate for the molecular weight of the noncrosslinked monomer was 45,000 ± 2000. The equation derived by the least squares method from the midpoints of the R_f ranges of the standards of known molecular weight was: $\log (MW) = -1.00 R_f + 5.04$ (Table 19).

TABLE 18. Effect of DMS on NPRTase Activity[a]

Sample	*Incubation Time For Activity Measurement*		
	1 min.	*3 min.*	*10 min.*
1. NPRTase without DMS	*0.1 cm.*	*0.2 cm.*	*0.5 cm.*
2. NPRTase with 15 µl. 5 mg./ml. DMS [30 sec.]	*0.1 cm.*	*0.2 cm.*	*0.4 cm.*
3. NPRTase with 15 µl. 5 mg./ml. DMS [4 hrs.]	*0.1 cm.*	*0.2 cm.*	*0.6 cm.*
4. NPRTase with Mg^{2+} & 15 µl. 5 mg./ml. DMS [30 sec.]	———	*0.05 cm.*	*0.4 cm.*
5. NPRTase with Mg^{2+} & 15 µl. 5 mg./ml. DMS [4 hrs.]	*0.1 cm.*	*0.2 cm.*	*0.4 cm.*

a) Activity measurements were as described in Table 12.

TABLE 19. SDS Electrophoresis of NPRTase

Treated with DMS in the Presence of Mg(II)

Sample Gel	Distance of Dye Migration	Distance of Protein Migration	Range of R_f	MW
1. Lysozyme	10.6 cm.	9.5–9.7 cm.	.896–.915	14,300
2. Trypsinogen	10.5 cm.	6.4–6.6 cm.	.610–.629	24,000
3. Ovalbumin	10.4 cm.	3.8–4.2 cm.	.366–.404	45,000
4. Bovine Serum Albumin	10.4 cm.	2.3–2.7 cm.	.221–.260	66,000
5. NPRTase w/o DMS	10.7 cm.	4.0–4.4 cm.	.374–,411	
6. NPRTase w/5 mg./ml. DMS [30 sec]	10.6 cm.	3.9–4.2 cm.	.368–.396	
7. NPRTase w/5 mg./ml. DMS [4 hrs]	10.6 cm.	3.9–4.2 cm.	.368–.396	
8. NPRTase w/Mg^{2+} & DMS [30 sec]	10.6 cm.	3.9–4.1 cm.	.368–.387	
9. NPRTase w/Mg^{2+} & DMS [4 hrs]	10.7 cm.	4.0–4.2 cm.	.374–.393	

In conclusion, there was no observable effect of Mg^{2+} on the electrophoretic pattern or on the activity of NPRTase treated with DMS.

NMR Results

Victor et. al. (13) have suggested that the kinetic mechanism of OPRTase involves an intermediate carbocation with a new sp geometry at the 1' carbon. One way of examining this mechanism is NMR and studies were carried out for both OMP and PRPP to characterize the proton spectra of these reactants. In Table 20 is presented the proton peak assignments for several ribose-containing compounds including PRPP and several nucleotides and deoxynucleotides (72) in addition to OMP. There is nothing remarkable about the ribose and base ring proton resonances of OMP when compared to other nucleotides. Interestingly, the H'_1-proton resonance of PRPP is shifted significantly downfield (relative to this resonance of ribose-5-phosphate) due to the attachment of PP_i.

The relaxation rates of the assigned resonances of PRPP under various conditions were then determined and these values are shown in Table 21. Three methods were employed to calculate these relaxation rates ($1/T_1$) and are included here (Table 21). The null point readings (procedure 2 of Table 21) provide only an estimate of the rates because of the selection of τ values in these experiments, whereas procedure 1 and 3 provide the best $1/T_1$ values. As shown in Table 21, the longitudinal relaxation rates of the protons of PRPP (pH = 8) in Tris/DCl are all within the range of 1.1-4.1 sec^{-1}, and these values are similar to those of ribose protons of nucleotides generally (73, 74). With the addition of the paramagnetic metal ion (Mn^{2+}) the relaxation rate of H_1 increases dramatically while the increases in the rates of the other protons are less

TABLE 20. Chemical Shifts of the Protons of Ribose- and Deoxyribose-Containing Compounds at 220 MHz

Compound	Proton						
	H_1	H_2	H_3	H_4	H_5	Other	Tris
Ribose	4.65	3.86	(3.71 — 3.40)[a]		3.28	———	3.49
Deoxyribose-5-P	5.98	2.25	4.27	3.79	3.48	———	3.48
Ribose-5-P	5.09	4.05	3.94	3.81	3.64	———	3.48
PRibosePP	5.51	4.15	(3.96 — 3.88)[a]		3.63	———	3.48
AMP[b]	6.04	4.77	4.46	4.35	4.01	———	———
GMP[b]	5.93	4.76	4.50	4.33	4.02	———	———
UMP[b]	5.98	4.41	4.34	4.25	4.00	———	———
CMP[b]	6.01	4.36	4.34	4.25	4.02	———	———
OMP	5.53	4.79	4.76	(4.11 — 3.92)[a]		5.77[c]	3.59
dAMP[b]	6.43	2.74	4.73	4.26	3.94	———	———
dGMP[b]	6.29	2.66	4.73	4.22	3.95	———	———
TMP[b]	6.33	2.36	4.57	4.16	3.99	———	———
dCMP[b]	6.33	2.38	4.55	4.15	3.95	———	———
dUMP[b]	6.32	2.36	4.56	4.15	3.95	———	———

a) overlapping resonances; b) from Davies and Danyluk (1974) Biochem. 13, 4417; c) proton of orotate ring.

significant. Moreover, the order of decrease in the paramagnetic effect is $H_1 > H_2 > H_3 > H_4 > H_5$, *indicating that* Mn^{2+} *is coordinated to the PRPP molecules close to the* H_1 *proton, presumably to the* PP_i *group. When OPRTase and a diamagnetic metal ion (*Mg^{2+}*) are added to PRPP there is very little effect on the relaxation rates of the PRPP protons as expected, although once again a slight effect was observed for the* H_1 *proton, suggesting that some component of the proton's motion has been hindered. Whether this implies that a single metal ion site exists or two sites exist cannot be ascertained by this qualitative experiment. Further analysis of the experiments described in Table 21 (experiments 4 and 5) will be discussed later.*

As shown in Table 22, the relaxation rates of the proton resonances of OMP were also calculated. These relaxation rates are typical of nucleotides and are unaffected by the addition of paramagnetic Co^{2+}. *Since metal ions can only bind to the 5' phosphate group of OMP (both the* PP_i *site of PRPP and the* $\overset{|}{N}H-C\overset{/}{H}-COO^-$ *site of orotate are no longer present in the OMP molecule), this coordination by* Co^{2+} *is quite loose and thus no real observable effect at this concentration of* Co^{2+} *is observed. However, there are small increases in the relaxation rates of the OMP resonances when OPRTase is added, again suggesting that OMP is binding to the enzyme under these conditions. The addition of* Mn^{2+} *to enzyme and OMP leads to measurable increases in the relaxation rates. The order of decreasing effect is* $H_0 > H_5, H_4 > H_3 > H_1 > H_2$, *suggesting that in the metal ion-enzyme-OMP complex, the position of the metal may be on top of the ribose ring close to the 5' phosphate and close to the orotate carboxyl group. This picture is reasonable for nucleotide metal interactions.*

TABLE 21. Longitudinal Relaxation Rates (sec^{-1}) of the Protons of PRPP

Solution	H_1	H_2	H_3	H_4	H_5	Procedure[a]
1) 100 mM PRPP[b]	1.9	1.5	1.4	1.1	3.9	1
in Tris/DCl (pH8)	2.2	2.1	2.1	1.5	4.1	2
	2.0	1.4	1.4	1.2	3.5	3
2) 100 mM PRPP[b]	6.7	3.3	2.8	1.8	4.1	1
in Tris/DCl (pH8)	8.7	3.9	2.9	2.3	4.6	2
20 μM Mn^{2+}	6.7	3.4	2.4	1.7	3.9	3
3) 100 mM PRPP	3.2	1.6	1.6	1.9	3.4	1
500 μM OPRTase	3.4	1.6	1.7	1.7	3.8	3
5 mM Mg^{2+}						
4) 15 mM PRPP	0.9	1.0	2.0	2.0	3.6	1
1 mM OPRTase	0.5	1.7	4.2	4.2	3.7	3
10 mM OMP						
5) 15 mM PRPP	7.8	5.1	6.0	6.0	2.8	1
10 mM OMP	9.5	4.8	6.1	6.1	5.3	3
1 mM OPRTase						
50 mM Mg^{2+}						

a) procedure 1 described by Mildvan and Gupta, Methods in Enzymology 49, 322, 1978; procedure 2 is a null-reading estimate described by Mildvan and Cohn, Adv. Enzymology 33, 1, 1970; procedure 3 is described by Sass and Ziessow, J. Mag. Res. 25, 263, 1977.

b) Victor, J., and Sloan, D.L., unpublished results.

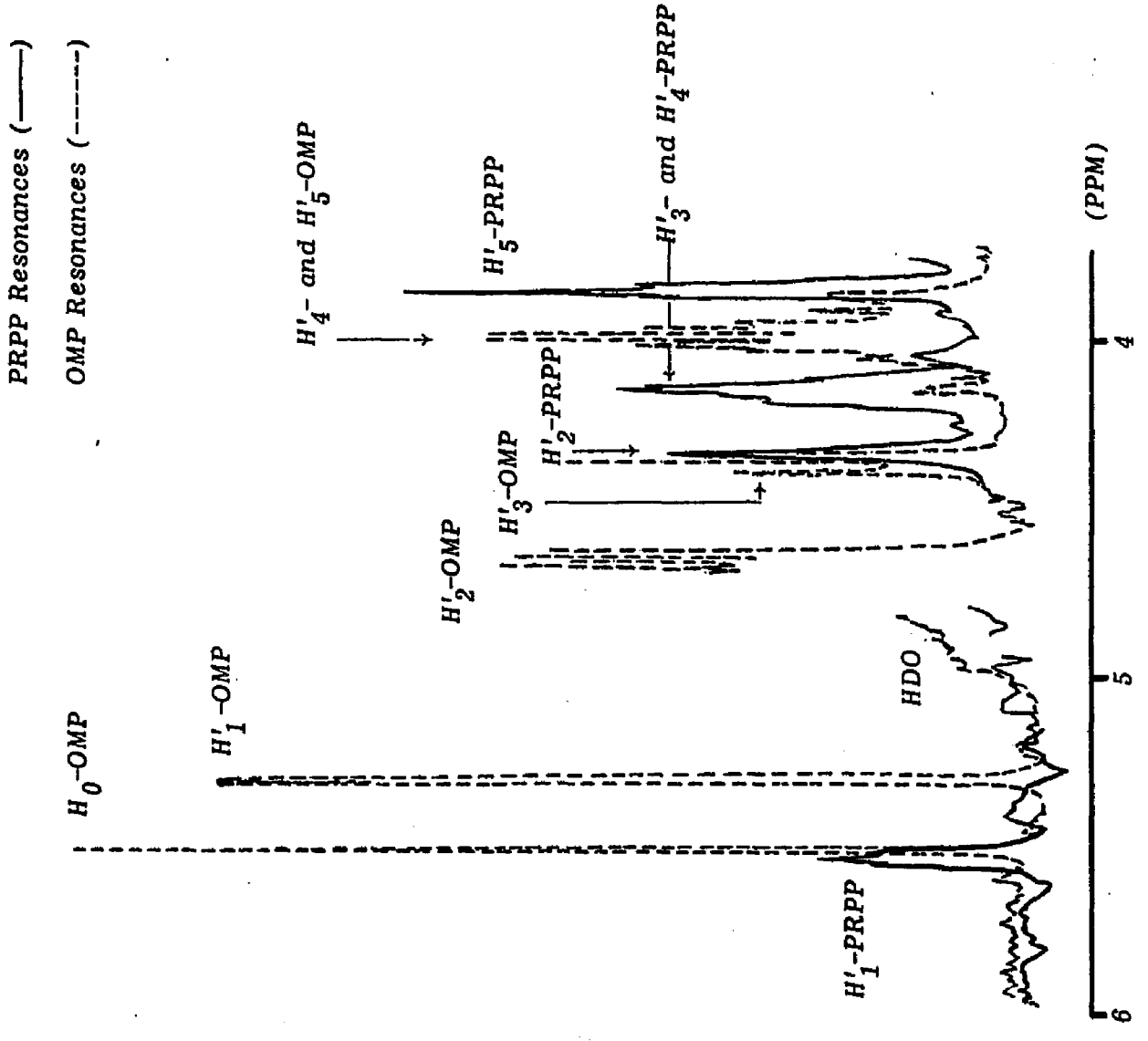

FIGURE 22. Overlapping NMR Spectrum of OMP and PRPP. Experimental Conditions: Tris/DCl (pD ≡ 8), 220 MHz, 19°C, 0.5 ml. sample volume.

An experiment was then run in order to examine if the ping pong kinetic mechanism can be observed using proton NMR. In this experiment the enzyme is provided with the ribose-containing substrate for both the forward (OMP formation) and reverse (orotate formation) reactions, but the other substrates for these reactions are not included. Since PRPP and OMP together include all of the substrates (OMP contains orotate for the forward reaction and PRPP contains PP_i for the reverse reaction) of the reversible reaction, it was concluded that if an E-RibP intermediate forms from either direction, the substrate for the other direction will have been provided. Thus if the ping pong mechanism applies, the phosphoribosyl intermediate will form only in the presence of a divalent metal cation: the OMP bound OPRTase will form in the absence of a divalent metal cation. The results of this experiment are shown in both Table 21 (experiments 4 and 5) and Table 22 (experiments 6 and 7).

When OPRTase and OMP were added to PRPP (Figure 22, Table 21) the relaxation rates of protons H_3 and H_4 of PRPP increased while those of H_1, H_2 and H_5 decreased slightly (exp #4 - #1). The order of decreasing effect was $H_4 > H_3 > H_2 > H_1 = H_5$. This suggests that protons H_4 and H_3 become more hindered upon binding of PRPP to OPRTase.

The addition of OPRTase, OMP, and Mg^{2+} to PRPP led to significant increases in the relaxation rates of protons H_1, H_2, H_3, and H_4. The rate for H_5 hardly changed at all (exp #5 - #1). The order of decrease of the effect was $H_1 > H_4 > H_3 > H_2 > H_5$. These results indicate that the motions of the protons H_1, H_4, H_3, and H_2 are more hindered, again suggesting that Mg^{2+} is coordinated close to the H_1 proton.

The relaxation rates of protons H_1, H_2, H_3, and H_4 of PRPP increased dramatically as a consequence of the addition of Mg^{2+} to PRPP, OPRTase,

TABLE 22. Longitudinal Relaxation Rates (1/sec) of the Protons of OMP

Solution	H_1	H_2	H_3	H_4	H_5	H_0	Procedure[a]
1) 100 mM OMP[b]	0.9	1.0	1.3	2.5		0.7	1
in Tris/DCl (pH8)	1.5	2.0	2.5	4.8		0.7	2
2) 100 mM OMP[b]	0.6	1.0	1.3	2.7		0.4	1
20 μM Co(II)							
3) 10 mM OMP[b]	0.8	1.6	1.4	2.8		0.4	1
20 μM Co(II)	1.2	1.6	2.0	4.5		0.8	2
4) 50 mM OMP	1.1	1.3	2.1	3.3		0.4	1
100 μM OPRTase	1.9	1.4	3.9	5.0		1.0	2
5) 50 mM OMP	1.3	—	2.7	2.3		0.8	1
100 μM OPRTase	2.2	1.5	3.9	6.9		1.9	2
20 μM Mn(II)							
6) 10 mM OMP	0.8	—	1.0	5.0		0.4	1
1 mM OPRTase	1.4	—	7.7	7.7		1.0	2
15 mM PRPP	0.8	—	1.7	5.9		0.4	3
7) 10 mM OMP	2.1	—	5.1	4.4		1.3	1
1 mM OPRTase	2.3	—	7.7	6.3		1.4	2
15 mM PRPP	1.6	—	4.8	4.3		0.8	3
50 mM Mg(II)							

a) procedures described in Table 21.

b) Victor, J., and Sloan, D.L., unpublished results.

and OMP (exp #5 - #4). Furthermore, the relaxation rate of proton H_5 hardly changed at all. The decreasing order of the effect was $H_1 > H_2 > H_3 = H_4 > H_5$. The increases of the rates suggest that the motion of proton H_1 is more hindered due to proximity to H_1 of the site of coordination of Mg^{2+}.

When PRPP was added to OPRTase and OMP (Figure 22, Table 22), the relaxation rates of protons H_4 and H_5 of OMP increased (exp #6 - #4). The order of decreasing effect was $H_4, H_5 > H_3 > H_0 > H_1$. This suggests the motions of H_4 and H_5 of OMP are hindered during the displacement of OMP by PRPP.

When PRPP and OPRTase were added to OMP (exp #6 - #1, Table 22) the relaxation rates of protons H_3, H_4, and H_5 of OMP increased. The order of decreasing effect was $H_4, H_5 > H_3 > H_0 > H_1$. This suggests that the motion of protons H_3, H_4, and H_5 of OMP is influenced by OMP binding to OPRTase.

When Mg^{2+} was added to OMP, OPRTase, and PRPP, the relaxation rate of proton H_3 of OMP increased while the change in the relaxation rates of the other protons was less significant (exp #7 - #6). The order of decreasing effect was $H_3 > H_0 > H_1 > H_4, H_5$. The relaxation rate for the overlapping resonances of protons H_4 and H_5 decreased. These results suggest that the motion of H_3 is more restricted in the phosphoribosyl intermediate than in either OMP-OPRTase or PRPP-OPRTase. Mg^{2+} may induce a conformational change in the macromolecule which not only alters the extent of association but also increases the relaxation rate for H_3 of OMP and decreases the relaxation rate for H_4, H_5 of OMP.

When OPRTase, PRPP, and Mg^{2+} were added to OMP, the relaxation rates of protons H_3, H_4, and H_5 of OMP increased (exp #7 - #1). The

TABLE 23. Amplitudes of the Resonances of OMP and PRPP at Pulse Sequence Delay (τ) of 2.0 sec. Effects of the Addition of Mg(II) to a Sample Containing Both Reactants and OPRTase.

	Proton Amplitudes (cm)				
PRPP Experiments (Table 21)	H_1	H_2	H_3, H_4	H_5	
Exp #4 ($-Mg^{2+}$)	17	43	45	70	
Exp #5 ($+Mg^{2+}$)	11	50	40	40	
Difference #5-#4	-6	+7	-5	-30	
OMP Experiments (Table 22)	H_1	H_2	H_3	H_4, H_5	H_0
Exp #6 ($-Mg^{2+}$)	33	—	43	70	25
Exp #7 ($+Mg^{2+}$)	40	—	50	118	65
Difference #7-#6	+7	—	+7	+48	+40

order of decreasing effect was $H_3 > H_4, H_5 > H_1 > H_0$. This suggests that the motions of H_3, H_4, and H_5 are more hindered in the phosphoribosyl intermediate than in OMP.

In summary, throughout the comparison of the experiments of Table 21 and 22, small effects (both diamagnetic and paramagnetic) were found, confirming the formation of metal ion complexes with enzyme, the enzyme and OMP, and the enzyme and PRPP. Interestingly, resonance amplitude changes were also observed which could not be explained in terms of line broadening effects. These results are presented below.

When Mg^{2+} was added to PRPP, OPRTase, and OMP, the amplitude of proton H_5 of PRPP decreased dramatically (Table 23). The order of decrease of the effect was $H_2 > H_3, H_4 > H_1 > H_5$. When Mg^{2+} was added to PRPP, OPRTase, and OMP, the amplitudes of protons H_4, H_5, and H_0 of OMP increased significantly (Table 23). The order of decrease of the effect was $H_4, H_5 > H_0 > H_3 = H_1$. The general loss of amplitude for PRPP and the general gain of amplitude for OMP may be attributed to the establishment of a new equilibrium reached by the consumption of PRPP by OPRTase to form more OMP. This suggests that upon addition of Mg^{2+}, PRPP and OMP are in equilibrium through a phosphoribosyl intermediate.

Thus only in the presence of Mg^{2+} can one observe a change in the peak amplitude confirming the result of Victor et. al. (13) that the ping pong mechanism proceeds only in the presence of Mg^{2+}. These NMR results provide evidence that there are several possible roles for the metal in this reversible reaction: binding of PRPP coordinating to the PP_i moiety and binding to the enzyme altering the extent of association. Because of this result, the previously described studies of the structure of the enzyme using crosslinking reagents were initiated to

see what effect metal ions would have on this structure.

Discussion of the Monomer/Dimer Equilibrium

As shown in Figure 23, the crosslinking reagents GTA and DMS can be envisioned to react with lysine residues in close proximity. These lysine residues can be present on adjacent monomer units of a dimer as illustrated in Figure 24. There can be no doubt, because of the electrophoresis results (both nondenaturing and denaturing), that a monomer dimer equilibrium exists for OPRTase but not for NPRTase. In the case of OPRTase, there are two possible routes for the formation of crosslinked dimer (structure C). The first route involves the formation of dimer, its covalent crosslinking and subsequent dissociation (A → D → E → F → C). The second route involves the formation of a complex of crosslinker and monomer, and the subsequent formation of a crosslink between monomers in solution (A → B → C). There are three good arguments for the former route taking precedence over the latter route. 1) The concentration of A, the monomeric unit, in a solution in which the crosslinker is in a > 1000 molecular abundance, should be minimal since most of the monomer should be in the form shown by structure B and two molecules of structure B cannot form a crosslinked dimer. 2) The crosslinking of two monomeric units has to be facilitated kinetically by the noncovalent interaction of units and thus structure E can easily form a crosslink whereas structure B must collide with structure A in the correct orientation. 3) Route A → B → C should not be affected by the presence of substrate or activator molecules whereas route A → D → E → F → C may indeed be affected by molecules which bind to the enzyme and affect the monomer/dimer equilibrium. Indeed, my observation of an effect of Mg^{2+} on the relative

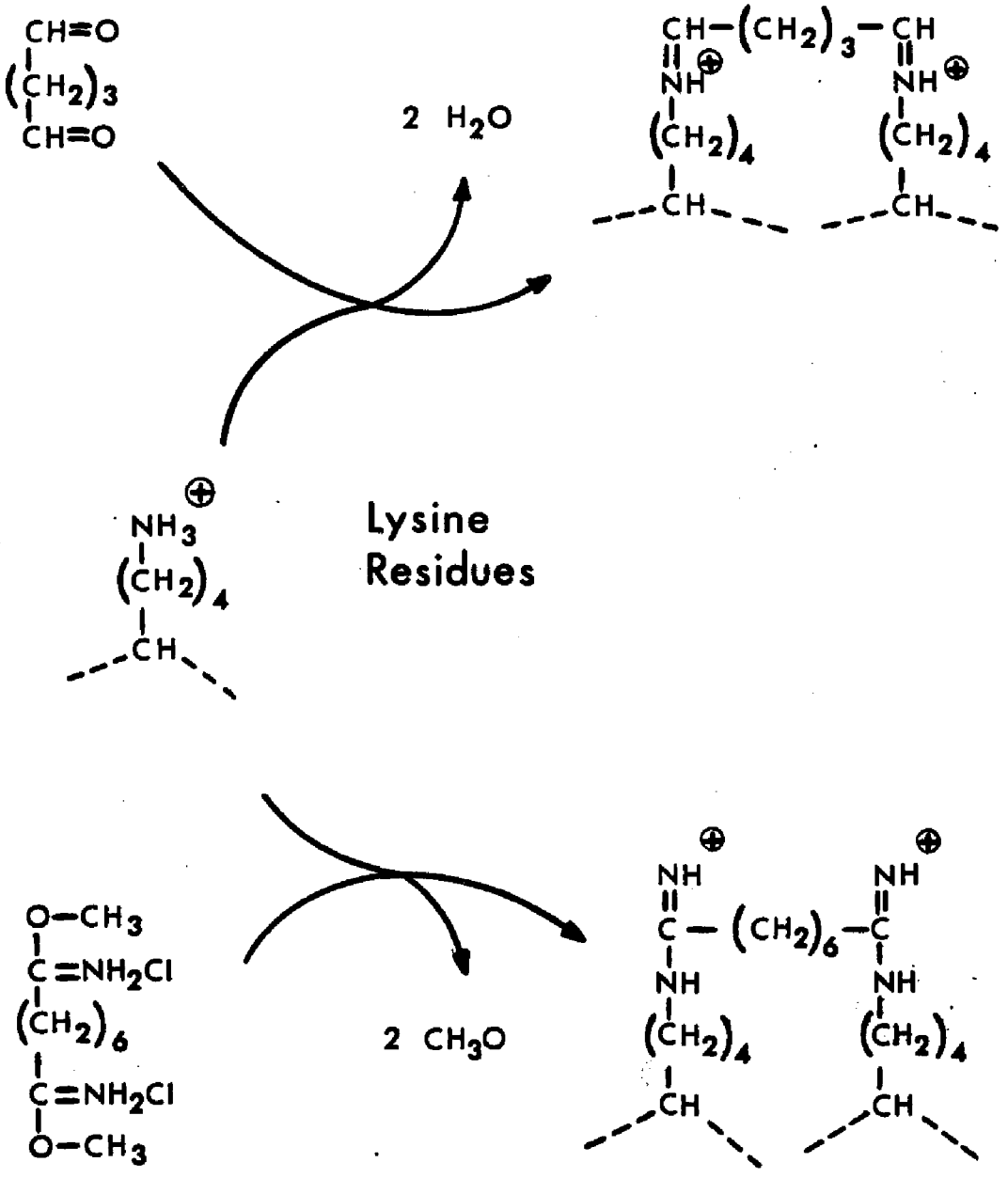

FIGURE 23. Crosslinking Reactions of GTA and DMS.

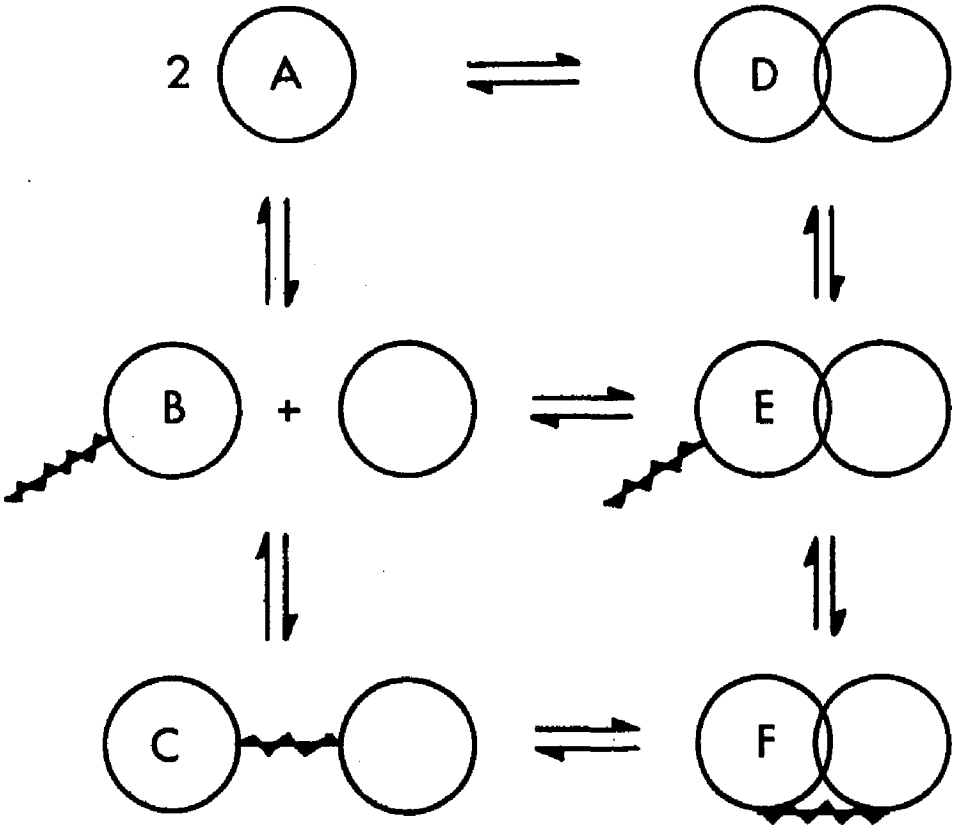

FIGURE 24. Mechanism of Crosslinking for a Monomer/Dimer Equilibrium

amount of dimer may prove the dimer's existence in the absence of GTA or DMS. Of course, this discussion assumes a single binding site for the crosslinker on each monomer. The existence of more than one binding site, which is probable, complicates the discussion but the conclusions should remain the same.

Observations of Other Phosphoribosyltransferase Monomer/Dimer Equilibria

The results of this research suggest that yeast OPRTase may exist in the form of a monomer or a dimer, and that the activity that has been characterized kinetically (13) is that of the dimer. Moreover, the enzymic dimer is probably the Mg^{2+}–enzyme dimeric complex which has been suggested to proceed via the ping pong kinetic mechanism (37). The overall kinetic mechanism in substrate addition and metal ion activation is shown in equations 3 and 4. Additionally this new data also explains why a sigmoidal binding isotherm is obtained from yeast OPRTase when Mn^{2+} binds to the enzyme (37). Perhaps Mn^{2+} as well as Mg^{2+} promotes the formation of dimer.

OPRTase from Ehrlich ascites cells has also been proposed to undergo an activity altering monomer/dimer equilibrium (25). Whereas the formation of dimers for yeast OPRTase is influenced by the presence of the cation Mg^{2+}, it is a function of the presence of anions in the solvent for OPRTase from Ehrlich ascites cells. In the presence of dithiothreitol, a change of anions alters the extent of dimer formation through rapid interconversion.

In this laboratory, hypoxanthine-guanine phosphoribosyltransferase from yeast (HGPRTase) has also been observed to be present in solution as both a monomer and a dimer using crosslinking reagents. Interestingly,

Mg^{2+} has no effect on this monomer/dimer equilibrium but the presence of Mg^{2+}–PRPP does promote the formation of the monomer. This difference in the effectors of monomer/dimer equilibria of two phosphoribosyltransferases of the same species may be a way in which the control of PRPP allocation among the two reactions is manifested. Certainly more experiments which define the similarities and differences between HGPRTase, NPRTase, and OPRTase structures and mechanisms are called for.

BIBLIOGRAPHY

1. Lieberman, I., Kornberg, A., and Simms, E.S. (1955) J. Biol. Chem. 215, 403-415

2. Raivio, K.O., and Seegmiller, J.E. (1970) in Current Topics in Cellular Regulation (Horecker, B.L., and Stadtman, E.R., eds) Vol. 2, pp. 201-225

3. Priess, J., and Handler, P. (1958) J. Biol. Chem. 233, 493-500

4. Kosaka, A., Spirey, H.O., and Gholson, R.F. (1971) J. Biol. Chem. 246, 3277-3283

5. Smith, O.H., and Yanosky, C. (1960) J. Biol. Chem. 235, 2051-2057

6. Ames, B.N., Martin, R.G., and Garry, B.J. (1961) J. Biol. Chem. 236, 2019-2026

7. Yoshimoto, A., Amaya, T., Kobayashi, K., and Tomita, K. (1978) in Methods in Enzymology (Hoffee, P.A., and Jones, M.E., eds) Vol. LI, pp. 69-79, Academic Press, New York

8. Belser, W.L., and Wild, J. R. (1978) in Methods in Enzymology (Hoffee, P.A., and Jones, M.E., eds) Vol. LI, pp. 135-143, Academic Press, New York

9. Silva, R.F., and Hatfield, D. (1978) in Methods in Enzymology (Hoffee, P.A., and Jones, M.E., eds) Vol. LI, pp. 143-154, Academic Press, New York

10. Jones, M.E., Prabhakar, R.K., and Traut, T.W. (1978) in Methods in Enzymology (Hoffee, P.A., and Jones, M.E., eds) Vol. LI, pp. 155-167, Academic Press, New York

11. Umezu, K., Amaya, T., Yoshimoto, A., and Tomita, K.(1971) J. Biochem. 70, 249-262

12. Musick, Wm. D.L.(1981) CRC Critical Reviews in Biochemistry 11(1), 1-34

13. Victor, J., Greenberg, L.B., and Sloan, D.L. (1979) J. Biol. Chem. 254, 2647-2655

14. Reyes, P., and Sandquist, R.B. (1978) Anal. Bioch. 88, 522-531

15. Dodin, G.(1981) FEBS Letters 134(1), 20-24

16. Traut, T.W. (1982) Trends in Biochemical Science 7, 255-257

17. Kasbekar, D.K., Nagabhushanan, A., and Greenberg, D.M. (1964) J. Biol. Chem. 239, 4245-4249

18. Appel, S.H. (1968) J. Biol. Chem. 243, 3924-3929

19. Shoaf, W.T., and Jones, M.E. (1973) Biochemistry 12, 4039-51

20. Brown, G.K., Fox, R.M., and O'Sullivan, W.J. (1972) Biochem. Pharmacol. 21, 2469-2477

21. Reyes, P., and Guganig, M.E. (1975) J. Biol. Chem. 250, 5097-5108

22. Brown, G.K., Fox, R.M., and O'Sullivan, W.J. (1975) J. Biol. Chem. 250, 7352-7358

23. Gero, A.M., and Coombs, G.H. (1980) FEBS Letters 118(1), 130-132

24. Qureschi, I.A., Letarte, J., and Ouellet, R. (1982) Experientia 38, 308-309

25. Jones, M.E. (1980) Ann. Rev. Bioch. 49, 253-279

26. Kavipurapu, P.R., and Jones, M.E. (1976) J. Biol. Chem. 251, 5589-5599

27. Traut, T.W., and Jones, M.E. (1977) J. Biol. Chem. 252, 8374-8381

28. Traut, T.W., and Jones, M.E. (1979) J. Biol. Chem. 254, 1143-1150

29. McClard, R.W., Black, M.J., Livingstone, L.R., and Jones, M.E. (1980) Biochemistry 19, 4699-4706

30. Jones, M.E. (1971) Adv. Enzyme Regulation (Weber, G., eds) 9, 19-49

31. Reyes, P., and Intress, C. (1978) Life Sciences 22(7), 577-582

32. Jones, M.E.(1972) in Current Topics Cellular Regulation (Horecker, B. L., and Stadtman, E. R., eds) Vol. 6, pp. 227-64, Academic Press, New York

33. Jund, R., and Lacroute, F. (1972) J. Bact. 109, 196-202

34. Lacroute, F. (1968) J. Bact. 95, 824-832

35. O'Donovan, G.A., and Neuhard, J. (1970) Bact. Rev. 34, 278-343

36. Goltein, R.K., Chelsky, D., and Parsons, S.M. (1978) J. Biol. Chem. 253, 2963-2971

37. Victor, J., Leo-Mensah, A., and Sloan, D.L. (1979) Amer. Chem. Soc. 18, 3597-3604

38. Priess, J., and Handler, P. (1958) J. Biol. Chem. 233, 493-500

39. Priess, J., and Handler, P. (1958) J. Biol. Chem. 233, 488-492

40. Imsande, J. (1961) J. Biol. Chem. 236, 1494-1497

41. Nishizuka, Y., and Hayaishi, O. (1963) J. Biol. Chem. 238, 3369-3377

42. Imsande, J., and Handler, P. (1961) J. Biol. Chem. 236, 525-530

43. Imsande, J., and Handler, P. (1964) Biochem. Biophys. Acta 85, 255-264

44. Ogasawara, N., and Gholson, R.K. (1966) Biochem. Biophys. Acta 118, 422-424

45. Honjo, T., Nakamura, S., Nishizuka, Y., and Hayaishi, O. (1966) Biochem. Biophys. Res. Commun. 25, 199-204

46. Kosaka, A., Spivey, H.O., and Gholson, R.K. (1971) J. Biol. Chem. 246, 3277-3283

47. Kosaka, A., Spivey, H.O., and Gholson, R.K. (1977) Arch. Biochem. Biophys. 179, 334-341

48. Seifert, R., Kittler, M., and Hilz, H. (1966) in Current Aspects of Biochemical Energetics (Kaplan, N.O., and Kennedy, E.P., eds) pp. 413-431, Academic Press, New York

49. Kahn, V., and Blum, J.J. (1967) Biochem. Biophys. Acta 146 305-308

50. Niedel, J., and Dietrich, L.S. (1973) J. Biol. Chem. 248, 3500-3505

51. Baecker, P.A., Yung, S.G., Rodriguez, M., Austin, E., and Andreoli, A.J. (1978) J. Bact. 133(3), 1108-1112

52. Sloan, D.L., Hanna, L.S., and Hess, S.L. (1982) Fed. Proc. 41, 1386

53. Foster, J.W., Kinney, D.M., and Moat, A.G. (1979) J. Bact. 138, 957-961

54. Hanna, L., Sloan, D.L. (1980) Anal. Biochem. 103, 230-234

55. Lowry, O.H., Rosebrough, N.J., Farr, L., and Randall, R.J. (1951) J. Biol. Chem. 193, 265-275

56. Bio-Rad Laboratories (1977) Technical Bulletin 1051, Richmond, A.

57. Brewer, J.M., Resce, A.J., and Ashworth, R.B. (1974) Experimental Techniques in Biochemistry pp. 128-160, Prentice Hall, Englewood Cliffs, New Jersey

58. Cooper, T.G. (1977) The Tools of Biochemistry pp. 194-208, John Wiley & Sons, New York

59. Davis, B.J. (1964) Ann. N. Y. Acad. Sci. 121, 404-427

60. Reynolds, J.A., and Tanford, C. (1970) Proc. Natl. Acad. Sci. U.S.A. 66(3), 1002-1007

61. Reynolds, J.A., and Tanford, C. (1970) J. Biol. Chem. 245, 5161-5165

62. Thomas, J.O. (1971) Techniques in the Life Sciences Vol. B1/1, B106, pp. 1-22, Elsevier/North Holland Scientific Publishers Ltd., County Clare, Ireland

63. Weber, K. and Osborn, M. (1975) in The Proteins (Neurath, H., and Hill, R. L., eds) Vol. 1, pp. 179-223, Academic Press, New York

64. Pople, J.A., Schneider, W.G., and Bernstein, H.J. (1950) High Resolution Nuclear Magnetic Resonance pp. 22-49, McGrawHill Book Co., N.Y.

65. Carrington, A., and McLachlan, A.P. (1969) Introduction to Magnetic Resonance (Rice, S.A., ed.) pp. 4-8, Harper & Row, New York

66. McLauchlan, K.A. (1972) Magentic Resonance pp. 1-20, Clarendon Press, Oxford

67. Kowalsky, A. and Cohn, M. (1964) Ann. Rev. Biochem. 33, 481-518

68. Wutrich, K. (1976) NMR In Biological Research: Peptides and Proteins pp. 123-133, North-Holland/American Elsevier, New York

69. Carr, H.Y. and Purcell, E.M. (1954) Phys. Rev. 94, 630-639

70. Carr, H.Y. and Purcell, E.M. (1952) Phys. Rev. 88, 415-416

71. Sass, M. and Ziessow, D. (1977) J. of Mag. Res. 25, 263-276

72. Davies, D.B. and Danyluk, S.S. (1974) Biochem. 13, 4417-4434

73. Sloan, D.L., Loeb, L.A., and Mildvan, A.S. (1975) J. Biol. Chem. 250, 8913-8920

74. Sloan, D.L. and Mildvan, A.S. (1976) J. Biol. Chem. 251, 2412-2420

75. Sloan, D.L., Ali, L.Z., and Joseph Jr., A. (1982) J. Clin. Chem. Clin. Biochem. 20, 419

CURRICULUM VITAE

NAME: Leonard Mayer

ADDRESS: 2835 Sedgwick Ave., Bronx, New York 10468

TELEPHONE NUMBER: (212) 543-6946

BIRTHDATE: January 28, 1951

CITIZENSHIP: U.S.A.

EDUCATION: Master in Philosphy, BIOCHEMISTRY, City University of New York, 1981

Nuclear Magnetic Resonance, Fordham University, 1976

Chemistry, New York University (Washington Square), 1975-1976

French, Universite de la Sorbonne Nouvelle, Paris, 1973-5

B.A., Mathematics, New York University (University Heights), 1973

TEACHING EXPERIENCE: Teaching Fellowship, Dept. of Chemistry, The City College, Feb. 1977-June 1977, and Sept. 1978-Jan. 1979

ACADEMIC HONORS: Graduate Fellowship

Graduate Assistantship

Dean's List

New York State Regent's Scholarship

MEMBERSHIP IN PROFESSIONAL SOCIETIES:

Sigma χi , The Scientific Research Society

American Association for the Advancement of Science

New York Academy of Science

American Chemical Society